DEVELOPMENT OF A PASSIVE VIBRATION ISOLATION ANALYSIS AND OPTIMIZATION SOFTWARE FOR MECHANICAL SYSTEMS

A THESIS SUBMITTED TO
THE GRADUATE SCHOOL OF NATURAL AND APPLIED SCIENCES
OF
MIDDLE EAST TECHNICAL UNIVERSITY

BY

OZAN YAVUZ BAYTEMİR

IN PARTIAL FULFILLMENT OF THE REQUIREMENTS
FOR
THE DEGREE OF MASTER OF SCIENCE
IN
MECHANICAL ENGINEERING

SEPTEMBER 2013

Approval of the thesis:

DEVELOPMENT OF A PASSIVE VIBRATION ISOLATION ANALYSIS AND OPTIMIZATION SOFTWARE FOR MECHANICAL SYSTEMS

submitted by **OZAN YAVUZ BAYTEMİR** in partial fulfillment of the requirements for the degree of **Master of Science in Mechanical Engineering Department, Middle East Technical University** by,

Prof. Dr. Canan Özgen ____________________
Dean, Graduate School of **Natural and Applied Sciences**

Prof. Dr. Suha Oral ____________________
Head of Department, **Mechanical Engineering**

Assist. Prof. Dr. Ender Ciğeroğlu ____________________
Supervisor, **Mechanical Engineering Dept., METU**

Assist. Prof. Dr. Gökhan O. Özgen ____________________
Co-Supervisor, **Mechanical Engineering Dept., METU**

Examining Committee Members:

Assoc. Prof. Dr. Serkan Dağ ____________________
Mechanical Engineering Dept., METU

Assist. Prof. Dr. Ender Ciğeroğlu ____________________
Mechanical Engineering Dept., METU

Assist. Prof. Dr. Gökhan O. Özgen ____________________
Mechanical Engineering Dept., METU

Assist. Prof. Dr. Yiğit Yazıcıoğlu ____________________
Mechanical Engineering Dept., METU

Assist. Prof. Dr. Selehattin Çağlar Başlamışlı ____________________
Mechanical Engineering Dept., Hacettepe University

Date: 09-09-2013

I hereby declare that all information in this document has been obtained and presented in accordance with academic rules and ethical conduct. I also declare that, as required by these rules and conduct, I have fully cited and referenced all material and results that are not original to this work.

Name, Last name :

Signature :

ABSTRACT

DEVELOPMENT OF A PASSIVE VIBRATION ISOLATION ANALYSIS AND OPTIMIZATION SOFTWARE FOR MECHANICAL SYSTEMS

Ozan Yavuz Baytemir

M.Sc., Department of Mechanical Engineering

Supervisor: Assist. Prof. Dr. Ender Ciğeroğlu

Co-Supervisor: Assist. Prof. Dr. Gökhan O. Özgen

September 2013, 131 Pages

In the design stage of a mechanical structure, the effects of vibration are taken into consideration as important design criteria. In order to eliminate the adverse effects of vibration sources, a direct intervention to the vibration source, structural reinforcement or the use of vibration isolators are encountered as the most popular vibration control methods. Among all, being compact, low cost, reliable and maintenance free, elastomeric passive vibration isolators with linear properties are examined within the scope of the present thesis study.

In this thesis, the mechanical structure mounted on elastomeric resilient elements is modeled theoretically. In this theoretical model, the mechanical structure is assumed to be a rigid body with 6 degrees of freedom. Having obtained system matrices and input vibration profile, modal analysis, static deflection analysis in addition to response analysis for harmonic and random type of excitations are made available in software developed. Additionally, in order to design an efficient vibration isolation system, both location and parameter optimization of elastomeric isolators are included in the present study. In comparison to similar studies in the literature, types of analysis, in addition to the optimization design variables are improved so that a more flexible design environment is introduced. For practical design purposes, a graphical user interface is also included. Using the developed software, a designer will be able to analyze an isolation system and optimize design variables considering various types of optimization problem scenarios.

Keywords: Passive vibration isolation analysis, multi-degree-of-freedom system, elastomeric isolators, location and parameter optimization, hybrid optimization, Monte Carlo simulations.

ÖZ

MEKANİK SİSTEMLER İÇİN PASİF TİTREŞİM İZOLASYON ANALİZ VE OPTİMİZASYON YAZILIMI GELİŞTİRİLMESİ

Ozan Yavuz Baytemir

Yüksek Lisans, Makine Mühendisliği Bölümü

Tez Yöneticisi: Yrd. Doç. Dr. Ender Ciğeroğlu

Ortak Tez Yöneticisi: Yrd. Doç. Dr. Gökhan O. Özgen

Eylül 2013, 131 Sayfa

Bir mekanik yapının tasarım aşamasında, titreşim etkileri önemli bir tasarım kriteri olarak dikkate alınmaktadır. Titreşim kaynağının olumsuz etkilerini azaltmak maksadıyla, titreşim kaynağına doğrudan müdahale, yapısal güçlendirme veya titreşim izolatörü kullanımı, titreşim kontrol metodları arasında en çok başvurulan yöntemlerdendir. Hepsinin arasında, kompakt, düşük maliyetli, güvenilir ve bakım gerektirmez olmaları dolayısıyla, sunulan tez çalışması kapsamında lineer özellikli elastomer malzemeli pasif titreşim izolatörleri incelenmiştir.

Bu tez raporunda, elastomer malzemeli yapılar üzerine monte edilen mekanik yapı teorik olarak modellenmiştir. Bu teorik modelde, mekanik yapı 6 serbestlik dereceli katı kütle şeklinde varsayılmıştır. Bu çalışmada, sistem matrisleri ve girdi titreşim profiline sahip olarak, modal analiz, statik sapma analizi ile harmonik ve rastgele titreşim için tepki analizleri gerçekleştirilebilir hale getirilmiştir. Ayrıca, sunulan çalışma, daha etkili titreşim izolasyon sistemi tasarımı elde etme amacıyla, elastomer

izolatörlerin pozisyon ve parametre optimizasyonu çalışmasını içermektektedir. Literatürdeki benzer çalışmalar ile karşılaştırıldığında, analiz tipleri ve optimizasyon tasarım değişkenleri geliştirilerek daha esnek bir tasarım ortamı tanıtılmıştır. Pratik uygulamalar için bir grafik arayüzü geliştirilmiştir. Geliştirilen yazılım ile kullanıcı, bir izolasyon sistemini analiz edebilecek ve çok çeşitli optimizasyon problemi senaryolarını dikkate alarak tasarım değişkenlerini optimize edebilecektir.

Anahtar kelimeler: Pasif titreşim izolasyonu, çok serbestlik dereceli system, elastomer izolatörler, pozisyon ve parametre optimizasyonu, hibrid optimizasyon, Monte Carlo simülasyonları.

ACKNOWLEDGEMENTS

I would like to thank my supervisor Assist. Prof. Dr. Ender Ciğeroğlu and co-supervisor Assist. Prof. Dr. Gökhan O. Özgen for their support and guidance during the thesis study. Without their valuable help and technical support, this study would never have come into life. I also thank them for their motivation and great patience during this long-term study.

I would also like to thank Ali Osman Boyacı, Manager of the Mechanical Design Department in Meteksan Defence Ind. Inc. for his executive support, tolerance and trust. I would also like to express my deepest appreciation for his moral support in the meeting of the thesis defence.

I specially would like to thank Burçak Özkök for his great discussions, comments, guidance and supports in all areas. Without him, it would be hard for me to gain self-confidence, complete the overall study and use it for practical purposes. I should also admit that I am so lucky to meet a man like him.

I am also grateful to all of my fellows in Meteksan Defence. Special thanks to Uğur Susuz, Sedat Ozan Koca, Kerem Ali Günbulut, Ahmet Levent Avşar, Ufuk Yiğit, Sinan Kurudere, Volkan Aban and Anıl Yaman for restoring my belief in completing the thesis report; Ebru Dülgergil, Yiğitcan Güden and Şaban Bilek for their valuable help in thesis format; Yusuf Yazar and Nuri Beştepe for their technical supports in all areas.

I owe to my friends, Osman Gürlevik, Emir Topkaraoğlu and Gökçe Ulusoy for all the things we have shared since Ankara Science High School years.

I also thank Dr. Ersoy Kontacı for his moral support and especially for his great stories that motivated me at the end of the thesis studies.

Finally, I would like to give my greatest thanks to my lovely parents, my dear fiancée, Bilgen Bilgi and my dear brother Özgür and his lovely wife for their

unconditional love, support, patience and encouragement. Without them, I never had the enthusiasm to conduct all these studies.

To My Parents

TABLE OF CONTENTS

LIST OF FIGURES

FIGURES

LIST OF TABLES

TABLES

CHAPTER 1

BACKGROUND AND LITERATURE SURVEY

1.1. Introduction

Vibration is an important issue in the design of various components of aerospace, marine and vehicular applications. In spite of the fact that those devices operate precisely in quiet environmental conditions, the user expects not to lose its function in harsh environmental conditions. The endurance of such equipment is defined primarily by the ability of their internal sensitive components to survive severe vibration without developing critical fatigue to the mounted components [1]. In order not to lose function and operational performance of the components, vibration isolation design involving the selection of optimum isolator properties and optimum isolator position appear to be a critical study.

Knowing the growing need for the vibration isolation system design, this thesis study aims to present the capabilities of two types of softwares developed:

- Software on vibration isolation system analysis;
- Software on vibration isolation system optimization.

Those softwares are capable of implementing modal analysis, response analysis for both random and harmonic types of excitations, static deflection analysis, Monte Carlo simulations in addition to study of parameter and location optimization for different types of isolation problem scenarios. Investigating the literature, there is no study developing a software-based tool that is capable of implementing all these analysis, simulation and optimization studies in one platform simultaneously. In this thesis study, the capabilities of a MATLAB based software having a graphical user interface for the analysis, simulation and optimization of a general vibration isolation design problem is developed and demonstrated.

In this study, the theoretical system model is generated for a 6 degree of freedom rigid body; where, the mechanical structure is assumed to be mounted on elastomeric isolators which are defined by three mutually orthogonal springs with stiffness coefficients and a loss factor. Static and dynamic analysis in addition to simulation and optimization studies are performed using the system matrices and forcing vectors obtained from the general equation of motion. The results obtained by following the given procedures for each type of analysis are verified by using a commercial finite element analysis software, ANSYS Workbench 14.0. For optimization, a hybrid method is used involving both global search and gradient-based methods. Defining the optimization design variables, different types of optimization scenarios are listed in detail. Using the software developed for the purposes of vibration isolation system analysis and optimization, three different case studies for a real application used in air platforms are implemented in order to demonstrate the capabilities of the analysis and optimization programs.

1.2. Thesis Layout

This thesis study is composed of six chapters. In Chapter 1, following an introduction to the thesis work performed, similar studies on passive vibration isolation analysis and optimization are listed and explained in detail. The vibration control techniques in addition to isolator and isolation system modeling are summarized for single and multi-degree of freedom systems. As the primary vibration excitation source, air platforms are considered and the vibration profile details of specific platforms found in military standards are detailed.

In Chapter 2, theoretical development of the mathematical model for a 6-degree of freedom rigid body suspended on flexible vibration isolators is explained and the equations of motion are listed. The equations are rearranged in matrix form and the system matrices are generated. For harmonic and random types of vibration excitation, the response analysis procedures are explained in detail. Additionally, detailed information on modal analysis and static deflection analysis are presented. Importance of Monte Carlo simulations is stated and the parameters deviated during those simulations are described. Finally, a variety of optimization problem scenarios with corresponding design variables and input parameters are tabulated and explained in detail.

In Chapter 3, the verification of the theoretical model using a commercial finite element program is implemented. Here, modal analysis, static deflection analysis in addition to response analysis to random and harmonic type of vibration are generated for isolators mounted orthogonal or inclined to the global reference frame. Additionally, the transmissibility functions obtained for different input-output relations are compared.

In Chapter 4, the details of the software developed for vibration isolation analysis and optimization purposes are given. For both analysis and optimization sections, existing buttons and panels encountered on the graphical user interfaces are described in detail.

In Chapter 0, case studies demonstrating the capabilities of the developed software are given in three main sections. In the first section, the analysis of a vibration isolation system mounted on a helicopter platform is considered. Here, modal analysis, static deflection analysis, response analyses for harmonic and random type of excitation in addition to Monte Carlo simulations are implemented for a specific mechanical system mounted on elastomeric isolators. In the second section, using the same mechanical structure, a variety of optimization problem scenarios is investigated and the results for different design parameters are compared with each other. In this section, the mechanical structure is the same as the one given in the first section. However, the vibrating platform is a military aircraft at this time. In the third and final sections, an optimization application for the same mechanical structure mounted on a helicopter platform is shown. In this section, a specific optimization problem is generated and the optimum design variables are computed.

In Chapter 6, the thesis study is summarized and the points in order to improve the present study are shared as future studies.

1.3. Literature Survey

Before examining a vibration isolation design problem in detail, it would be beneficial to investigate other studies in literature. Below, the review of the studies on vibration isolation system design is presented. The isolator and isolation system modeling are summarized referring to other studies found in literature. Finally, the air platforms as vibrating platforms are investigated using military standards.

1.3.1. Review of the Studies on Vibration Isolation System Design

In literature, there are a variety of studies investigating the adverse effects of vibration on several devices. For instance, Kamesh *et al.* [2] mentioned about the effects of micro-vibrations in a spacecraft. In this study, it is stated that the vibration produced by functioning of on-board equipment such as gyroscopes, thrusters, electric motors and data storage devices has adverse effects on sensitive payloads like sensors, laser communication devices in addition to the telescopes. In one another study, Yoon [3] explained the output errors encountered in micro-electromechanical systems (MEMS) due mechanical vibration. Here, it is generalized that those errors cannot be compensated with electronics and they generate systemic problems. In Hati and his friends' study [4], the effects of vibration on oscillators used in unmanned aerial vehicle are stated. Additionally, other electronic components such as microwave cables, circulators and amplifiers are described as vibration sensitive electronic components. Griffith [5] and Knott [6] related the performance reduction in a radar antenna to the occurrence of vibration on air platforms. According to the observations, the generated vibration causes phase errors, bore sight errors and increased side and back lobe levels, thus results in a decrease in the quality of the transmitted signals.

Being aware of the adverse effects of vibration on a number of devices as mentioned above, it is possible to find many other researchers in literature studying passive vibration isolation system design in order to minimize such destructive effects due vibration. Many of them develop their own softwares for vibration analysis and optimization purposes for specific cases. In Table 1.1 and Table 1.2, the studies found in literature are tabulated and compared with each other in detail.

Table 1.1 Studies on Vibration Isolation Analysis and Optimization

Owner of the Study	Software Used	Analysis	Optimization	
			Method	Variables
Song [7]	EMTOOLS	-Static -Modal -Response	DSA(*)	-Stiffness -Location
Ponslet *et al*. [8]	DAKOTA	-Static -Modal -Response	GA(**)	-Location
Esat *et al.* [9]	VIBRATIO	-Modal -Response	GA(**)	-Stiffness -Location -Orientation
Swanson *et al.* [10]	SIXOPT	-Static -Modal -Response	CVMOT (†)	-Stiffness -Orientation
Vibrant Technology [11]	ME'scopeVES	-Modal -Response	None	None
BAuA [12]	ISOMAG	-Static -Modal -Response	None	None
Mechartes Simulation Experts [13]	VISP	-Modal -Response	N/A	-Stiffness -Location
Vejsz [14]	ProE/Mechanica	-Modal -Response	None	None
Chen *et al*. [15]	ANSYS	-Modal -Response	None	None
Zehsaz *et al.* [16]	ANSYS	-Modal -Response	Iterative	-Stiffness -Damping
Basavaraj *et al.* [17]	LS-Dyna	-Modal -Response	Iterative	-Engine Mount Sys.
Mallick *et al.* [18]	N/A	-Response	GA(**)	-Stiffness -Damping -Location
Alkhatib [19]	N/A	-Response	GA(**)	-Stiffness -Damping
Kaul [20]	MATLAB based	-Modal -Response	Meta-Modelling	-Stiffness -Damping -Location -Orientation
Wang [21]	MATLAB based	-Static -Modal -Response -Parameters Sensitivity	SQP(††) (fmincon)	-Stiffness -Damping -Location -Orientation
Cinarel [22]	MATLAB Based	-Static -Modal -Response -Monte Carlo Sim.	Hybrid	-Stiffness -Damping

(*) Based on Design Sensitivity Analysis; (**) Genetic Algorithm; (†) The Constrained Variable Metric Optimization Technique; (††) Sequential Quadratic Programming.

Table 1.2 Comparison of the Studies

Owner of the Study	**Analysis**				**Optimization Design Variables**		
					Isolator Properties		
	Static	Modal	Response	M.C.Sim.	Char.	Location	Orientation
Song [7]	✓	✓	✓		✓	✓	
Ponslet [8]	✓	✓	✓			✓	
Esat [9]		✓	✓		✓	✓	✓
Swanson[10]	✓	✓	✓		✓		✓
V.Tech.[11]		✓	✓				
BAuA [12]	✓	✓	✓				
M.S.Exp.[13]		✓	✓		✓	✓	
Vejsz [14]		✓	✓				
Chen [15]		✓	✓				
Zehsaz [16]		✓	✓		✓		
Basavaraj[17]		✓	✓				
Mallick[18]			✓		✓	✓	
Alkhatib [19]			✓		✓		
Kaul [20]		✓	✓		✓	✓	✓
Wang [21]	✓	✓	✓		✓	✓	✓
Cinarel[22]	✓	✓	✓	✓	✓		
Present Thesis Study	✓	✓	✓	✓	✓	✓	✓

Following the given in Table 1.1 and Table 1.2, the studies can be summarized as follows.

Song [7] developed MSC ADAMS based vibration isolation analysis and design optimization software, called EMTOOLS. This program is specialized in static analysis and vibration analysis such as modal analysis in addition to response analysis of engine mount systems. Using this software, it is possible to implement idle and engine shake analysis for 6 and 16 degrees of freedom models. In [7], an optimization analysis is also performed in order to find the optimum location and the stiffness values for the engine mounts in order to maximize the roll modal purity of the engine. The optimization process is based on design sensitivity analysis.

One another software, capabilities of which are demonstrated in Ponslet *et al.* [8], is called DAKOTA. This software is actually developed as an optimization tool for general purposes. However, in this paper [8], DAKOTA is used to investigate the effects of isolator location on the vibration isolation performance. In this study, discrete location optimization of isolators for an optical table has been performed by using genetic algorithm. The system is modeled in MATLAB and coupled with the developed software. The stiffness and damping coefficients, in addition to the mounting angle of the isolators are fixed. The objective of the optimization analysis is to minimize the value of transmissibility function of a point at a constant frequency. The point of interest is located near the corner of the optical table. For the defined design constraints, the developed software is also capable of implementing static analysis, modal analysis in addition to response analysis.

VIBRATIO is the name of another commercial software used for optimization of vibratory behavior of the system. Esat *et al.* [9] used this software in their study. Similar to DAKOTA, VIBRATIO also uses genetic algorithm as an optimization method. The difference is in the design variable. In this study not only the locations of isolators, but also the stiffness values and angular orientation of the mounts can be optimized concerning the design purposes.

Swanson *et al.* [10] demonstrated the simulation and numerical optimization of the mounting system for an aircraft engine. For this purpose, an interactive computer program, called SIXOPT is developed. In this study, an optimization problem is studied to determine the optimum design parameters such as stiffness and the orientation angle of the mount in order to minimize the transmitted forces. For the optimization study, the constrained variable metric optimization technique is used. Additionally, using the developed software, it is possible to implement static analysis, modal analysis in addition to response analysis for predefined design parameters.

ME'scopeVES, ISOMAG and VISP are other commercially developed softwares used by Vibrant Technology [11], BAuA [12] and Mechartes Simulation Experts [13], respectively. From those three computer programs, the first two are only capable of implementing vibratory analysis; on the other hand, the last, VISP is able to implement modal analysis and response analysis in addition to parameter and location optimization for a specified vibration problem.

Investigating Table 1.1, it is easily observed that many other studies are found in literature where vibratory analysis and optimization studies are performed using best-selling commercial tools such as ProE/Mechanica, ANSYS or LS-Dyna. From those studies, Vejsz [14] used ProE/Mechanica for modal analysis in addition to response analysis of a computer hard drive subjected to random vibration in his thesis study.

The results obtained are verified by experiments. On the other hand, Chen *et al.* [15] and Zehsaz [16] used finite element analysis software, ANSYS in their studies. Chen *et al.* [15] built an equivalent analysis model for engine powertrain mounting system. In this study [15], an example for an automotive engine powertrain with three mounting components is investigated and modal analysis is implemented. Similarly, Zehsaz *et al.* [16] used ANSYS software in order to optimize passive suspension parameters of a tractor's cabin for minimizing the transmitted vibration via iterative method. In this study [16], modal and response analysis of the tractor, which is exposed to random vibration, are performed. Finally, Basavaraj *et al.* [17] used LS-Dyna simulation in order to investigate dynamic behavior of the engine mount. For different engine mount systems, modal and response analysis are implemented. The results are compared with each other and the best suited design is selected.

Observing Table 1.1, it is possible to find other studies demonstrating the analysis and optimization capabilities of custom softwares developed for specific cases. In the study of Mallick *et al.*[18], the optimization technique is based on genetic algorithm. The design variables are selected as the stiffness and damping coefficients of the isolators in addition to location of the isolators. An isolator platform design problem is built for electronic systems mounted on police vehicles. Using the developed software, the optimum design parameters are computed and the corresponding response analyses are performed.

In literature, it is also possible to find a number of thesis reports investigating vibration isolation analysis and optimization studies for different types of applications in real world. One of them is about modeling and vibration control of turboprop installations in aircrafts. In this thesis study, Alkhatib [19] utilized Lagrange's technique in order to obtain the equations of motion for the proposed model. The design of the engine mounting is considered as an optimization problem and genetic algorithm is developed to compute the optimum values of the design variables such as stiffness and damping coefficients of the isolators. For the optimization of the passive vibration isolation system, a simple two degree of freedom model is used and frequency response functions are obtained and employed in the process.

In Kaul's thesis study [20], different models representing the vibration isolation problem of a motorcycle system have been developed. Those models include simplified models with assumptions and a complete motorcycle model with all sub-systems and connection elements. Having obtained analytical models for different cases, optimization of the isolation system is performed using MATLAB based software in order to minimize the load transmitted from the engine mount system to the frames. The stiffness and damping coefficients of the isolators in addition to the location and orientation of the mounts are defined as the optimization design variables. Meta-modeling technique is used to simplify the governing equations in addition to reducing the computational time required for the solution of the optimization problem.

Thesis study of Wang [21] is one another study investigating the vibration isolation of engine mount systems similar to the studies of Song [7], Chen [15], Basavaraj [17] and Alkhatib [19]. Differently, MATLAB based software is developed and an optimization algorithm, fmincon that is found in MATLAB's Optimization Toolbox is used for the purpose of optimizing the defined design variables. In this study [21], stiffness and damping coefficients of the isolators in addition to the location and orientation angle of the engine mounts are selected as the optimization design parameters. In all design purposes, static deflection analysis, modal analysis and response analysis are performed in. Additionally, by implementing parameter sensitivity analysis, it is possible to check and decide parameters which have primary influence on the selected objective function.

Finally, another thesis study including MATLAB based software is Çınarel's study [22]. In this thesis report, vibration isolation and optimization studies have been conducted for an inertial measurement unit mounted on air platforms. In this thesis study [22], hybrid method is used as an optimization algorithm. This hybrid method includes genetic algorithm and fmincon function that are both available in MATLAB's Optimization Toolbox. The stiffness and damping coefficients of the isolators are selected as the optimization design parameters. For different objectives and design constraints, a set of case studies are implemented. Having obtained optimum values for the design parameters, static deflection analysis, modal analysis and response analysis are carried out. Additionally, being aware of the deviations in the characteristics of isolators in real world, Monte Carlo simulations are performed and the variations in the selected parameters are plotted separately. Finally, a graphical user interface is developed for the implementation of analysis and optimization capabilities using MATLAB Guide Tool.

1.3.2. Vibration Control, Isolator and Isolation System Modeling

In order to analyze a vibration isolation system accurately, it is important to generate correct analytical models for isolators and corresponding isolation system. In order to obtain those correct models, the designer should define the isolation problem first.

According to Kelly [23] and Silva [24], the vibration isolation problems are grouped in two classes basically:

- Protection of foundation against large forces of equipment (Figure 1.1a);
- Protection of equipment against motion of foundation (Figure 1.1b).

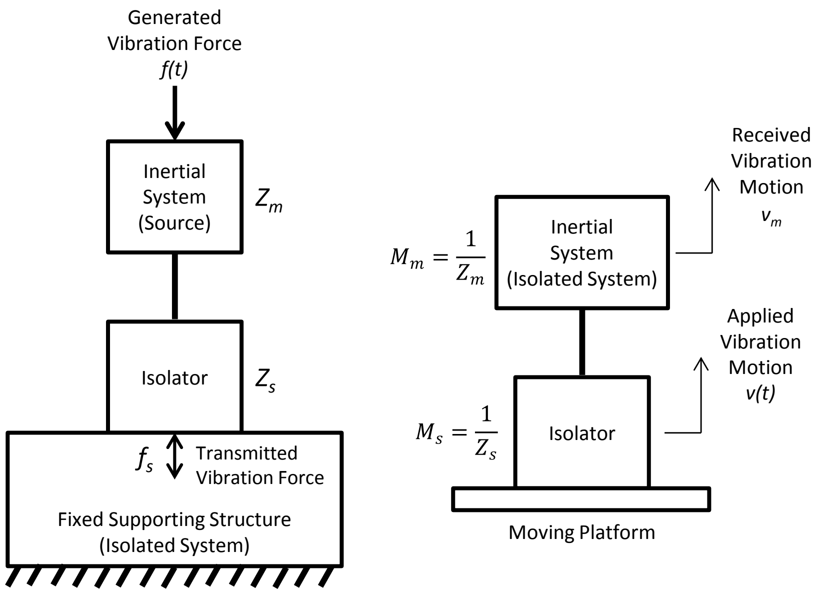

(a) (b)

Figure 1.1 Typical Vibration Isolation Systems [24]

Considering the given typical vibration isolation problems, Kelly [23] and Rao [25] proposed the following vibration control methods.

- Elimination of the external vibration excitation or reduction in its magnitude,

- Control of system parameters such as inertia, stiffness and damping by an optimized structural design,
- Reduction of force or motion transmission by the use of vibration isolators or absorbers mounted on the mechanical structure.

The first method is related to the source of vibration. Considering this method, the designer may change the location of the vibration sensitive device away from the sources of excitation or reduce the amplitude of vibration source directly. However, in most cases, the method is considered as improper due to the existence of such integration constraint for the device and the possibility of direct intervention to the vibration source unpreferably.

The second method is actually related to structural reinforcement. Such vibration control method is encountered as a research topic in literature. Baran [26] has proposed topology and stiffener parameter optimization for minimizing the adverse effects of structural vibrations of a radar antenna on its functional performance in his thesis study. Such a vibration control method might be beneficial for a mechanical structure in design stage. However, what if the mechanical system is manufactured and a need for reduction in the destructive effects of the vibration without any structural modification exists?

The third and final control method is the most preferable one for real type of applications. In this method, reduction in the dynamic response of the system is achieved by using a variety of devices such as resilient members, springs, pneumatic or hydraulic mounts, auxiliary mass damper or the usage of magnetorheological fluids. Besides, as Rao [25] mentions, the isolation system is defined as an active or passive depending on the necessity of external control of the devices to perform their function.

Although Alkhatib [19] remarks that there is an increase in research in the area of active vibration control in recent years, being compact, low cost, reliable, maintenance free and having long service life, passive vibration isolation devices are still most preferable in vibration isolation problems [27].

In passive vibration isolation systems, isolators produce a resistant force across the device without any use of power supply. In literature, the passive vibration isolators come up in different forms. However, for each type, a force resistance element or an energy dissipater is common. Metal springs, pneumatic springs, elastomer springs in addition to wire rope isolators, negative-stiffness isolators and elastomeric pads and sheets can be given as examples used in passive vibration isolation systems.

Within the scope of the presented thesis study, elastomeric passive vibration isolators are used in order to minimize the transmitted forces from the moving platform to the isolated system by shifting the natural frequencies away from the excitation frequency. In literature, Voigt model is highly used for elastomeric isolator modeling due to its simplicity in analysis and parameter identification [28]. Voigt model is a two-element model consisting of a spring and viscous damper as shown in Figure 1.2. Since the elastomer is a polymer with viscoelasticity, the Voigt model is proper to some extent. However, according to Zhang and Richards [29], dynamic stiffness experiments show the frequency dependent features of elastomeric isolators and thus the Voigt model is not sufficient.

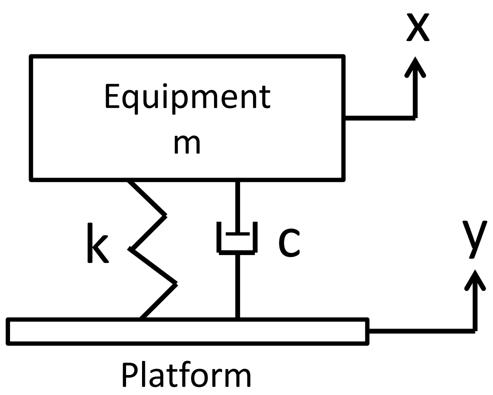

Figure 1.2 Single Degree of Freedom Voigt Model

As Kaul [20] mentions, the mechanical properties of rubber like materials are usually expressed in frequency domain. Those mechanical properties are the dynamic-to-static stiffness ratio in addition to damping characteristics. Both factors change with the excitation frequency, amplitude of the loading in addition to temperature. Therefore it is best to obtain the information on the mechanical properties of those elastomeric isolators by implementation of experiments. However, as Cinarel [22] mentions, in order to obtain a reliable characterization of the mechanical properties, a high number of experiments with good accuracy are needed. This results in high cost and longer times for isolation analysis and optimization processes. Due to this reason, for simplicity the dynamic to static stiffness ratio is assumed to be set to unity in this thesis study. Additionally, since the structural damping is the most commonly used model for commercial isolators [22], instead of using viscous damping, the isolators are defined in terms of structural damping characteristics. For those types of elastomer mounts, complex spring stiffness is used to model the dynamic behavior as;

$$k^{*} = k(1 + i\eta), \tag{1}$$

where k is the stiffness coefficient, η is the loss factor and i is the complex number.

In this thesis study, the elastomer mounts are modeled as 3 mutually orthogonal springs with stiffness coefficients and a loss factor. The isolator mounts are assumed to be massless and are free to be located in any point on the rigid body in any orientation as seen in Figure 1.3. With the elastomer mounts, the isolated system is assumed to be a rigid body with 6 degrees of freedom consisting of 3 translational motion along the global reference frame and 3 rotary motion around the global reference frame which is assumed to be located at the center of mass of the rigid body.

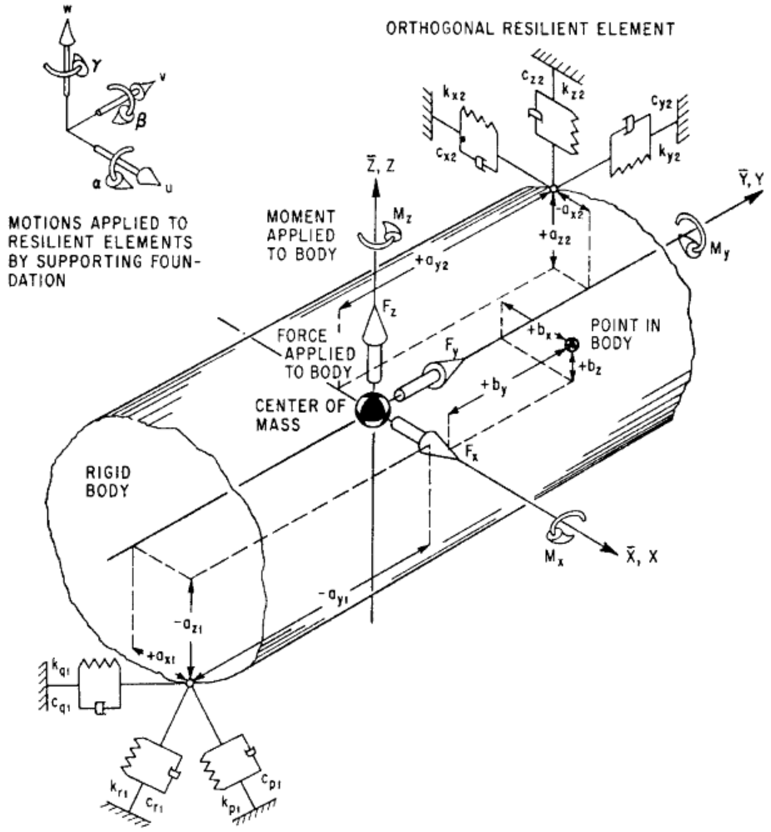

Figure 1.3 General Representation of a Multi-Degree of Freedom System [30]

Having obtained the isolator model in addition to the isolation system model, it is possible to obtain all equations of motion from the free body diagram which can also be put in a matrix form. Thus, the system matrices such as mass matrix, stiffness matrix and forcing vector can be generated. The details are presented in Chapter 2.

1.3.3. Air Platforms as Vibrating Platforms

In order to compute the response vector at any point on the rigid body, the type of input vibration profile should be well defined. In this thesis study, the air platforms are considered as the vibrating platform. However, it should be stated that the procedure followed in the *Theoretical Development* chapter can be implemented for any known vibration profile.

It should be noted that the selection of the proper vibration compensation technique and implementing the selected technique in a proper way is highly relevant to the information obtained from the vibrating platform.

In this thesis study, air platforms are taken into consideration as the vibrating platform. The sources of vibration encountered in those platforms can be listed as follows [31]:

- For both commercial and military aircrafts and helicopters;
  - Propulsion system,
  - Aerodynamic flow noise,
  - Landing impact.
- For military aircrafts and helicopters;
  - Gunfire.
- For carrier based military aircrafts only;
  - Catapult take-offs,
  - Arrested Landing.
- For commercial and military helicopters;
  - Main and tail rotors,
  - Drive shafts and gear boxes.

Considering the above list, vibration exposure levels for each case should be well known to define the existing vibration problem properly. In order to obtain such information, it is possible to use the applicable specifications and standards. For instance, for commercial air-platforms, typical vibration, shock and noise levels can be obtained from the manufacturers' specifications; on the other hand, for military air-platforms, military standards such as MIL-E-5400, MIL-E-5272 and MIL-STD-810 can be used as reference.

In this thesis study, military standard MIL-STD-810-F [32] is taken into consideration. In this standard, except from other laboratory test methods, a section on vibration testing is given in detail. In MIL-STD-810-F [32], the test plan including the information of vibration level and test duration can be easily defined by selecting the proper vibrating platform from the Table 1.3 below.

Table 1.3 Vibration Environment Categories [32]

Life Phase	Platform	Category	Material Description	Level & Duration Annex A	Test 1/
Manufacture / Maintenance	Plant Facility/ Maintenance Facility	1.Manufacture / Maintenance processes	Material/assembly/part	2.1.1	2/
		2.Shipping,handling	Material/assembly/part	2.1.2	2/
		3.ESS	Material/assembly/part	2.1.3	3/
Transportation	Truck/ Trailer/ Tracked	4.Restrained Cargo	Material as restrained cargo	2.2.1	I
		5.Loose Cargo	Material as loose cargo	2.2.2	II
		6.Large Assembly Cargo	Large assemblies, shelters, van and trailer units	2.2.3	III
	Aircraft	7.Jet	Material as cargo	2.2.4	I
		8.Propeller	Material as cargo	2.2.5	I
		9.Helicopter	Material as cargo	2.2.6	I
	Ship	10.Surface Ship	Material as cargo	2.2.7	I
	Railroad	11.Train	Material as cargo	2.2.8	I
Operational	Aircraft	12.Jet	Installed Material	2.3.1	I
		13.Propeller	Installed Material	2.3.2	I
		14.Helicopter	Installed Material	2.3.3	I
	Aircraft Stores	15.Jet	Assembled stores	2.3.4	IV
		16.Jet	Installed in stores	2.3.5	I
		17.Propeller	Assembled/Installed in stores	2.3.6	IV/I
		18.Helicopter	Assembled/Installed in stores	2.3.7	IV/I
	Missiles	19.Tactical Missiles	Assembled/Installed in missiles (free flight)	2.3.8	IV/I
	Ground	20.Ground Vehicles	Installed in wheeled/tracked/trailer	2.3.9	I/III
	Watercraft	21.Marine Vehicles	Installed Material	2.3.10	I
	Engines	22.Turbine Engines	Material Installed on	2.3.11	I
	Personnel	23.Personnel	Material carried by/on personnel	2.3.12	2/
Supplemental	All	24.Minimum Integrity	Installed on Isolators/Life cycle not defined	2.4.1	I
	All Vehicles	25.External Cantilevered	Antennae, airfoils, masts, etc.	2.4.2	2/

Although the thesis study concentrates on the air-platforms, it is also possible to investigate the responses for other platforms used in marine and vehicular applications. For these types of vibrating platforms, the information given in can as well be used.

As observed in MIL-STD-810-F [32], the aerial platforms are grouped as follows:

- Jet Aircraft,
- Propeller Aircraft,
- Helicopter.

The vibration level for each platform is well defined and given in Figure 1.4, Figure 1.5 and Figure 1.6, respectively.

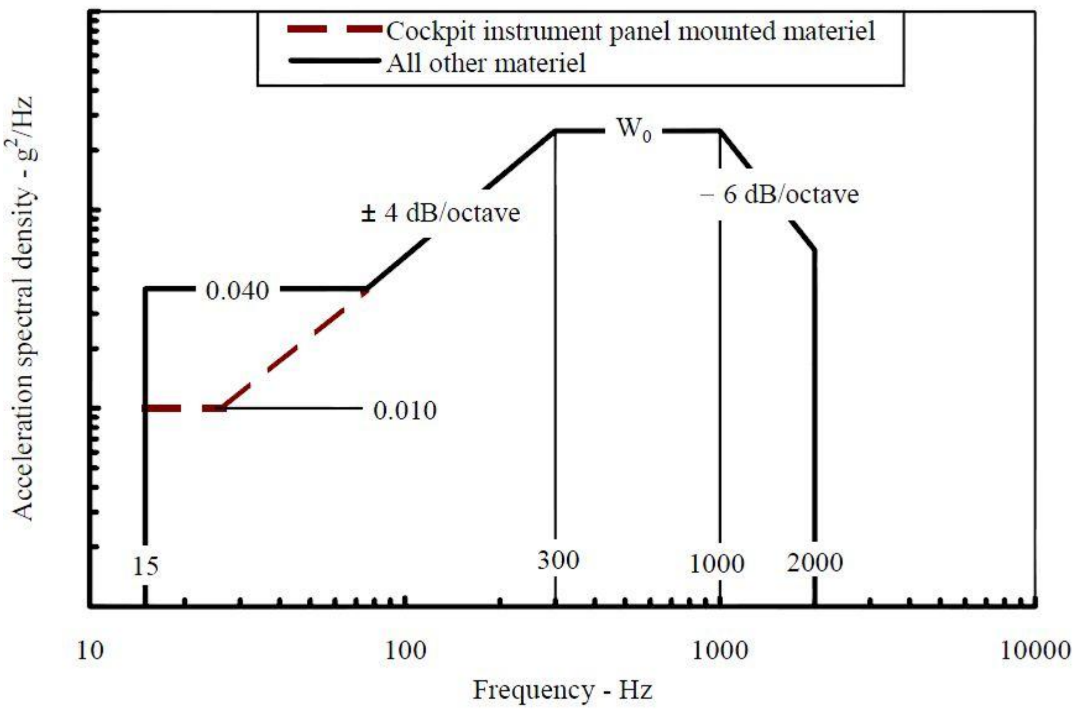

Figure 1.4 Jet Aircraft Vibration Exposure [32]

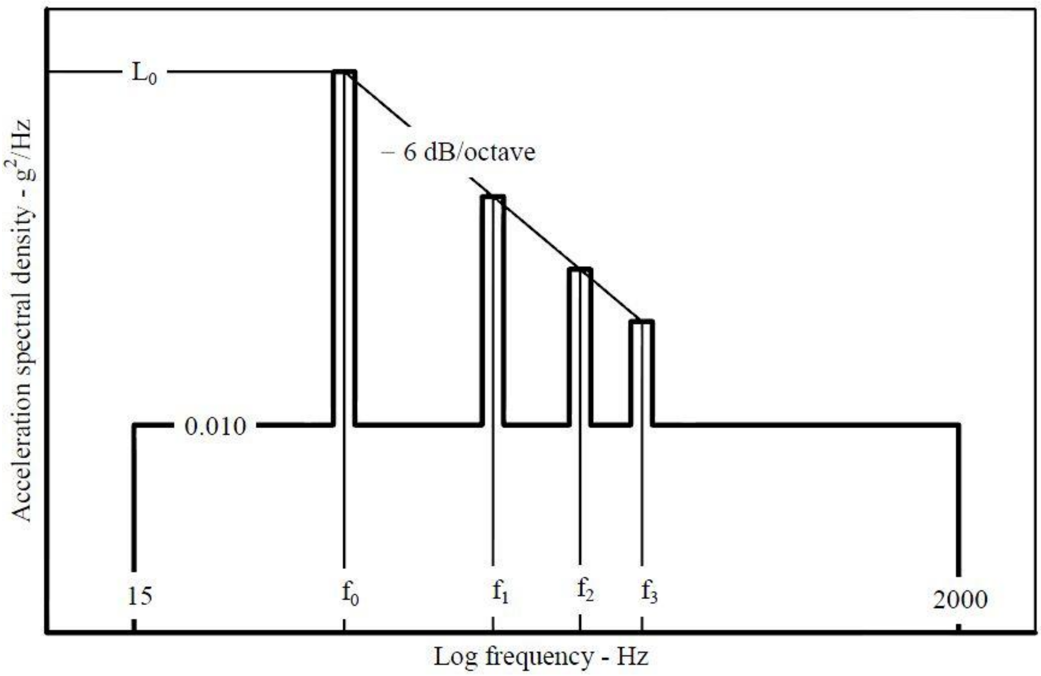

Figure 1.5 Propeller Aircraft Vibration Exposure [32]

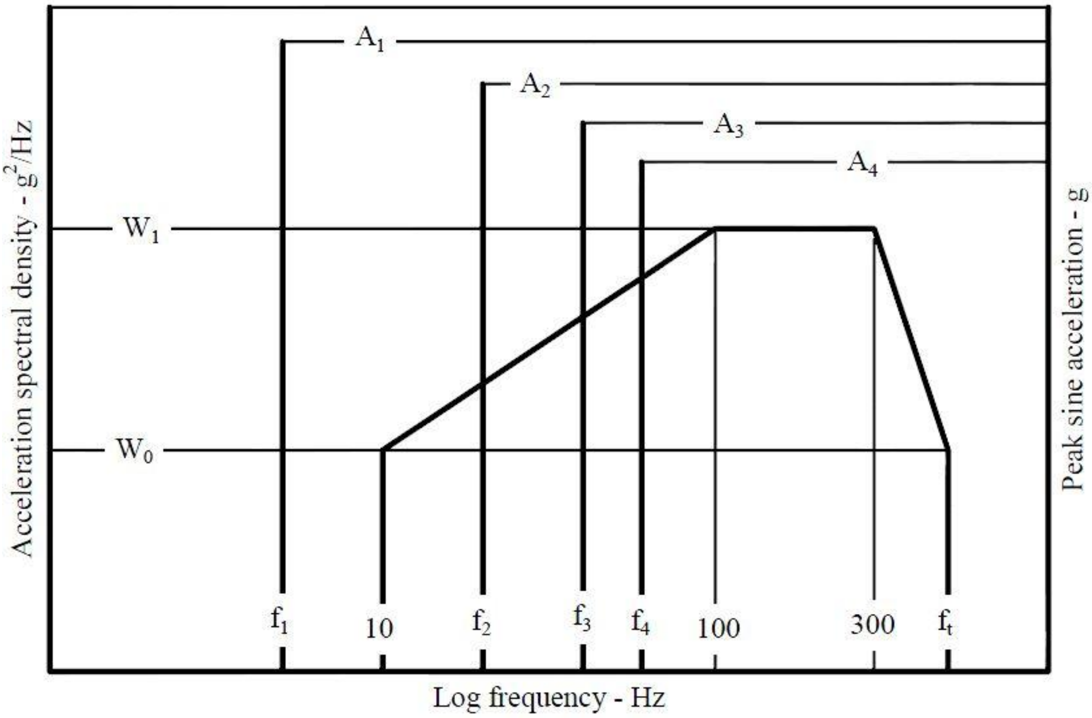

Figure 1.6 Helicopter Vibration Exposure [32]

If the figures are investigated, for jet aircraft vibration exposure, the acceleration PSD amplitude value W_0; for propeller aircraft vibration exposure, the acceleration PSD amplitude value L_0 and the frequency values f_0, f_1, f_2 and f_3; for helicopter vibration exposure, the acceleration PSD amplitude values W_0, W_1 and harmonic acceleration amplitudes A_1, A_2, A_3 and A_4, and the frequency values f_1, f_2, f_3, f_4 and f_t are all defined in the relevant tables in MIL-STD-810-F [32]. In the *Case Studies* chapter, the values for those parameters will be obtained for the selected vibrating air platform.

If the profiles given on the figures are taken into consideration, it can be stated that the jet aircraft is exposed to only random vibration over a wide frequency band. On the other hand, for propeller aircraft and helicopter platforms, both random and harmonic vibration exposure is encountered. Although the random and harmonic vibration profiles are given separately for helicopter platform, the harmonic vibration information is superimposed on pink noise random vibration for propeller aircraft.

It should also be noted that the sources of random vibration is aerodynamic flow noise; on the other hand, the sources of harmonic vibration are the engine, main rotor (plus tail rotor if available), drive shaft and the gear boxes. Vibration sources of a helicopter platform demonstrated in Figure 1.7.

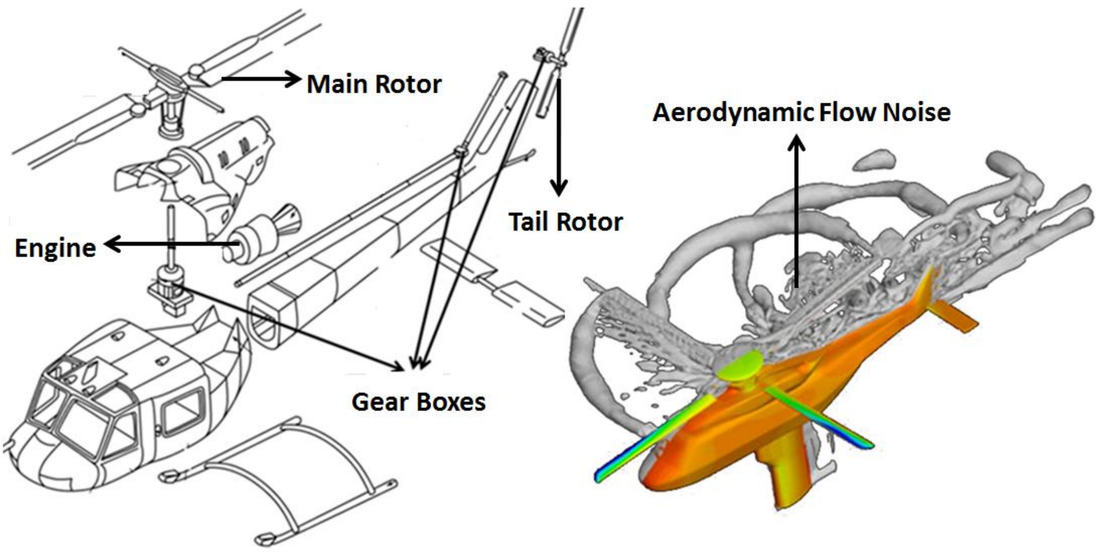

Figure 1.7 Harmonic and Random Vibration Sources on Helicopter Platform [33]

CHAPTER 2

THEORETICAL DEVELOPMENT

2.1. Introduction

In this section detailed information on isolator and isolation system modeling is presented. Converting the equations of motion into matrix form, system matrices such as mass and stiffness matrices as well as the forcing vector are obtained. Getting the required system matrices in addition to the forcing vectors, analysis of the vibration isolation system is presented. In this chapter, the parameters used for Monte Carlo simulations in addition to isolation system optimization processes are also listed in detail. Finally, possible scenarios that are all available within the scope of the presented thesis study are mentioned and tabulated briefly.

2.2. Isolator Modeling

In this thesis study, since it is usually reasonable to assume constant parameters and linear relationships [34] in derivation of a simple mathematical model to represent the dynamics of the mechanical structure, the isolators are assumed to have linear stiffness and structural damping characteristics. Similar with Tao’s study [35], the isolators used in this paper are of a rubber bonded to metal or elastomeric isolators. For these types of mounts, complex spring stiffness is used to model the dynamic behavior as given in Eq. (1).

As mentioned before, the elastomer mounts can be modeled using 3 linear simple spring elements which are mutually orthogonal to each other. The springs are assumed to be massless and modeled with constant stiffness coefficient and a constant loss factor (i.e. hysteretic damping coefficient). The elastomer mounts are not restricted to be mounted orthogonal to the global reference frame used to represent the vibrational response of the 6 DOF rigid body. This global reference frame is generally located at the mass center. Isolators may be located in any point on the rigid body and in any orientation of choice w.r.t. the global reference frame as shown in Figure 2.1.

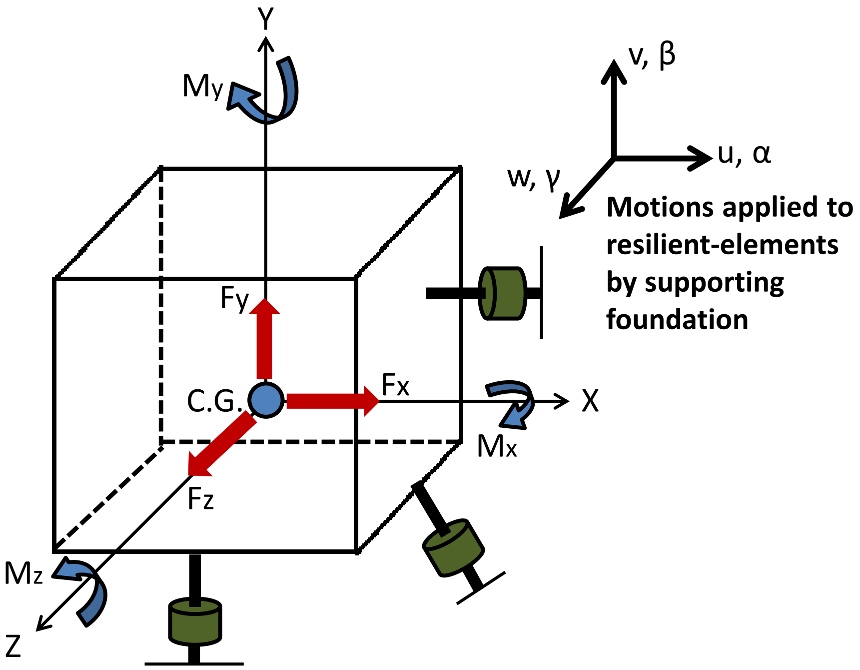

Figure 2.1 Representative 6-DOF Vibration Isolation System

The principal elastic axis of the elastomer mounts may be designated by P, Q and R [30]. The global reference frame and the principal elastic axis are shown in Figure 2.2.

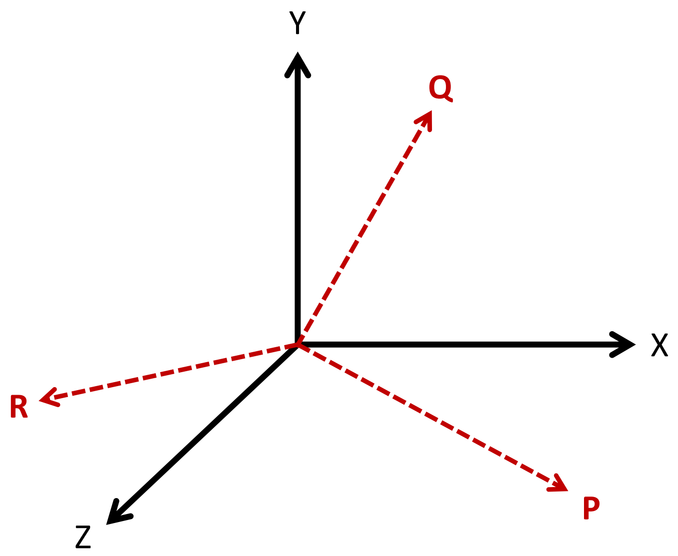

Figure 2.2 Global Reference Frame and Principal Elastic Axis

If the stiffness coefficients along those principal elastic axis are defined as k_p , k_q and k_r, then the stiffness values in global reference frame for the isolators mounted orthogonal to this frame can be obtained as follow [30]:

$$k_{xx} = k_p \ , \tag{2}$$

$$k_{yy} = k_q \ , \tag{3}$$

$$k_{zz} = k_r \ , \tag{4}$$

where k_{xx} , k_{yy} and k_{zz} are the proper translational stiffness coefficients.

However, if the isolators are mounted inclined with respect to the global reference frame as shown in Figure 2.2, then the stiffness values defined with respect to global coordinates, X, Y and Z can be formulized as follows [36]:

$$k_{xx} = k_p\lambda_{xp}^2 + k_q\lambda_{xq}^2 + k_r\lambda_{xr}^2 \ , \tag{5}$$

$$k_{yy} = k_p\lambda_{yp}^2 + k_q\lambda_{yq}^2 + k_r\lambda_{yr}^2 \ , \tag{6}$$

$$k_{zz} = k_p\lambda_{zp}^2 + k_q\lambda_{zq}^2 + k_r\lambda_{zr}^2 \ , \tag{7}$$

$$k_{xy} = k_p\lambda_{xp}\lambda_{yp} + k_q\lambda_{xq}\lambda_{yq} + k_r\lambda_{xr}\lambda_{yr} \ , \tag{8}$$

$$k_{xz} = k_p\lambda_{xp}\lambda_{zp} + k_q\lambda_{xq}\lambda_{zq} + k_r\lambda_{xr}\lambda_{zr} \ , \tag{9}$$

$$k_{yz} = k_p\lambda_{yp}\lambda_{zp} + k_q\lambda_{yq}\lambda_{zq} + k_r\lambda_{yr}\lambda_{zr} \ , \tag{10}$$

where k_{xy} , k_{xz} , k_{yz} are the cross translational stiffness coefficients; λ_{xp} , λ_{xq} , λ_{xr} are the cosines of the angles between X axis and the principal elastic axes; λ_{yp} , λ_{yq} , λ_{yr} are the cosines of the angles between Y axis and the principal elastic axes; λ_{zp} , λ_{zq} and λ_{zr} are the cosines of the angles between Z Axis and the principal elastic axes.

Finally, it should also be stated that the angular stiffness of the isolators is neglected within the scope of the thesis study, in the characteristics of elastomeric type of vibration isolators since their torsional resistance is negligible compared to the resistive moments created by the linear forces transmitted through the isolators [36].

2.3. Modeling of Isolation System

In this thesis study, the isolated structure is assumed to be a rigid body with 6 degrees of freedom (DOF), comprised of 3 translational and 3 rotational displacements. As shown in Figure 2.1, the structure modeled as a rigid body is suspended on resilient members (vibration isolators) which are connected to the supporting foundation. The point of attachment of each resilient member is positioned at distances of a_x, a_y and a_z with respect to the global reference frame located at mass center.

Equations of motion for this 6 DOF vibration isolation system model can be obtained easily and also given in literature [30] as follows:

$$m\ddot{x} + \sum k_{xx}(x-u) + \sum k_{xy}(y-v) + \sum k_{xz}(z-w) + \sum\left(k_{xz}a_y - k_{xy}a_z\right)(\alpha - \boldsymbol{\alpha}) + \sum(k_{xx}a_z - k_{xz}a_x)(\beta - \boldsymbol{\beta}) + \sum\left(k_{xy}a_x - k_{xx}a_y\right)(\gamma - \boldsymbol{\gamma}) = F_x, \tag{11}$$

$$m\ddot{y} + \sum k_{xy}(x-u) + \sum k_{yy}(y-v) + \sum k_{yz}(z-w) + \sum\left(k_{yz}a_y - k_{yy}a_z\right)(\alpha - \boldsymbol{\alpha}) + \sum\left(k_{xy}a_z - k_{yz}a_x\right)(\beta - \boldsymbol{\beta}) + \sum\left(k_{yy}a_x - k_{xy}a_y\right)(\gamma - \boldsymbol{\gamma}) = F_y, \tag{12}$$

$$m\ddot{z} + \sum k_{xz}(x-u) + \sum k_{yz}(y-v) + \sum k_{zz}(z-w) + \sum\left(k_{zz}a_y - k_{yz}a_z\right)(\alpha - \boldsymbol{\alpha}) + \sum(k_{xz}a_z - k_{zz}a_x)(\beta - \boldsymbol{\beta}) + \sum\left(k_{yz}a_x - k_{xz}a_y\right)(\gamma - \boldsymbol{\gamma}) = F_z, \tag{13}$$

$$I_{xx}\ddot{\alpha} - I_{xy}\ddot{\beta} - I_{xz}\ddot{\gamma} + \sum\left(k_{xz}a_y - k_{xy}a_z\right)(x-u) + \sum\left(k_{yz}a_y - k_{yy}a_z\right)(y-v) + \sum\left(k_{zz}a_y - k_{yz}a_z\right)(z-w) + \sum\left(k_{yy}a_z^2 + k_{zz}a_y^2 - 2k_{yz}a_y a_z\right)(\alpha - \boldsymbol{\alpha}) + \sum\left(k_{xz}a_y a_z + k_{yz}a_x a_z - k_{zz}a_x a_y - k_{xy}a_z^2\right)(\beta - \boldsymbol{\beta}) + \sum\left(k_{xy}a_y a_z + k_{yz}a_x a_y - k_{yy}a_x a_z - k_{xz}a_y^2\right)(\gamma - \boldsymbol{\gamma}) = M_x, \tag{14}$$

$$I_{yy}\ddot{\beta} - I_{xy}\ddot{\alpha} - I_{yz}\ddot{\gamma} + \sum(k_{xx}a_z - k_{xz}a_x)(x-u) + \sum\left(k_{xy}a_z - k_{yz}a_x\right)(y-v) + \sum(k_{xz}a_z - k_{zz}a_x)(z-w) + \sum\left(k_{xz}a_y a_z + k_{yz}a_x a_z - k_{zz}a_x a_y - k_{xy}a_z^2\right)(\alpha - \boldsymbol{\alpha}) + \sum(k_{xx}a_z^2 + k_{zz}a_x^2 - 2k_{xz}a_x a_z)(\beta - \boldsymbol{\beta}) + \sum\left(k_{xy}a_x a_z + k_{xz}a_x a_y - k_{xx}a_y a_z - k_{yz}a_x^2\right)(\gamma - \boldsymbol{\gamma}) = M_y, \tag{15}$$

$$I_{zz}\ddot{\gamma} - I_{xz}\ddot{\alpha} - I_{yz}\ddot{\beta} + \sum\left(k_{xy}a_x - k_{xx}a_y\right)(x-u) + \sum\left(k_{yy}a_x - k_{xy}a_y\right)(y-v) + \sum\left(k_{yz}a_x - k_{xz}a_y\right)(z-w) + \sum\left(k_{xy}a_y a_z + k_{yz}a_x a_y - k_{yy}a_x a_z - k_{xz}a_y^2\right)(\alpha - \boldsymbol{\alpha}) + \sum\left(k_{xy}a_x a_z + k_{xz}a_x a_y - k_{xx}a_y a_z - k_{yz}a_x^2\right)(\beta - \boldsymbol{\beta}) + \sum\left(k_{xx}a_y^2 + k_{yy}a_x^2 - 2k_{xz}a_x a_y\right)(\gamma - \boldsymbol{\gamma}) = M_z, \tag{16}$$

where m is the mass of the rigid body; I_{xx}, I_{yy}, I_{zz}, I_{xy}, I_{xz} and I_{yz} are the moments of inertia and products of inertia with respect to global reference frame; x, y, z are the translational responses of the mass center about X, Y and Z axes; α, β and γ are the rotational responses of the mass center around X, Y and Z axes; a_x, a_y and a_z are the distances of the point of the elastomer mount with respect to the global reference frame; u, v and w are the translational displacement of the foundation in X, Y and Z directions; $\boldsymbol{\alpha}$, $\boldsymbol{\beta}$ and $\boldsymbol{\gamma}$ are rotational displacement of the foundation about X, Y and Z axes; F_x, F_y and F_z are the forces, M_x, M_y and M_z are the moments applied directly to the rigid body.

The above six equations are derived from force and moment equilibrium equations which describe a 6 DOF model completely. Investigating the equations, the system dynamics is dependent on the mass of the rigid body, the moments of inertia with the products of inertia, the proper and cross translational stiffness constants, the location of the isolators and the input forcing and moments acting on the rigid body, and the displacement amplitudes of the foundation. In this thesis study, the forces and the moments are assumed to be zero; hence, the excitation on the rigid body is due to the motion of the foundation only. Additionally, it should also be noted that the rotational displacement of the foundation about X, Y and Z axes are assumed to be zero ($\boldsymbol{\alpha} = \boldsymbol{\beta} = \boldsymbol{\gamma} = 0$). In other words, the excitation of the foundation is dependent only on translational displacements in X, Y and Z directions.

Using the equations of motion and assuming isolators are modeled using stiffness coefficient and a loss factor, a general equation of motion in matrix form can be obtained as follows.

$$[M]\{\ddot{q}\} + i\,\eta[K]\{q\} + [K]\{q\} = \{F\}, \tag{17}$$

where $[M]$ and $[K]$ are 6x6 mass and stiffness matrices, $\{F\}$ is a 6x1 forcing vector, $\{q^T\} = \{x \quad y \quad z \quad \alpha \quad \beta \quad \gamma\}$ is a 6x1 response vector defined at the mass center. In this matrix form, the structural damping is proportional to stiffness matrix by a factor of loss factor, η.

Here, it is possible to expand the system matrices and forcing vector as follows

$$[M] = \begin{bmatrix} m & 0 & 0 & 0 & 0 & 0 \\ 0 & m & 0 & 0 & 0 & 0 \\ 0 & 0 & m & 0 & 0 & 0 \\ 0 & 0 & 0 & I_{xx} & -I_{xy} & -I_{xz} \\ 0 & 0 & 0 & -I_{xy} & I_{yy} & -I_{yz} \\ 0 & 0 & 0 & -I_{xz} & -I_{yz} & I_{zz} \end{bmatrix}. \tag{18}$$

As seen in Eq. (18), mass matrix includes the parameters which depend on the isolated equipment's physical properties such as mass and moments of inertia and products of inertia with respect to the reference frame at the mass center.

$$[K] = \begin{bmatrix} K_{11} & K_{12} & K_{13} & K_{14} & K_{15} & K_{16} \\ K_{21} & K_{22} & K_{23} & K_{24} & K_{25} & K_{26} \\ K_{31} & K_{32} & K_{33} & K_{34} & K_{35} & K_{36} \\ K_{41} & K_{42} & K_{43} & K_{44} & K_{45} & K_{46} \\ K_{51} & K_{52} & K_{53} & K_{54} & K_{55} & K_{56} \\ K_{61} & K_{62} & K_{63} & K_{64} & K_{54} & K_{66} \end{bmatrix}, \tag{19}$$

where,

$$K_{11} = \sum k_{xx}\,, \tag{20}$$

$$K_{12} = K_{21} = \sum k_{xy}\,, \tag{21}$$

$$K_{13} = K_{31} = \sum k_{xz} , \tag{22}$$

$$K_{14} = K_{41} = \sum k_{xz}a_y - k_{xy}a_z , \tag{23}$$

$$K_{15} = K_{51} = \sum k_{xx}a_z - k_{xz}a_x , \tag{24}$$

$$K_{16} = K_{61} = \sum k_{xy}a_x - k_{xx}a_y , \tag{25}$$

$$K_{22} = \sum k_{yy} , \tag{26}$$

$$K_{23} = K_{32} = \sum k_{yz} , \tag{27}$$

$$K_{24} = K_{42} = \sum k_{yz}a_y - k_{yy}a_z , \tag{28}$$

$$K_{25} = K_{52} = \sum k_{xy}a_z - k_{yz}a_x , \tag{29}$$

$$K_{26} = K_{62} = \sum k_{yy}a_x - k_{xy}a_y , \tag{30}$$

$$K_{33} = \sum k_{zz} , \tag{31}$$

$$K_{34} = K_{43} = \sum k_{zz}a_y - k_{yz}a_z , \tag{32}$$

$$K_{35} = K_{53} = \sum k_{xz}a_z - k_{zz}a_x , \tag{33}$$

$$K_{36} = K_{63} = \sum k_{yz}a_x - k_{xz}a_y , \tag{34}$$

$$K_{44} = \sum k_{yy}a_z^2 + k_{zz}a_y^2 - 2k_{yz}a_y a_z , \tag{35}$$

$$K_{45} = K_{54} = \sum k_{xz}a_y a_z + k_{yz}a_x a_z - k_{zz}a_x a_y - k_{xy}a_z^2 , \tag{36}$$

$$K_{46} = K_{64} = \sum k_{xy}a_y a_z + k_{yz}a_x a_y - k_{yy}a_x a_z - k_{xz}a_y^2 , \tag{37}$$

$$K_{55} = \sum k_{xx}a_z^2 + k_{zz}a_x^2 - 2k_{xz}a_x a_z , \tag{38}$$

$$K_{56} = K_{65} = \sum k_{xy}a_x a_z + k_{xz}a_x a_y - k_{xx}a_y a_z - k_{yz}a_x^2 , \tag{39}$$

$$K_{66} = \sum k_{xx}a_y^2 + k_{yy}a_x^2 - 2k_{xy}a_x a_y \,. \tag{40}$$

As seen from the equations, the stiffness matrix includes the coefficients of stiffness of each isolator; in addition to the distances between the isolators and the reference axis. Here, it should also be noted that the isolator stiffness values used in stiffness matrix are assumed to be the same for both static and dynamic cases in this thesis.

$$\{F\} = \begin{Bmatrix} F_1(t) \\ F_2(t) \\ F_3(t) \\ F_4(t) \\ F_5(t) \\ F_6(t) \end{Bmatrix}, \tag{41}$$

where,

$$F_1(t) = (\sum k_{xx} + i\,\eta\, k_{xx})u(t) + (\sum k_{xy} + i\,\eta\, k_{xy})v(t) + (\sum k_{xz} + i\,\eta\, k_{xz})w(t), \tag{42}$$

$$F_2(t) = (\sum k_{yy} + i\,\eta\, k_{yy})v(t) + (\sum k_{xy} + i\,\eta\, k_{xy})u(t) + (\sum k_{yz} + i\,\eta\, k_{yz})w(t), \tag{43}$$

$$F_3(t) = (\sum k_{zz} + i\,\eta\, k_{zz})w(t) + (\sum k_{xz} + i\,\eta\, k_{xz})u(t) + (\sum k_{yz} + i\,\eta\, k_{yz})v(t), \tag{44}$$

$$\begin{gathered} F_4(t) = -(\sum k_{yy}a_z + i\,\eta\, k_{yy}a_z)v(t) + (\sum k_{zz}a_y + i\,\eta\, k_{zz}a_y)w(t) + \\ (\sum k_{xz}a_y + i\,\eta\, k_{xz}a_y)u(t) - (\sum k_{xy}a_z + i\,\eta\, k_{xy}a_z)u(t) + (\sum k_{yz}a_y + \\ i\,\eta\, k_{yz}a_y)v(t) - (\sum k_{xz}a_z + i\,\eta\, k_{xz}a_z)w(t), \end{gathered} \tag{45}$$

$$\begin{gathered} F_5(t) = (\sum k_{xx}a_z + i\,\eta\, k_{xx}a_z)u(t) - (\sum k_{zz}a_x + i\,\eta\, k_{zz}a_x)w(t) - (\sum k_{xz}a_x + \\ i\,\eta\, k_{xz}a_x)u(t) + (\sum k_{xy}a_z + i\,\eta\, k_{xy}a_z)v(t) - (\sum k_{yz}a_x + i\,\eta\, k_{yz}a_x)v(t) + \\ (\sum k_{xz}a_z + i\,\eta\, k_{xz}a_z)w(t), \end{gathered} \tag{46}$$

$$\begin{gathered} F_6(t) = -(\sum k_{xx}a_y + i\,\eta\, k_{xx}a_y)u(t) + (\sum k_{yy}a_x + i\,\eta\, k_{yy}a_x)v(t) - \\ (\sum k_{xy}a_x + i\,\eta\, k_{xy}a_x)u(t) - (\sum k_{xy}a_y + i\,\eta\, k_{xy}a_y)v(t) + (\sum k_{yz}a_x + \\ i\,\eta\, k_{yz}a_x)w(t) - (\sum k_{xz}a_y + i\,\eta\, k_{xz}a_y)w(t). \end{gathered} \tag{47}$$

Similarly, from Eqs. (42) to (47), the forcing vector includes coefficient of stiffness and loss factor of the isolators; in addition to the distances between the isolators and mass center along X, Y and Z directions. Differently, the terms u, v and w

identifying the motion applied to resilient elements by supporting foundation are also present in the forcing vector.

2.4. Analysis

Having obtained the system matrices and forcing vector, it is possible to perform a variety of analysis such as modal analysis, static deflection analysis, response analysis for harmonic and random type of inputs. Those analysis are detailed separately in the following sections.

2.4.1. Modal Analysis

Knowing the mass and stiffness matrices, it is possible to calculate natural frequencies for all modes. The designer needs to know those values in order to compare them with the excitation frequencies. If possible, stiffness values of the isolators are selected in such a way that excitation frequencies and the natural frequencies do not coincide. Additionally, monitoring the values obtained for the first natural frequency gives an idea about the system whether it is stable or not. This monitoring action is also considered in the optimization part as a design constraint.

In modal analysis, the natural frequencies are calculated for the undamped free vibration case where foundation is assumed to be fixed. Therefore, the general equation of motion is revised as follows

$$[M]\{\ddot{q}\} + [K]\{q\} = \{0\}. \tag{48}$$

If it is assumed that $\{q\} = \{U\}e^{i\omega t}$, then the eigenvalue problem can be obtained as follows

$$[K]\{U\} = \omega^2[M]\{U\}. \tag{49}$$

In order to calculate the eigenvalues, in other words, the natural frequencies the eigenvalue problem defined by Eq. (49) should be solved which results in

$$\det([K] - \omega^2[M]) = 0. \tag{50}$$

In the software developed for vibration isolation analysis and optimization, MATLAB function *eig (*$[K]$, $[M]$*)* is used in order to solve for the eigenvalues.

2.4.2. Static Deflection Analysis

Stiffness characteristics of isolators for an isolation system not only change the dynamic behavior of the structure but also determine the static load carrying capacity of the mechanical system. Using manufacturers' catalogs [37][38], static load carrying capacity values may be available for an off-the shelf isolator. In vibration isolation design, the designer should check the static deflection value for all isolators. In order to compute those deflection values, the stiffness matrix, $[K]$, total mass of the mechanical structure, the direction and amplitude of the gravitational acceleration and the exact location information for the isolators should as well be known. Similar with the previous analysis, monitoring for the static deflection of isolators in each axis is also encountered in optimization software as a design constraint.

The vector used for static deflection at mass center can be obtained as

$$\{q\}_{static} = [K]^{-1}\{F\}_{static}, \tag{51}$$

where $\{F\}_{static}$ is 6x1 static forcing vector consisting of the total mass of the rigid body in addition to the gravitational acceleration amplitude and direction information. For instance, if the total mass of the rigid body is m and the amplitude of gravitational acceleration is g and it is in –Y direction, then the static forcing vector is defined as $\{F\}_{static}^{T} = \{0 \quad -mg \quad 0 \quad 0 \quad 0 \quad 0\}$.

Using the static deflection vector found for mass center from Eq. (51), it is also possible to obtain the deflection values at isolator locations as follows

$$\{q\}_{static,isolator} = [R]_{static}\{P\}_{isolator} - \{P\}_{isolator} + \{q\}_{static,trans}, \tag{52}$$

where $\{q\}_{static,isolator}$ is the 3x1 static deflection vector of the isolator of interest; $\{P\}_{isolator}$ is the 3x1 position vector of the isolator of interest with respect to mass center in global coordinate frame; $[R]_{static}$ is the 3x3 three dimensional static rotational matrix from principal elastic axis to global coordinate frame and

$\{q\}_{static,trans}$ is 3x1 translational static deflection vector at mass center in global coordinate frame.

If noticed, the translational static deflection vector at mass center is obtained from Eq. (51). Here, only the first three components of $\{q\}_{static}$ is used for $\{q\}_{static,trans}$. On the other hand, the three dimensional static rotational matrix can be computed as follows.

$$[R]_{static} = \begin{bmatrix} 1 & 0 & 0 \\ 0 & \cos(\alpha) & -\sin(\alpha) \\ 0 & \sin(\alpha) & \cos(\alpha) \end{bmatrix} \begin{bmatrix} \cos(\beta) & 0 & \sin(\beta) \\ 0 & 1 & 0 \\ -\sin(\beta) & 0 & \cos(\beta) \end{bmatrix} \begin{bmatrix} \cos(\gamma) & -\sin(\gamma) & 0 \\ \sin(\gamma) & \cos(\gamma) & 0 \\ 0 & 0 & 1 \end{bmatrix}, \qquad (53)$$

where the variables α, β and γ are obtained from the last three components of the static deflection vector at mass center found in Eq. (51).

2.4.3. Response Analysis

The main purpose of a vibration isolation system is to decrease the response level of the mechanical structure mounted on a vibrating platform (i.e. foundation). Knowing mass and stiffness matrices, $[M]$ and $[K]$, loss factor and the location information of the point of interest, it is possible to compute the response function with respect to frequency of any point on the rigid body. Moreover, these values obtained from response analysis then can be used in the objective function defined in the optimization algorithm.

As mentioned before, for response analysis, the knowledge of the input vibration profile is critical. In the following sections, procedures for harmonic and random types of excitations are presented. Additionally, the transmissibility functions defined in physical and modal domain are also considered beneficial to be shared.

2.4.3.1. Harmonic Type of Excitation

Harmonic response of a system is as follows

$$\{q\} = \begin{Bmatrix} x \\ y \\ z \\ \alpha \\ \beta \\ \gamma \end{Bmatrix} = [\alpha]\{F\}, \tag{54}$$

where $\{x \quad y \quad z \quad \alpha \quad \beta \quad \gamma\}^T$ are the components of the response vector at mass center; $[\alpha]$ is the 6x6 receptance matrix and $\{F\}$ is the 6x1 forcing vector. If the corresponding equations are investigated, it is observed that the forcing vector is dependent on the stiffness of the isolators, loss factor, and location information in addition to the displacement amplitude of the input harmonic vibration occurring in defined directions. For small sized systems, receptance matrix can be obtained as

$$[\alpha] = (-\omega^2[M] + [K] + i\,\eta[K]\,)^{-1}. \tag{55}$$

The response vector found in Eq. (54) is for the mass center. Similar with the case mentioned in static analysis section, by using 3 dimensional dynamic rotational matrix, it is possible to obtain response vector of any point on the rigid body. Here, response vector on any point, $\{q\}_P$ located on the mechanical structure can be computed as

$$\{q\}_P = [R]\{P\} - \{P\} + \{q\}_{trans}, \tag{56}$$

where $[R]$ is the 3x3 three dimensional rotational matrix from principal elastic axis to global coordinate frame, $\{P\}$ is the 3x1 position vector of the point of interest and $\{q\}_{trans}$ is the 3x1 translational response vector of the mass center consisting of the first three components of the response vector in global coordinate frame. On the other hand, the three dimensional rotational matrix can be obtained as follows

$$[R] = \begin{bmatrix} 1 & 0 & 0 \\ 0 & \cos(\alpha) & -\sin(\alpha) \\ 0 & \sin(\alpha) & \cos(\alpha) \end{bmatrix} \begin{bmatrix} \cos(\beta) & 0 & \sin(\beta) \\ 0 & 1 & 0 \\ -\sin(\beta) & 0 & \cos(\beta) \end{bmatrix} \begin{bmatrix} \cos(\gamma) & -\sin(\gamma) & 0 \\ \sin(\gamma) & \cos(\gamma) & 0 \\ 0 & 0 & 1 \end{bmatrix}, \tag{57}$$

where the variables α, β and γ are rotation of the rigid body around X, Y and Z axes, respectively.

2.4.3.2. Random Type of Excitation

For random vibration of a multi-degree of freedom system, which can be excited in three translational directions simultaneously, response of the mass center can only be obtained by coordinate transformation. In physical domain, the power spectral density (PSD) function for the displacement is defined as follows.

$$[S_q] = \frac{\{q\}\,\{q\}^{T^*}}{T}, \tag{58}$$

where T is the total measurement period and $\{q\}$ is the response vector in physical domain.

On the other hand, the coordinate transformation between modal and physical domains can be implemented as follows.

$$\{q\} = [\phi]\,\{\eta\}, \tag{59}$$

where $[\phi]$ is the mass normalized mode shape matrix and $\{\eta\}$ is the response vector in modal domain.

Substituting Eq. (59) into Eq. (58), the following equation is obtained

$$[S_q] = \frac{[\phi]\,\{\eta\}\,([\phi]\,\{\eta\})^{T^*}}{T} = \frac{[\phi]\,\{\eta\}\,\{\eta\}^{T^*}\,[\phi]^{T^*}}{T}. \tag{60}$$

Similar to Eq. (58), power spectral density (PSD) function for the displacement in modal domain can be defined as follows

$$[S_\eta] = \frac{\{\eta\}\,\{\eta\}^{T^*}}{T}. \tag{61}$$

Substituting Eq. (61) into Eq. (60), the relationship between power spectral density (PSD) in modal and physical domains is obtained as

$$[S_q] = [\phi]\,[S_\eta]\,[\phi]^{T^*}. \tag{62}$$

Similarly,

$$[S_\eta] = [\phi]^{-1}\,[S_q][\,\phi^{T^*}]^{-1}. \tag{63}$$

In modal domain, system response can be calculated as follows:

$$[S_{\eta_{out}}] = [\bar{T}]\,[S_{\eta_{in}}]\,[\bar{T}]^{T^*}, \tag{64}$$

where $[S_{\eta_{in}}]$ is the input PSD function for modal displacements, on the other hand $[S_{\eta_{out}}]$ is the output PSD function for modal displacements. Additionally, $[\bar{T}]$ is defined as the transmissibility function defined in modal domain and given as

$$[\bar{T}] = [\bar{K}](1 + i\,\lambda)\,[\bar{\alpha}], \tag{65}$$

where $[\bar{K}]$ is the modal stiffness matrix, λ is the loss factor and $[\bar{\alpha}]$ is the diagonal modal receptance matrix. Those matrices are given below; on the other hand, the details on how transmissibility function in modal domain is obtained are presented in the Appendix A.

Modal stiffness matrix $[\bar{K}]$ is defined as follows

$$[\bar{K}] = [\phi]^T[K][\phi] = \begin{bmatrix} \omega_1^2 & \cdots & 0 \\ \vdots & \ddots & \vdots \\ 0 & \cdots & \omega_n^2 \end{bmatrix}, \tag{66}$$

where ω_n is the n^{th} natural frequency of the isolation system.

Additionally, modal receptance matrix, $[\bar{\alpha}]$ can be computed as follows.

$$[\bar{\alpha}] = \left[[\bar{K}] - \omega^2[\bar{M}] + i\,\lambda\,[\bar{K}]\,\right]^{-1}, \tag{67}$$

where $[\bar{M}]$ is the modal mass matrix which is identity matrix

$$[\bar{M}] = [\phi]^T[M][\phi] = [I]. \tag{68}$$

Obtaining the system response PSD in modal domain and substituting it in Eq. (62), it is possible to obtain the response of the mass center as follows;

$$[S_{q_{out}}] = [\phi]\,[S_{\eta_{out}}]\,[\phi]^{T^*}. \tag{69}$$

2.5. Monte Carlo Simulation

The analyses described above, modal, static deflection and response analyses, are used to obtain these results for fixed values of the isolator characteristics. However in real life, isolator stiffness and loss factor, location and mounting angle of the isolators deviate from the theoretically determined and selected values to some extent. Therefore, static and dynamic behaviors of the isolation system also deviate.

In this thesis study, the design parameters that are considered to deviate in Monte Carlo Simulations are listed below:

- Stiffness coefficient of the isolators,
- Loss factor,
- Coordinates of the isolators,
- Angular Orientation of the isolators,
- Position of the point of interest.

Implementing the Monte Carlo simulations, it is possible to observe the deviations in a number of results as follows:

- Natural frequencies,
- Static deflection of all isolators in orthogonal axis,
- PSD of acceleration response of the point of interest in orthogonal directions for the given frequency range,
- PSD of displacement Response of the point of interest in orthogonal directions for the given frequency range,
- Root mean square (RMS) of acceleration response of the point of interest in orthogonal directions,
- RMS of displacement response of the point of interest in orthogonal directions,
- Harmonic amplitude of the acceleration of the point of interest in orthogonal directions for all input excitation frequencies,
- Harmonic amplitude of the displacement of the point of interest in orthogonal directions for all input excitation frequencies.

2.6. Optimization

Optimization of vibration isolation parameters is another main topic of this thesis. It is simply defined as the selection of the best element from a set of available alternatives. When defining an optimization problem, an objective function is defined, optimization parameters are designated and a set of design constraints, equalities or inequalities that the members of the candidates for the designated parameters have to satisfy are specified. In order to implement an optimization process, it is possible to use various types of optimization algorithms. According to the type of the problem and the number of the optimization parameters, the algorithm type should be selected properly. By selecting the proper algorithm, the possibility of obtaining the global minimum value for a defined objective function increases. Otherwise, a proposed solution would not be a global minimum, but a local minimum point. Thus, the user could not reach the goal of the existence of optimization processes properly.

Investigating similar studies on vibration isolation system design in literature, it seems reasonable to use a global search algorithm. As mentioned before, a hybrid method involving both global search and gradient-based methods is used in this study. For this type of hybrid method, genetic algorithm and *fmincon* function found in MATLAB Optimization Toolbox are used successively as in the case of Çınarel [22] and Çınarel and Ciğeroğlu [39]. Here, it is aimed to obtain more successful results by using the values of the optimum design parameters obtained from genetic algorithm as the initial guesses for the gradient based optimization. Therefore, optimum values are expected to be calibrated in preferable manner.

In all optimization alternatives for different types of vibration isolation problems, the user is required to set common properties. In general, the flowchart given in Figure 2.3 is followed for the optimization processes. According to this flowchart, before running an optimization process, there are some points to be set. These points can be summarized as common properties of the rigid body and vibration level, objective function and design constraints. Additionally, the type of optimization should be well defined. According to the selected optimization type, the optimization parameters, in addition to the properties of the isolators should be set as input parameters. For the design parameters used in the optimization, limits should be designated properly.

After the optimization settings are adjusted considering the size of the optimization work space, the algorithm is ready to be run.

Details for the points described above are explained in the following sub-sections.

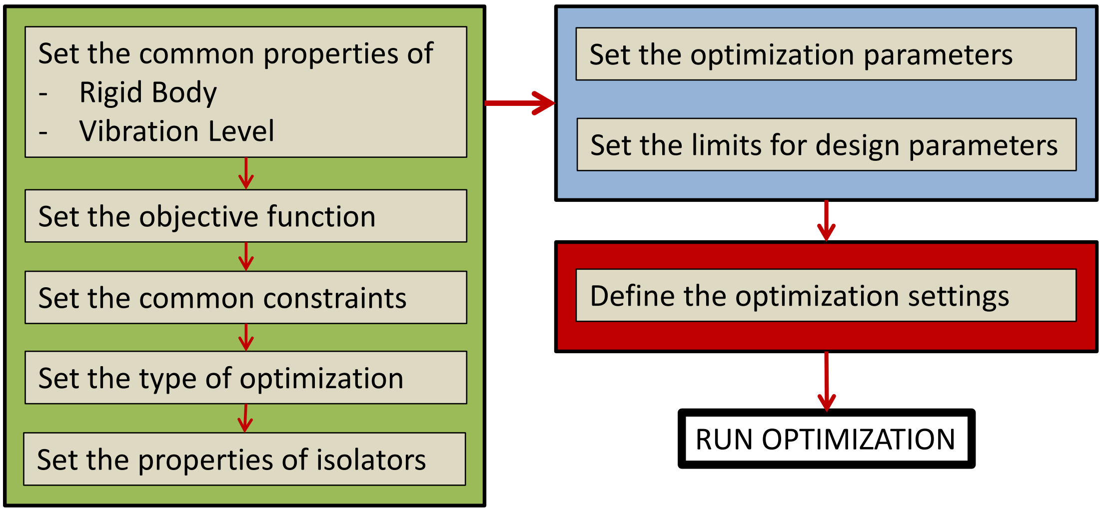

Figure 2.3 Procedure Followed In All Optimization Alternatives

2.6.1. Rigid Body Properties

Here, the rigid body is the mechanical structure that is required to be isolated from unwanted vibration levels. The properties of the rigid body used in the optimization process are listed below.

- Mass of the rigid body in units *kg*,
- Moments of inertia in units kgm^2.

2.6.2. Vibration Level Information

The vibration level can be obtained for any air-platform or a ground vehicle platform. Accordingly, the type of vibration can be either harmonic or random. For harmonic vibration, the amplitudes of vibration at the corresponding excitation frequencies should be well defined. These amplitude values can be in any form such as displacement or acceleration. On the other hand, for random type of vibration, power spectral density (PSD) functions should be defined properly in a specific frequency range. That PSD information can involve either acceleration or displacement power spectral density values with respect to frequency. For both harmonic and random vibration inputs, the direction of excitation should also be assigned. The directions of excitation could be in any three orthogonal directions, X, Y or in Z axes.

2.6.3. Objective Function

Objective function is an important function that should be specified properly in the optimization process. In an optimization process, the algorithm selects the alternative parameters successively in order to minimize the value of that function.

In this study for the selected points of interest with weight factors two types of objective functions are considered:

- Acceleration minimization,
- Displacement minimization.

The formulas for objective functions used in the optimization process are as follow.

$$objective_{acceleration} = \frac{\sum_{j=1}^{n} K_j (a_{x_j} + a_{y_j} + a_{z_j})}{\sum_{j=1}^{n} K_j}, \tag{70}$$

$$objective_{displacement} = \frac{\sum_{j=1}^{n} K_j (q_{x_j} + q_{y_j} + q_{z_j})}{\sum_{j=1}^{n} K_j}. \tag{71}$$

where j represents the point of interest; n is the total number of points of interest; K_j is the weight factor; a_x, a_y and a_z represent response acceleration responses encountered along X, Y and Z axes, respectively; q_x, q_y and q_z represent displacement responses in X, Y and Z directions, respectively.

2.6.4. Design Constraints and Penalty Functions

Assigning values for constraints is also other important issue in the optimization process. The values used as a design constraint for each parameter actually defines the flexibility of the process. In this thesis study, the constraints defined for the parameters are as follows:

- Maximum acceleration response limit for random vibration of the points of interest in addition to the point at C.G. in any translational direction,
- Maximum acceleration response limit for harmonic vibration of the points of interest in addition to the point at C.G. in any translational direction,
- Maximum displacement response limit for random vibration of the points of interest in addition to the point at C.G. in any translational direction,
- Maximum displacement response limit for harmonic vibration of the points of interest in addition to the point at C.G. in any translational direction,
- Maximum deflection limit of isolators due static loading in any translational direction,
- Maximum angular rotation limit of the rigid body due static loading,
- Response PSD envelope defined over a specified frequency range,
- Alignment constraint,
- Stability constraint.

According to the above list, except from the last two constraints, the given parameters are related to the response limits for the given random or harmonic type of excitation and gravitational forcing. However, the alignment and stability constraints are directly related to the undamped characteristics of the isolators in addition to the location and orientation of those elastomer mounts. For those types of constraints, the first natural frequency of the isolation system is monitored. In this thesis study, alignment constraint is used in order not to have a value for the first natural frequency as zero, which corresponds to rigid body rotation. Otherwise, the system stiffness matrix will be singular and the static equilibrium cannot be obtained. Additionally, stability constraint is used in order not to have a loose system mounted on highly soft elastomers.

In the event of exceeding the design constraints, penalty functions are generated and added into the objective function that is aimed to be minimized during optimization process. Hence, the optimum values for design variables are selected in such a way that the constraints are not exceeded. Being aware of the existence of penalty functions, the final objective function can be obtained as follows.

$$objective = objective_{\substack{acceleration \\ or \\ displacement}} + \sum_{i=0}^{9} penalty_i. \tag{72}$$

Here, $objective_{\substack{acceleration \\ or \\ displacement}}$ is defined as in Eqs. (70) and (71). According to the aim of the optimization study, one of the equations is to be selected. On the other hand, $\sum_{i=0}^{9} penalty_i$ is the total penalty function that is added in the final objective function. Here, $penalty_1$ and $penalty_2$ are the penalty functions in case the maximum acceleration response limit is exceeded for random and harmonic type of excitations, respectively; $penalty_3$ and $penalty_4$ are the penalty functions in case the maximum deflection response limit is exceeded for random and harmonic type of excitations, respectively; $penalty_5$ is the penalty function in case the maximum static deflection limit for the isolators is exceeded; $penalty_6$ is the penalty function in case the maximum angular rotation limit of the rigid body is exceeded; $penalty_7$ is the penalty function in case the response PSD acceleration function exceeds the predefined PSD envelope for the given frequency range; $penalty_8$ and $penalty_9$ are the penalty functions in case the alignment and stability constraints are violated, respectively. If there is no violation of the design constraints, those penalty functions are equal to zero separately.

In this thesis study, except from $penalty_7$, other penalty functions are set to a constant value. On the other hand, $penalty_7$ can be considered as gradual penalty function and defined as below.

$$penalty_7 = \sum_{i=1}^{n} \Delta a_i. \tag{73}$$

where Δa is the difference between the response PSD acceleration and the given PSD envelope at the corresponding frequency. Here, Δa is defined only when the amplitude response function exceeds the given PSD envelope. Otherwise, it is zero.

To be clear, a representative response functions regarding and disregarding the given PSD envelope are plotted in Figure 2.4. For acceleration minimization, the optimum design variables are selected in such a way that the system natural frequencies are reduced. However, considering constraint on the PSD envelope as a design constraint, the value of the penalty function is aimed to be minimized by maintaining the amplitude of the response PSD function below the given envelope. Therefore, although the reduced values for the natural frequencies increase, the value of the penalty function reduces in order to minimize the total objective function which can clearly be seen in Figure 2.4.

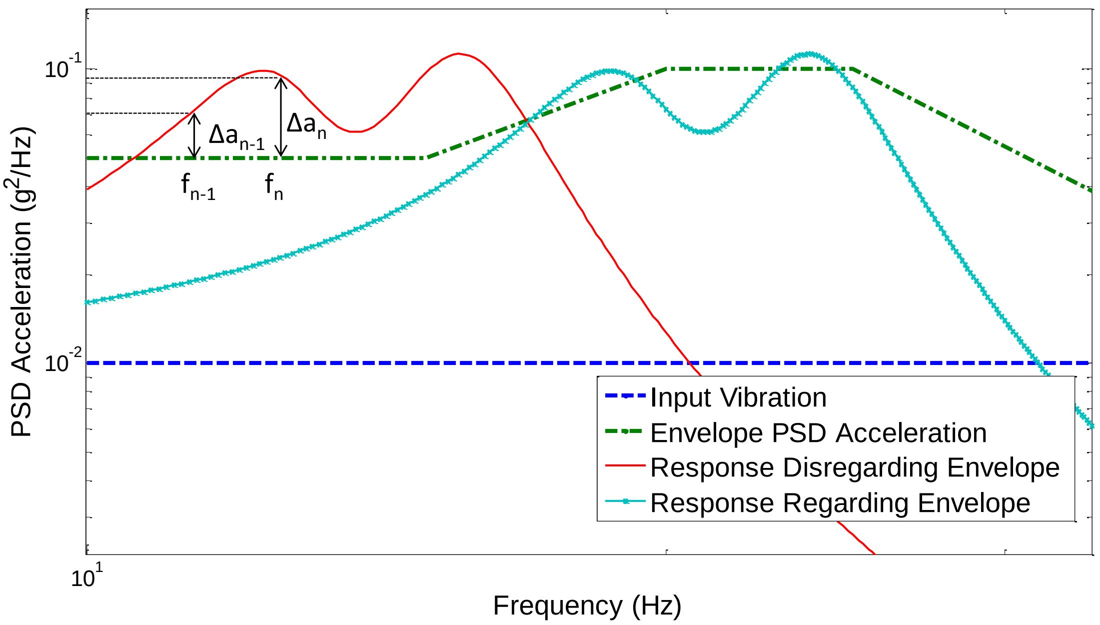

Figure 2.4 Representative Response Functions Disregarding and Regarding PSD Envelope

2.6.5. Type of Optimization, Properties of Isolators, Optimization Parameters and Limits of Design Parameters

In this study, two types of optimization problems are discussed in general. These can be given as follows:

- Parameter optimization,
- Location optimization.

In parameter optimization, the main focus is to obtain optimum values for the parameters defining each vibration isolator. On the other hand, for location optimization, the focus is on finding the optimum location of each isolator. However, it is also possible to consider both cases simultaneously as can be found in the present study.

The properties of isolators, the optimization parameters and the limits of design parameters depend on the type of the optimization problem and the corresponding subsections. The subsections available within this thesis study are tabulated in Table 2.1. If the given table is investigated, it is seen that the parameter optimization is divided into two sections:

- Single Type Isolators,
- Different Type Isolators.

As understood, in the first type, the isolators are of single type, sharing the same characteristics. On the other hand, in the second type, isolators may have different stiffness values and loss factor. For each type, the mounting angle of the isolators can also be selected as an optimization parameter or an input isolator property. Accordingly, the number of optimization design parameters may increase due to the optimization structure of problem.

On the other hand, for the case of location optimization, it is clearly seen that the possible location of isolators can be defined as;

- Continuous,
- Discrete,
- Predetermined points.

For continuous location optimization, the boundaries of the possible isolator location should be identified. On the other hand, for discrete location optimization, not only the boundary information, but also the number of possible discrete points in each axis should be well defined. Finally, for predetermined points, the coordinate information of possible isolator locations should be set and the whole set of points is automatically designated. Additionally, within the thesis scope, it is also possible to select the isolator parameters as an optimization design variable or an input isolator property in location optimization. Thereby, the number of design parameters will automatically change.

Table 2.1 Available Optimization Types and Corresponding Parameters

Type Of Optimization			Optimized Isolator Parameters				Input Isolator Properties							
			Axial Stiffness	Axial to Radial Stiffness Ratio	Position of Isolators	Inclination Angle	Number of Isolators	Loss Factor	Axial Stiffness	Radial Stiffness	Axial to Radial Stiffness Ratio	Position of Isolators	Available Positions of Isolators	Inclination Angle of Isolators
Parameter Optimization	Single Type Isolators	Fixed Orientation	✓	✗	✗	✗	✓	✓	✗	✗	✓	✓	✗	✓
		Free Orientation	✓	✗	✗	✓	✓	✓	✗	✗	✓	✓	✗	✗
	Different Type Isolators	Fixed Orientation	✓	✓	✗	✗	✓	✓	✗	✗	✗	✓	✗	✓
		Free Orientation	✓	✓	✗	✓	✓	✓	✗	✗	✗	✓	✗	✗
Location Optimization	Continuous Points with Fixed Parameters		✗	✗	✓	✗	✓	✓	✓	✓	✗	✗	✓	✓
	Continuous Points with Unfixed Parameters		✓	✓	✓	✗	✓	✓	✗	✗	✗	✗	✓	✓
	Dicrete Points with Fixed Parameters		✗	✗	✓	✗	✓	✓	✓	✓	✗	✗	✓	✓
	Discrete Points with Unfixed Parameters		✓	✓	✓	✗	✓	✓	✗	✗	✗	✗	✓	✓
	Predetermined Points with Fixed Parameters		✗	✗	✓	✗	✓	✓	✓	✓	✗	✗	✓	✓
	Predetermined Points with Unfixed Parameters		✓	✓	✓	✗	✓	✓	✗	✗	✗	✗	✓	✓

After defining optimization design parameters, the designer is required to set the limits for each parameter properly. Similar with the design constraints, the limits set for the design parameters are directly related to the flexibility of the optimization process.

CHAPTER 3

VERIFICATION OF THE THEORETICAL MODEL

3.1. Introduction

In this part, it is aimed to verify the mathematical model used in the analysis and optimization parts of the developed MATLAB based software. Here, the verification is implemented by using the results of a finite element analysis program, ANSYS Workbench 14.0. As a model, a rigid body with 6 degrees of freedom is used. For simplicity, the body is modeled as a rectangular prism with dimensions of 50x100x200 mm. The rigid body of which the physical properties are given in Table 3.1 is supported by 4 resilient members as shown in Figure 3.1.

Table 3.1 Physical Properties of the Model

MASS	2.2271	kg
Ixx	0.002162	$kg\text{-}m^2$
Iyy	0.009304	
Izz	0.007719	
Ixy	0	
Ixz	0	
Iyz	0	

As shown in Figure 3.1 below, those resilient members are mounted on the rigid body asymmetrically in orthogonal and inclined directions. The stiffness values and the orientations of each isolator are given in Table 3.2 and, Table 3.3 respectively.

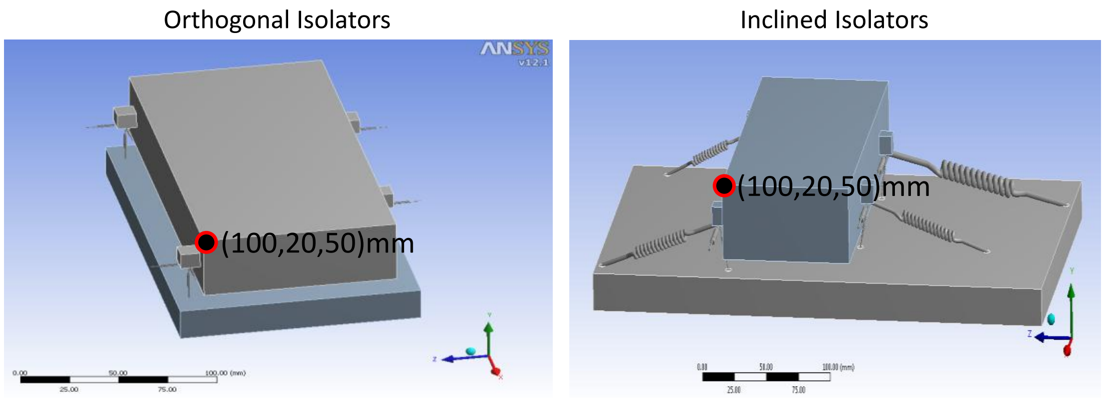

Figure 3.1 Isolated System Model Built in ANSYS Workbench

Table 3.2 Physical Properties and Location Information of the Isolators

Isolator Number	Stiffness (N/m)			Loss Factor	Location w.r.t Mass Center (mm)		
	X	Y	Z		X	Y	Z
1	6000	4000	6000	0.2	35	-5	-55
2	6000	4000	6000		-55	-5	-55
3	6000	8000	6000		-85	-5	55
4	6000	8000	6000		85	-5	55

Table 3.3 Rotation of the Isolators about X-Axis

Isolator	**Rotation About X-Axis (degrees)**
Isolator-1	15
Isolator-2	10
Isolator-3	-20
Isolator-4	-15

In this report, the verification has been implemented for both orthogonal and inclined isolator cases. Here, the following results obtained by using the mathematical model and the finite element model are compared. The analysis performed during verification process is summarized in Figure 3.2 and itemized below as:

- Eigenvalue problem solution in order to find the values of natural frequencies for all 6 modes.
- Calculation of static deflection of each isolator mounted on different locations of the rigid body under standard gravitational acceleration.

- Response analysis of mass center and a selected point (point on the corner labeled with a red dot in Figure 3.1) on the rigid body under a predefined random vibration input.
- Response analysis of mass center and a selected point (point on the corner labeled with a red dot in Figure 3.1) on the rigid body under a predefined harmonic vibration input.
- Transmissibility function of mass center and a selected point (point on the corner labeled with a red dot in Figure 3.1) on the rigid body.

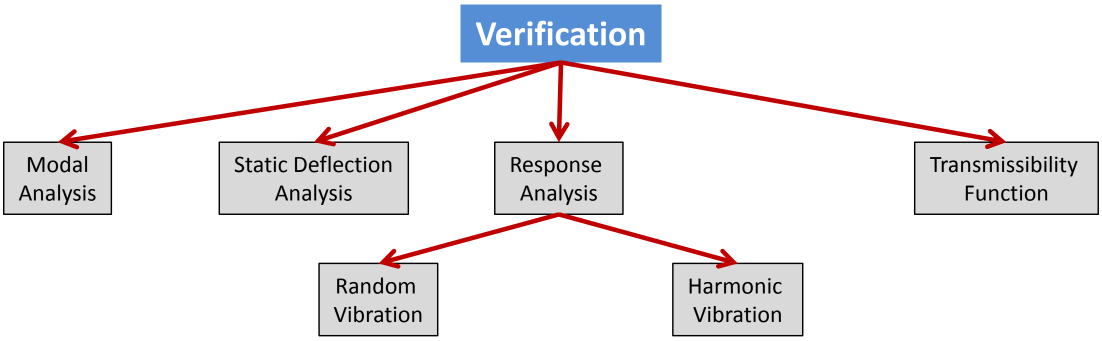

Figure 3.2 Analyses Performed for Verification

3.2. Modal Analysis

In this part, the results for the natural frequencies are compared. In Table 3.4 and Table 3.5, the results are obtained for the isolators mounted orthogonal and inclined to the global reference frame, respectively. As seen, the results obtained from both the mathematical and finite element models are very close to each other. This means that the mass and the stiffness matrices are well defined and the eigenvalue problem solution is correct.

Table 3.4 Comparison of Natural Frequencies of the Rigid Body supported on Orthogonal Isolators

Mode Number	Frequency (Hz)		Difference (%)
	Mathematical Model	Finite Element Model	
1	15.05	15.048	0.013
2	16.4231	16.423	0.001
3	16.4713	16.472	-0.004
4	21.0105	20.990	0.098
5	22.4706	22.452	0.083
6	30.0476	29.958	0.298

Table 3.5 Comparison of Natural Frequencies of the System on Inclined Isolators

Mode Number	Frequency (Hz)		Difference (%)
	Mathematical Model	Finite Element Model	
1	15.1251	15.119	0.040
2	16.4021	16.402	0.001
3	16.4659	16.466	-0.001
4	20.5758	20.541	0.1691
5	22.8393	22.831	0.036
6	29.9562	29.858	0.3278

3.3. Static Deflection Analysis

In this part, the results of the deflection values for each isolator due static loading are given for both orthogonal and inclined cases (foundation assumed to be fixed). Here, it is assumed that the standard gravitational acceleration vector is in –Y direction and has a value of 9.81 m/s^2. If the results obtained from both methods are compared in Table 3.6 and Table 3.7, it is observed that the values of static deflection of each isolator under standard gravitational acceleration are very close to each other. Therefore, it can be concluded that both mass and stiffness matrices in addition to the 3 dimensional rotational matrices due to static loading are defined correctly.

Table 3.6 Comparison of Static Deflection of Orthogonal Isolators in Y Axis

Isolator Number	Deflection in Y Direction (mm)		Difference (%)
	Mathematical Model	Finite Element Model	
1	1.4027	1.4044	-0.121
2	1.3281	1.3308	-0.203
3	0.6122	0.6110	0.196
4	0.7531	0.7527	0.053

Table 3.7 Comparison of Static Deflection of Inclined Isolators in Y Axis

Isolator Number	Deflection in Y Direction (mm)		Difference (%)
	Mathematical Model	Finite Element Model	
1	1.3753	1.3758	-0.036
2	1.3066	1.3061	0.038
3	0.6393	0.6397	-0.063
4	0.7690	0.7675	0.195

3.4. Response Analysis for Random Vibration Input

Response analysis of mass center and a randomly selected point on the rigid body is also verified by comparing the results obtained from the mathematical model and the finite element model. In this case, a pink noise random vibration is applied in Y direction only. The amplitude of input power spectral density of the acceleration is 0.05 g^2/Hz for the frequency range 10 to 50 Hz as shown in Figure 3.3. In Table 3.8 and Table 3.9, the RMS acceleration values of the mass center and the selected point on the corner (see Figure 3.1) are given for isolators mounted in orthogonal and inclined directions, simultaneously.

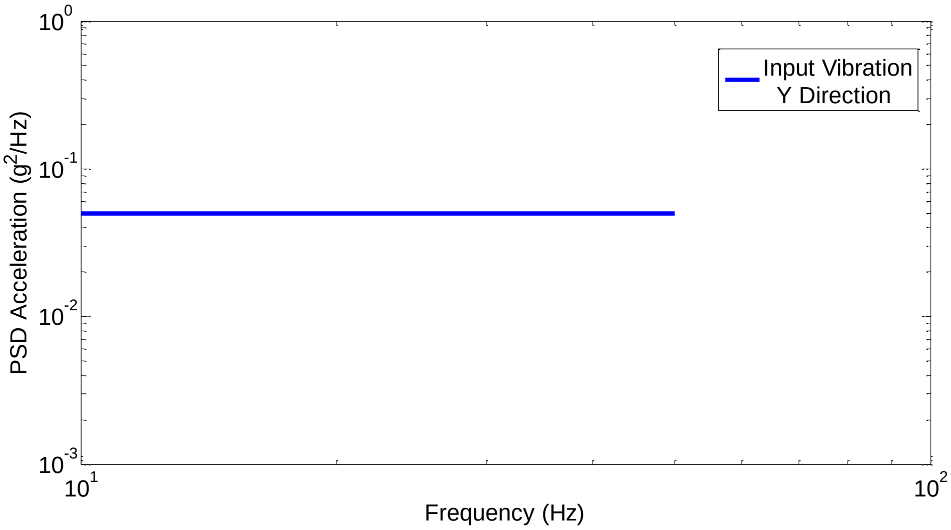

Figure 3.3 Input Vibration Profile in Y Axes

Table 3.8 Response RMS Acceleration of the Rigid Body supported on Orthogonal Isolators

Point of Interest	**Response RMS Acc. (g^2/Hz)**						**Difference (%)**		
	Mathematical Model			Finite Element Model					
	X	Y	Z	X	Y	Z	X	Y	Z
Mass Center	0.089	2.14	0.361	0.087	2.16	0.355	2.2	-0.9	1.7
Corner	0.147	2.161	0.739	0.145	2.188	0.728	1.4	-1.2	1.5

Table 3.9 Response RMS Acceleration of the Rigid Body supported on Inclined Isolators

Point of Interest	Response RMS Acc. (g^2/Hz)						Difference (%)		
	Mathematical Model			Finite Element Model					
	X	Y	Z	X	Y	Z	X	Y	Z
Mass Center	0.087	2.159	0.302	0.085	2.180	0.294	2.3	-1.0	2.6
Corner	0.098	2.162	0.628	0.096	2.190	0.608	2.0	-1.3	3.2

If the response values for the mass center and the point on the corner are compared for each orthogonal axis, it is observed that the response RMS acceleration values are close to each other; however, a slight difference exists. The difference is due to using different damping models in each model. However, it should be noted that the same analysis are repeated for a very low damping values and as expected the difference is eliminated for that case. In this study, the structural damping model is used; on the other hand, in ANSYS Workbench, the damping model that can only be selected is the viscous damping model in random vibration analysis. Considering the fact that the majority of the passive vibration isolator manufacturers share information on the damping property of isolators as structural damping, it is feasible to use this model. However, it will be beneficial to investigate and compare the acceleration response PSD results for the defined frequency range as shown in the following figures.

Response PSD acceleration values with respect to the defined frequency range for the mass center point and corner point are given in Figure 3.4 to Figure 3.7 and from Figure 3.8 to Figure 3.11, respectively. For all cases, the isolators are mounted orthogonal or inclined with respect to the global reference frame.

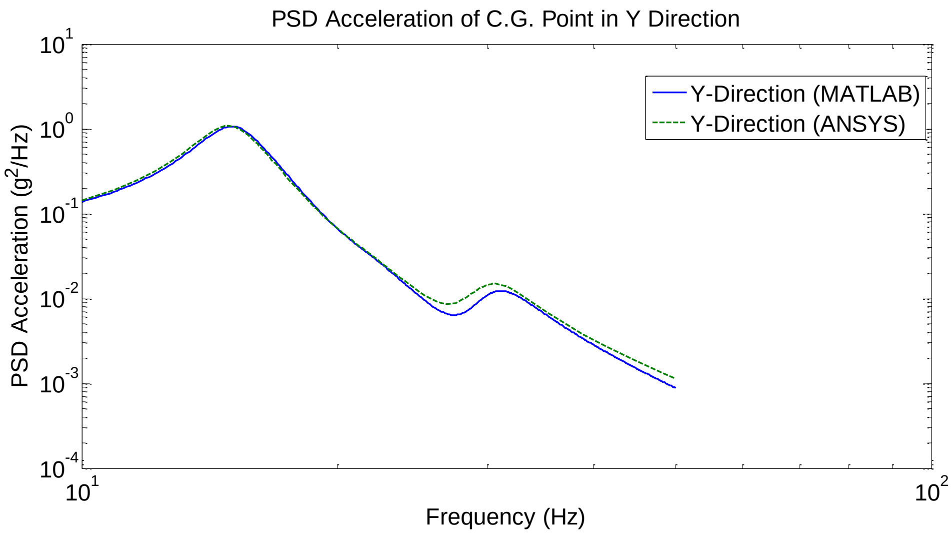

Figure 3.4 PSD Acceleration of C.G. in Y Direction for Orthogonal Isolators

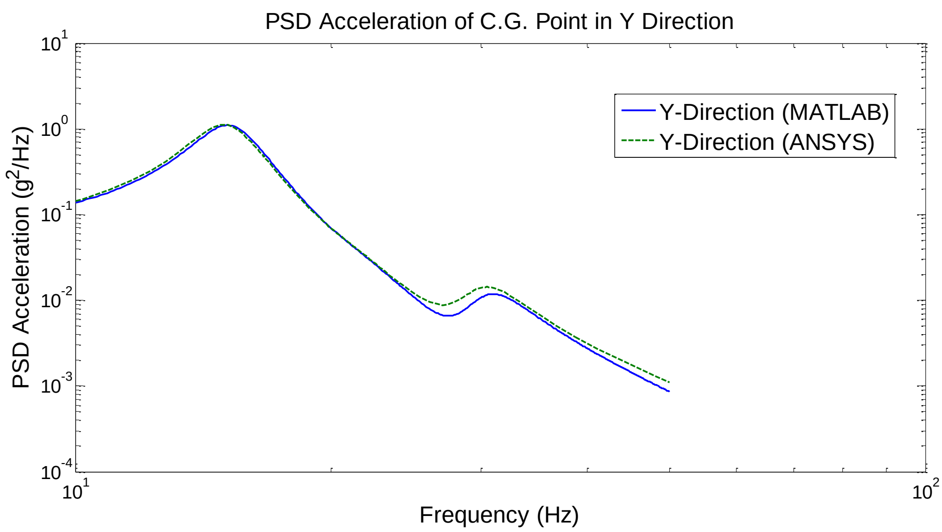

Figure 3.5 PSD Acceleration of C.G. in Y Direction for Inclined Isolators

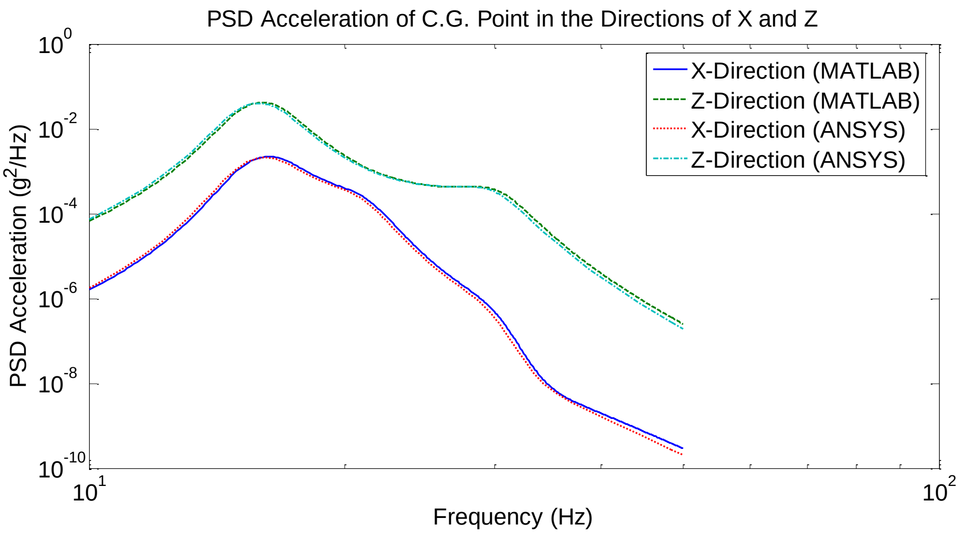

Figure 3.6 PSD Acceleration of C.G. in X and Z Directions for Orthogonal Isolators

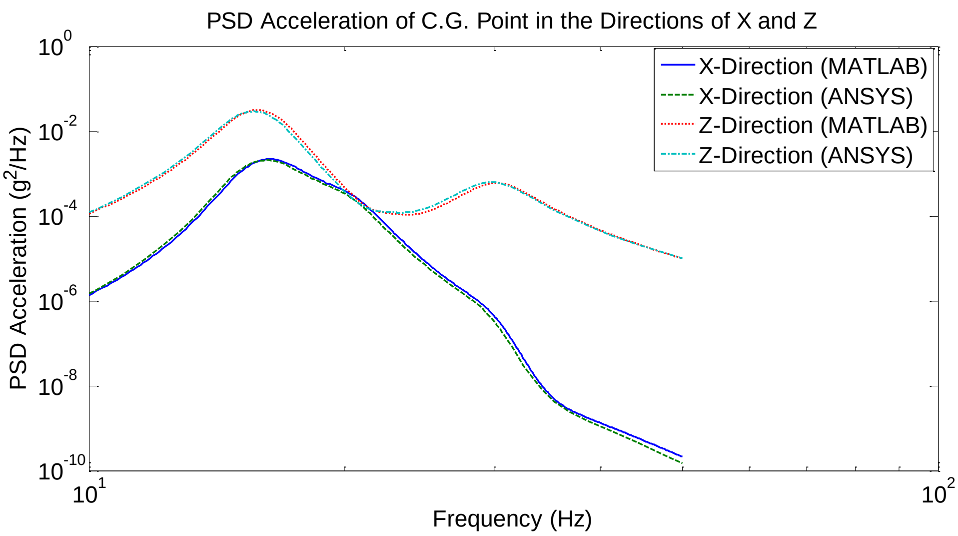

Figure 3.7 PSD Acceleration of C.G. in X and Z Directions for Inclined Isolators

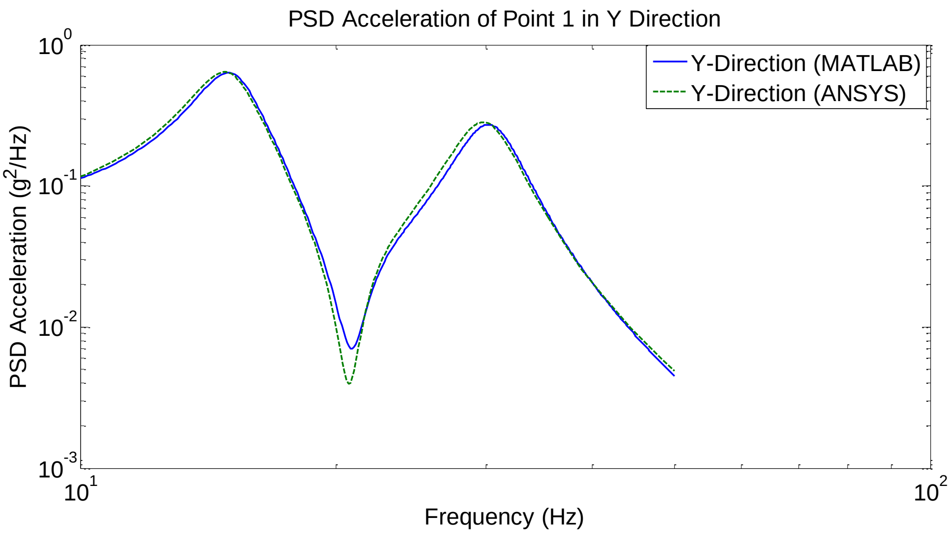

Figure 3.8 PSD Acceleration of Corner Point in Y Direction for Orthogonal Isolators

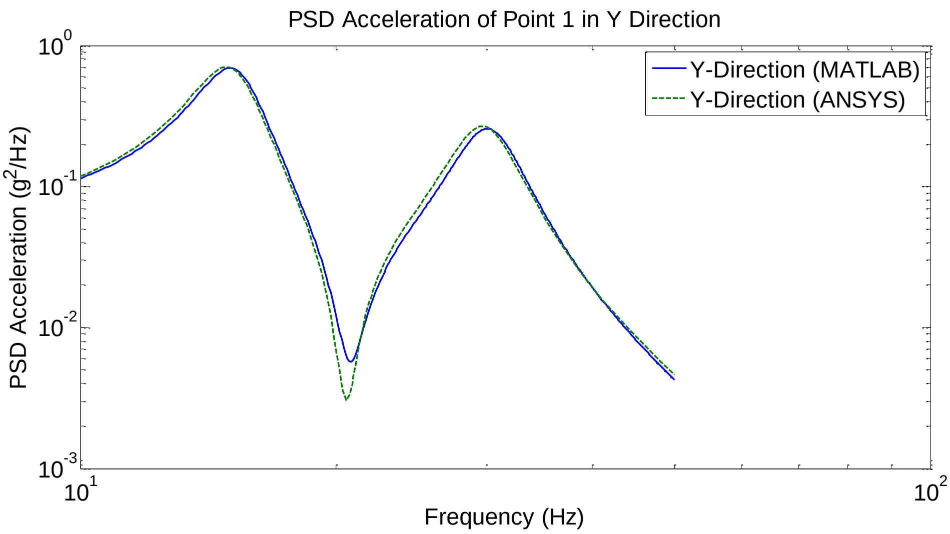

Figure 3.9 PSD Acceleration of Corner Point in Y Direction for Inclined Isolators

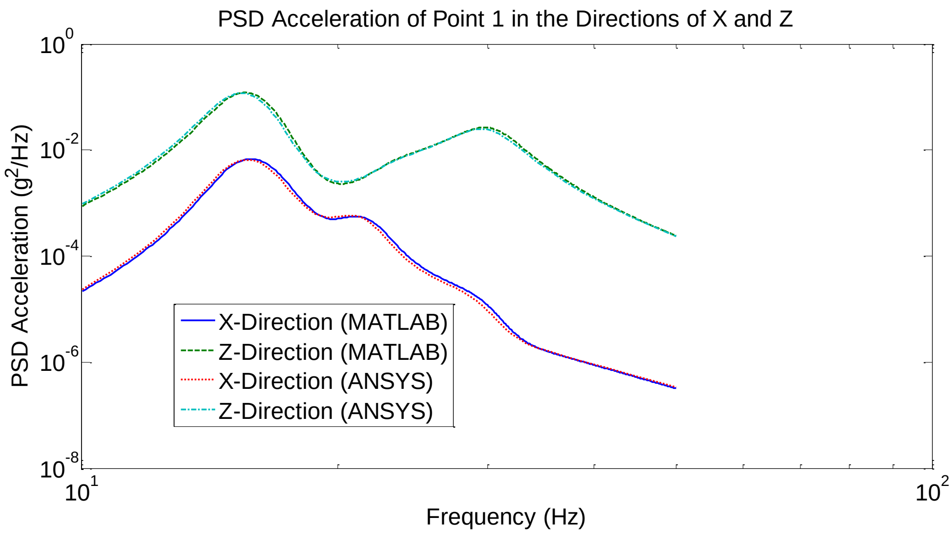

Figure 3.10 PSD Acceleration of Corner Point in X and Z Directions for Orthogonal Isolators

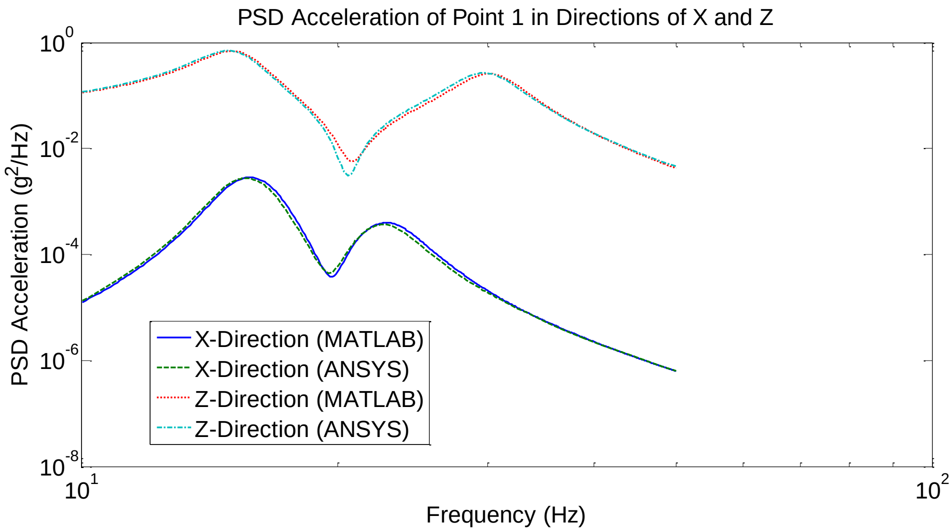

Figure 3.11 PSD Acceleration of Corner Point in X and Z Directions for Inclined Isolators

3.5. Response Analysis for Harmonic Vibration Input

In this part, the purpose is to verify the results obtained from the harmonic response analysis for the point on the corner. Here, it is assumed that the base is excited at constant acceleration amplitude of 0.90 g at 15 Hz which is close to the first natural frequency. The results can be obtained for both orthogonal and inclined mounted isolators simultaneously.

If the results shown in Table 3.10 and Table 3.11 are compared with each other, it is observed that they are close to each other.

Table 3.10 Response Displacement Amplitude of Corner Point for Orthogonal Isolators

	X (mm)	**Y (mm)**	**Z (mm)**
MATLAB	0.31457	3.5319	1.4264
ANSYS	0.31139	3.5253	1.4273
Difference (%)	1.0	0.2	-0.1

Table 3.11 Response Displacement Amplitude of Corner Point for Inclined Isolators

	X (mm)	**Y (mm)**	**Z (mm)**
MATLAB	0.20624	3.6937	0.43393
ANSYS	0.20026	3.7057	0.42424
Difference (%)	0.1	-0.3	2.2

3.6. Transmissibility Function

In this part, the verification has been implemented for the results of transmissibility functions. Here, the frequency range is selected as 1 to 50 Hz which involves all natural frequencies. Additionally, the base is assumed to be excited at constant amplitude of displacement of 1.0 mm in Y direction only. In the following figures, from Figure 3.12 to Figure 3.17, the transmissibility values for the corresponding frequencies are plotted for the point on the corner. The verification for the transmissibility function has been implemented for both orthogonal and inclined isolator cases.

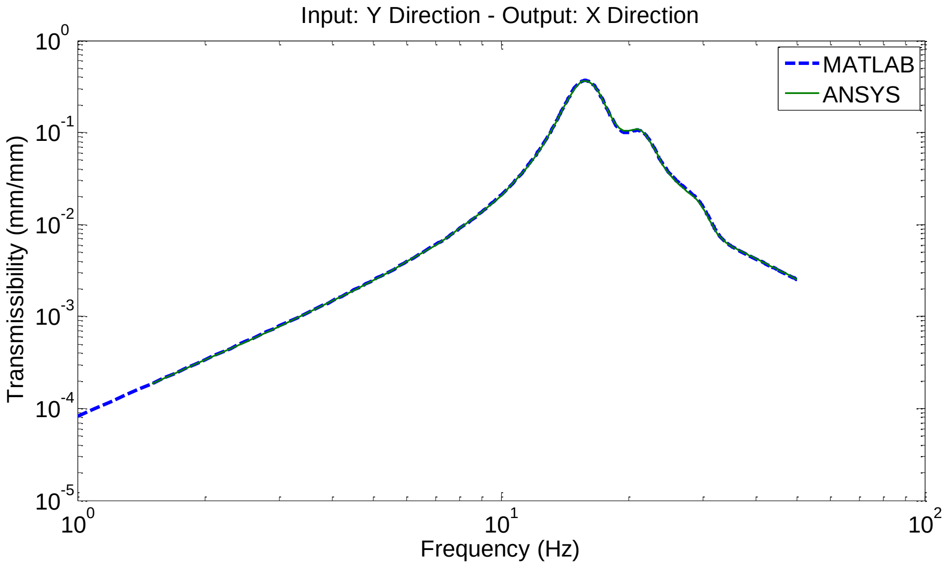

Figure 3.12 Transmissibility Function at Corner Point for Orthogonal Isolators - Input in Y; Output in X Directions

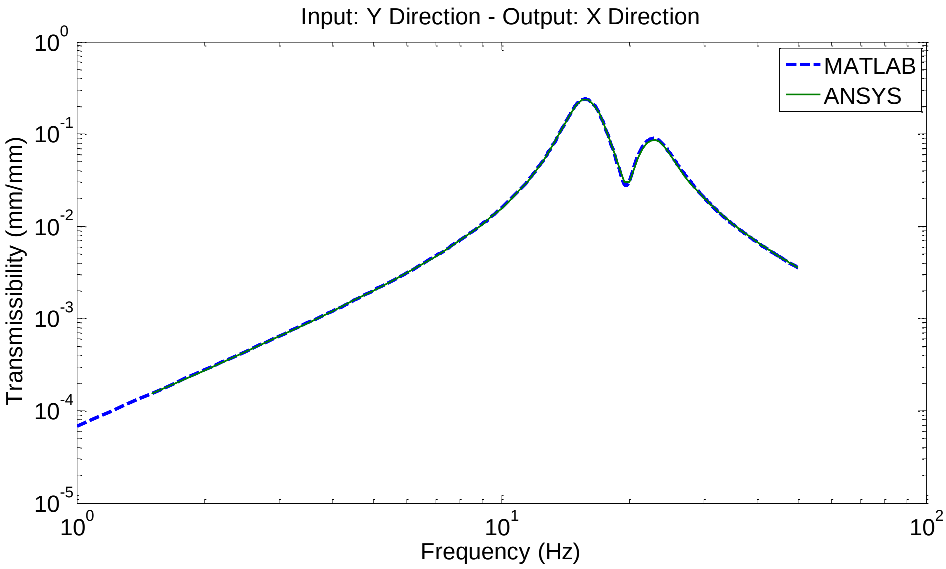

Figure 3.13 Transmissibility Function at Corner Point for Inclined Isolators - Input in Y; Output in X Directions

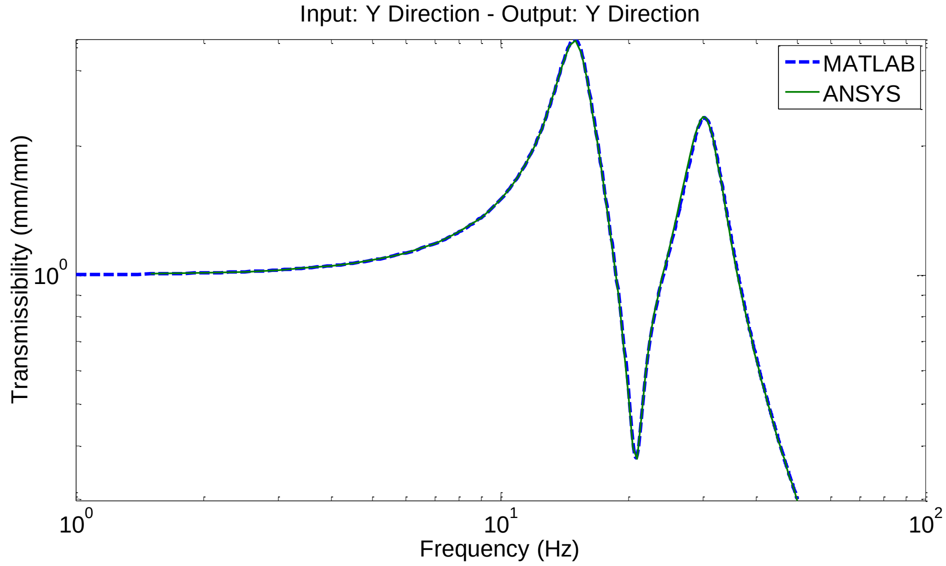

Figure 3.14 Transmissibility Function at Corner Point for Orthogonal Isolators - Input in Y; Output in Y Directions

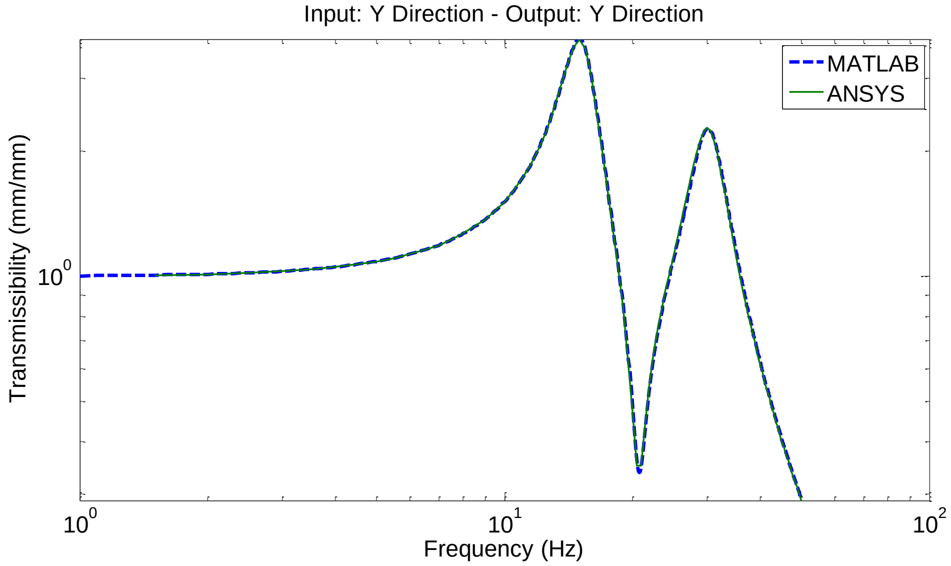

Figure 3.15 Transmissibility Function at Corner Point for Inclined Isolators - Input in Y; Output in Y Directions

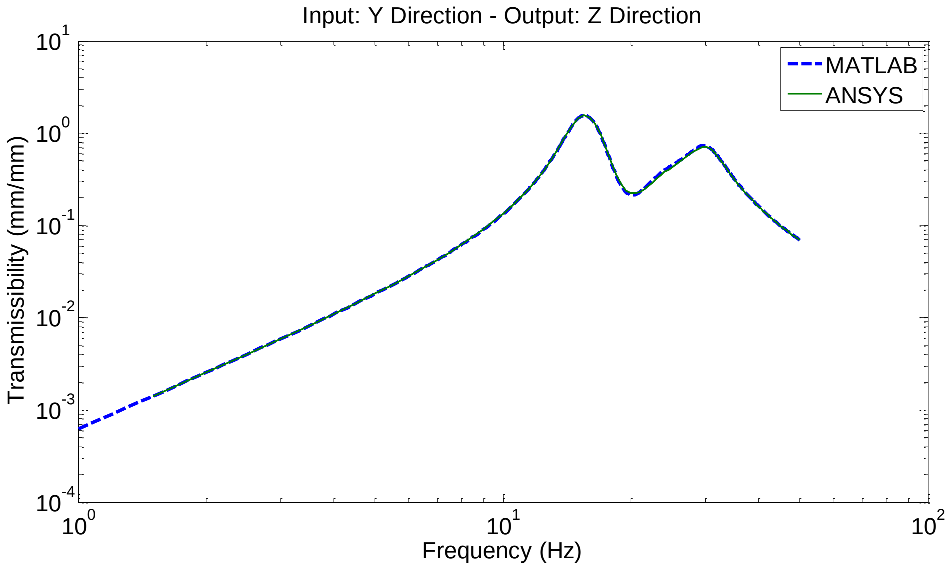

Figure 3.16 Transmissibility Function at Corner Point for Orthogonal Isolators - Input in Y; Output in Z Directions

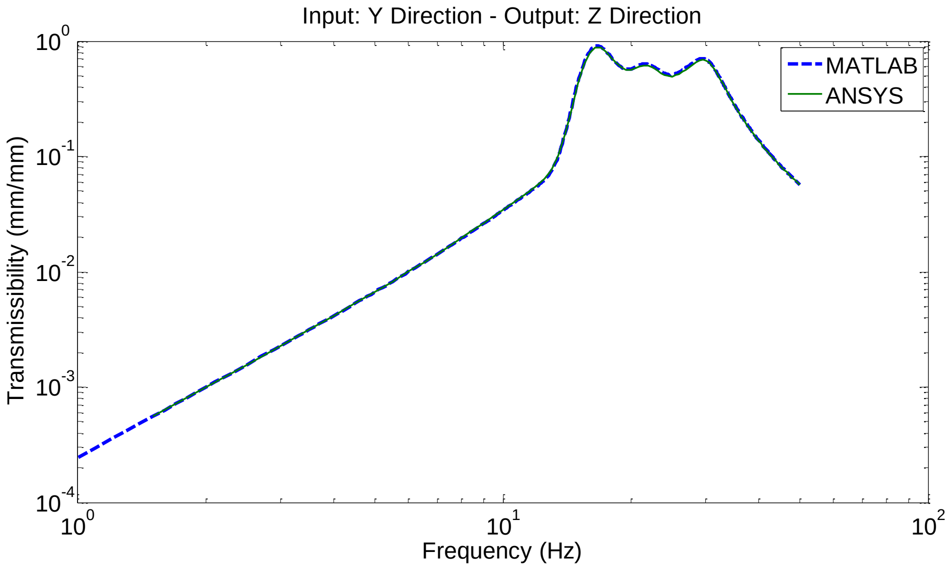

Figure 3.17 Transmissibility Function at Corner Point for Inclined Isolators - Input in Y; Output in Z Directions

CHAPTER 4

DEVELOPMENT OF THE SOFTWARE ENVIRONMENT

4.1. Introduction

In this part of the study, software developed for the analysis and optimization sections are introduced.

4.2. Analysis Section

The software for the analysis section is prepared in order to obtain static and dynamic behaviors of the designed vibration isolation system. The environment of the software consists of three main panels including control buttons, input data entries and results section. Additionally, as shown in Figure 4.1, the software has a toolbar at the top including data cursor, zoom in, zoom out and pan. As followed from the figure, the control panel includes the following buttons:

- Input data panel buttons such as rigid body properties, isolator unit properties, gravity, location of interest and vibration profile;
- Computation button;
- Result buttons such as figures, numerical results and transmissibility function;
- Monte Carlo simulation button;
- Data management buttons such as report, save and load data.

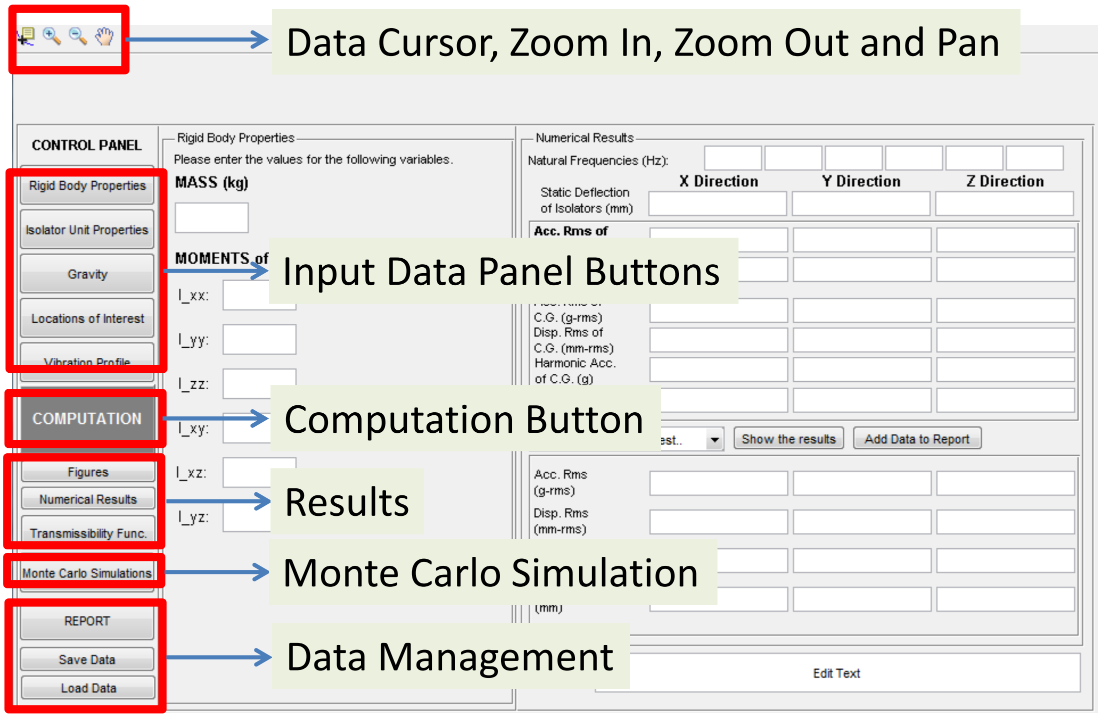

Figure 4.1 GUI Developed For Vibration Isolation System Analysis

Even though the vibration isolation analysis software is easy to use, before running the software, the user should be aware of the relationship between input parameters and results. If it is desired to use all capabilities of the analysis software, the input parameters given in Figure 4.2 should be well defined.

According to the figure, the user is expected to know the properties of the rigid body in addition to the isolators. Additionally, the amplitude and direction of gravitational acceleration and the information of vibration profile for the exciting platform should be well known. If a point different from the mass center is taken into consideration, the user should set the location information with respect to the global reference frame completely. The user may also expect to know the behavior of the transmissibility function of an isolation system. If so, the interested frequency range in addition to the direction information for input and response excitation should be set in the corresponding panel. Finally, in order to implement Monte Carlo simulations, the user is required to define parameters such as the number of simulation and the percentage deviations in the position stiffness and loss factor of the isolators.

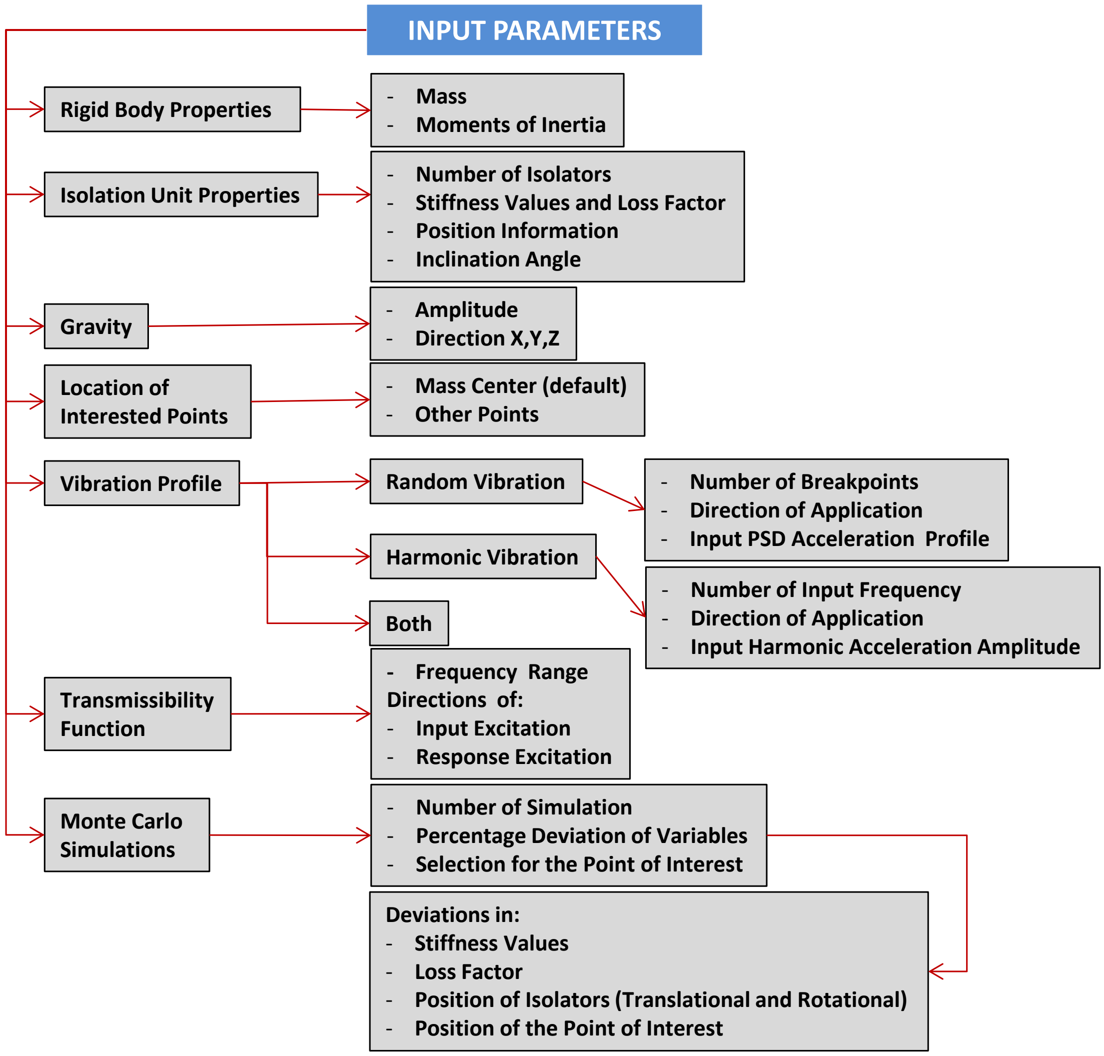

Figure 4.2 Input Parameters Used in Developed Software

Filling in the relevant portions of the analysis software, the user is capable to obtain a variety of information on a vibration isolation system. As can be seen from Figure 4.3, the numerical results involving the natural frequencies, static deflection of isolators and response to the input vibration excitation for the points of interest can be computed using the software. Additionally, a variety of plots can be obtained considering the transmissibility and the response PSD acceleration & displacement functions for any selected point in any direction.

Additionally, if a Monte Carlo simulation is implemented using the generated analysis software, it is possible to observe the deviations in natural frequencies, static deflection of isolators, response PSD acceleration and displacement functions, and the corresponding RMS values in addition to the harmonic acceleration and displacement amplitudes for the selected point.

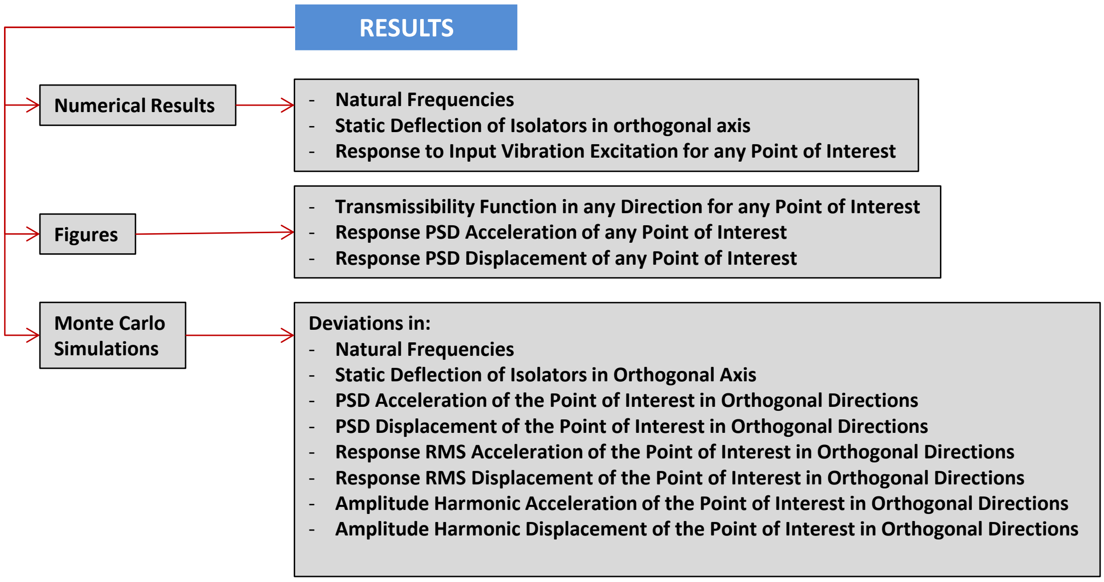

Figure 4.3 Output Parameters of the Developed Software

4.3. Optimization Section

One other software developed in this study is for obtaining the optimum design parameters for a defined vibration isolation problem. In the opening window, as shown in Figure 4.4, the user encounters two main panels including control buttons and the input section.

In control panel, like in the analysis software, the user finds buttons used to switch between panels easily. Using those buttons, the user is expected to define input design parameters, the type of optimization, design constraints and objective function used in the optimization software.

Here, the input design parameters consist of rigid body properties and the information on gravity and the location of points of interest. Additionally, in this panel, the user is expected to define the type of vibration profile and set the corresponding vibration level.

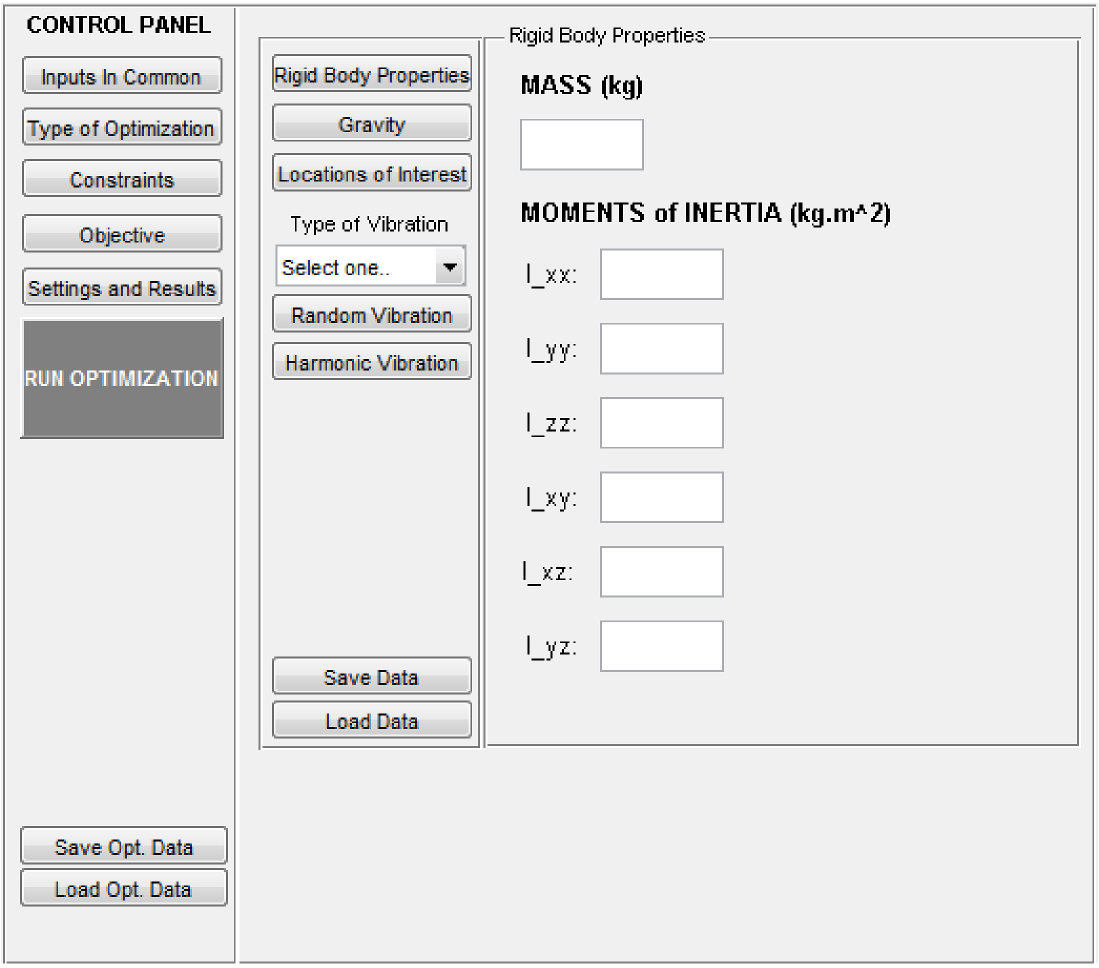

Figure 4.4 GUI Developed for Vibration Isolation System Design Parameter Optimization

Following the procedure given in Figure 2.3, the user should also define the type of the optimization, design constraints and the objective function. In the present study, a number of possible optimization scenarios are defined. If Table 2.1 is investigated, parameter and location optimization types are encountered as the two major topics. Investigating the given other sub-types such as single and different types of isolators, discrete and continuous location optimization with fixed and unfixed isolator properties, the user is able to implement an optimization process for a specific type of isolation problem scenario.

Selecting the optimization type from Table 2.1, the optimization design parameters in addition to the input isolator properties are automatically determined. For instance, if a user selects a parameter optimization of different types of isolators with fixed inclination angle, a new panel with a new set of parameters appears as in Figure 4.5.

Here, due to the selected optimization type, the axial to radial stiffness ratio in addition to the isolator stiffness coefficient are set as optimization design parameters. In the opening panel, the user is expected to set the range of these design parameters and define corresponding isolator properties such as the total number of isolators, loss factor, position and mounting angle information of isolators.

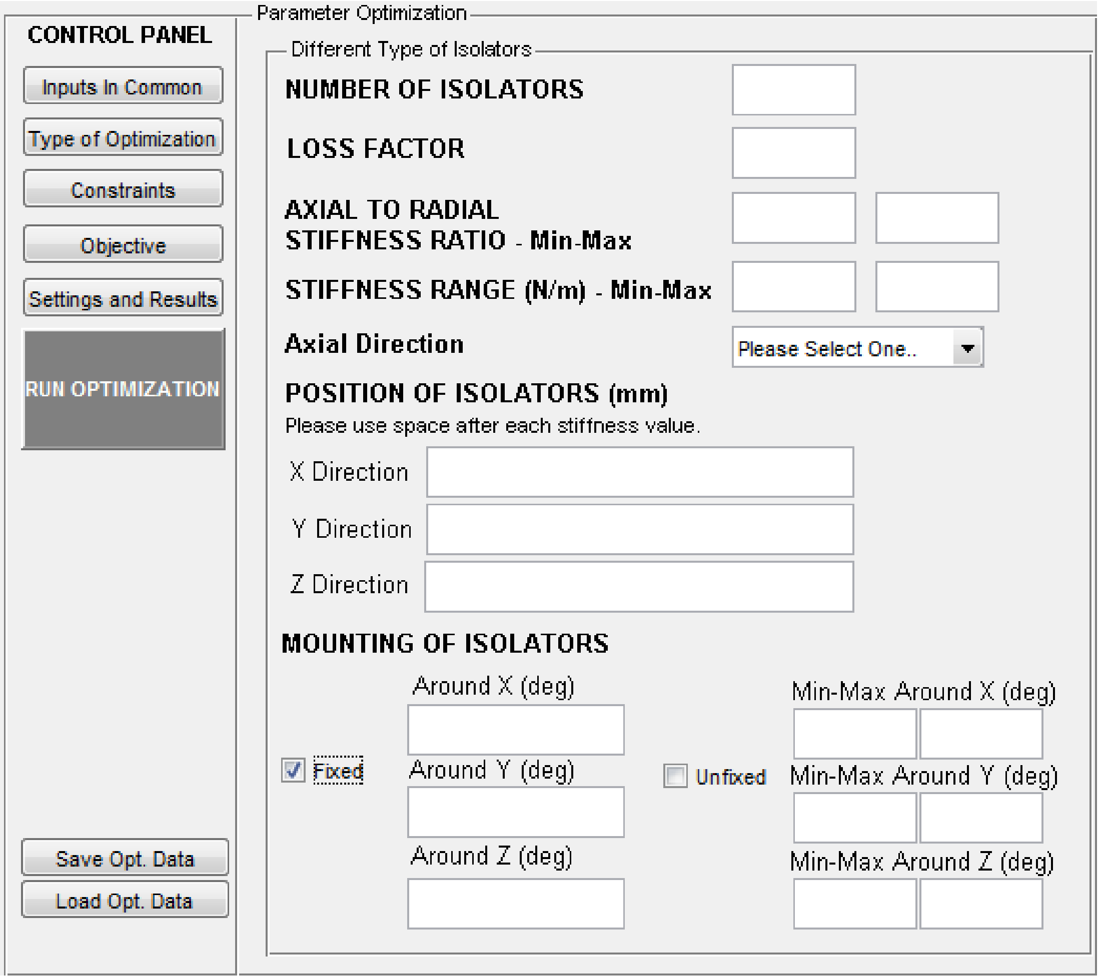

Figure 4.5 Environment for Parameter Optimization - Different Type of Isolators

After setting the mentioned parameters, the design constraints should be well defined. In the present study, the design constraints can be listed as follows:

- Maximum acceleration limit for defined vibration response,
- Maximum displacement limit for defined vibration response,
- Maximum static deflection limit for the isolators,
- Maximum angular rotation of the rigid body due static loading,
- Constraints for alignment and stability.

Thereafter the user is expected to define the objective function. According to the purpose of the optimization process, the objective function might be the minimization of acceleration or displacement. According to the number of points of interest, there might be a necessity to use weight factor in defining objective function.

Before running the optimization process, the user should set parameters that are related with the genetic algorithm. These parameters are the population size and stall generation limit. In addition to these, the time limit to the optimization running time is another point that should be defined in this section.

CHAPTER 5

CASE STUDIES

5.1. Introduction

This section is prepared in order to demonstrate the analysis and optimization capabilities of the software developed. For this purpose, the case studies have been implemented in order to show the abilities of the graphical user interfaces prepared for analysis and optimization sections. Here, the case studies are divided in 3 main parts as given in Figure 5.1.

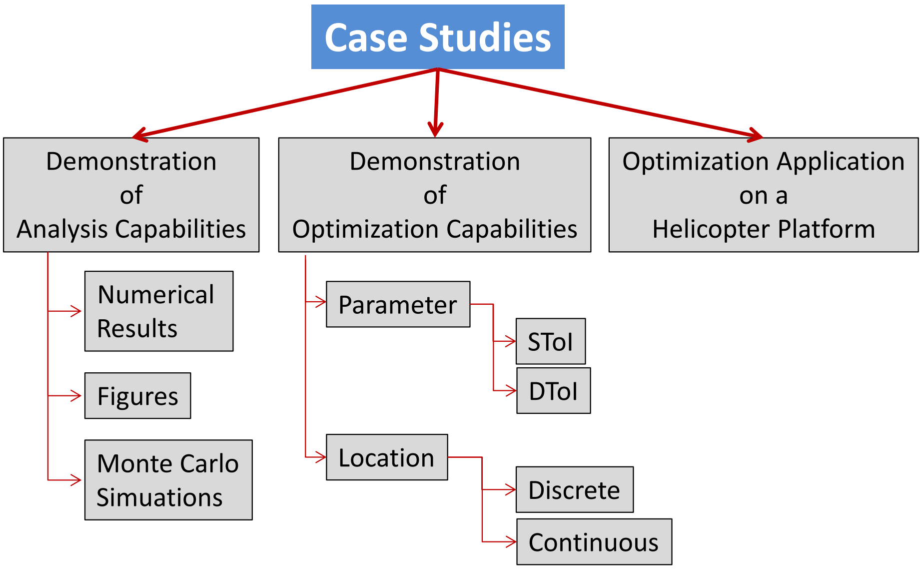

Figure 5.1 Flowchart for Case Studies

For each part, the isolated system is selected as an optomechanical system which is used to determine the altitude of any air-platform. With the electronic devices and optical lenses used, the mechanical structure can be considered as an optomechanical system. The system with the dimensions and physical properties given in Figure 5.2 and Table 5.1 has two points of interest. One is at the mass center and the other is at the point where the optical lens is located.

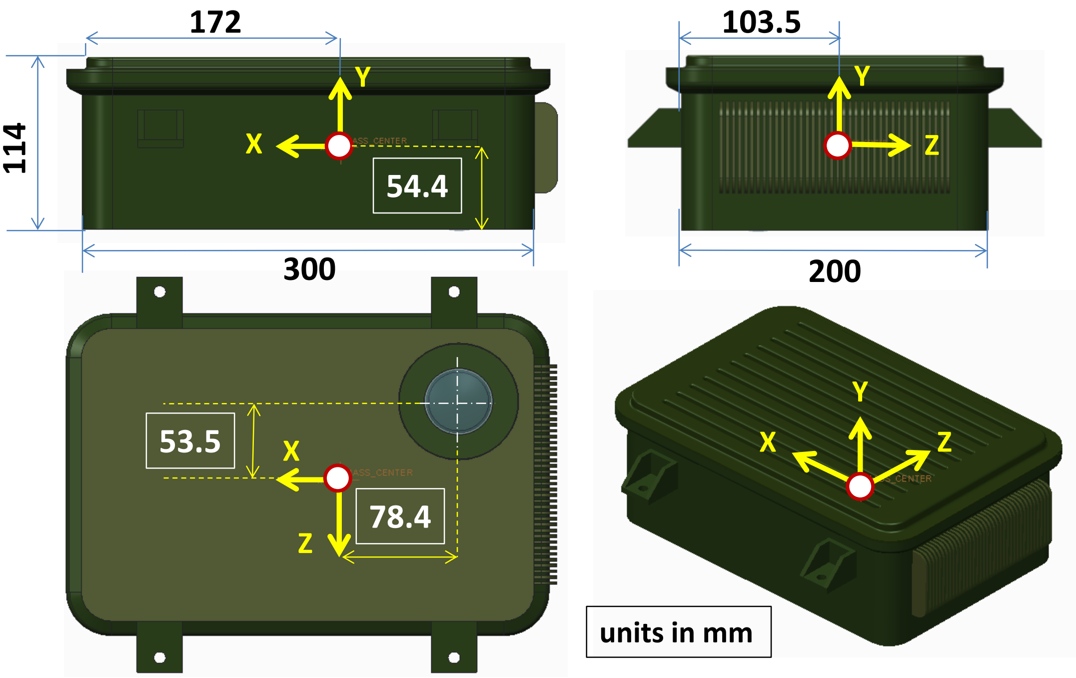

Figure 5.2 Dimensions of the Optomechanical System

Table 5.1 Physical Properties of the Optomechanical System

Property	Value	Unit
Mass	6.4	kg
Ixx	0.032372241	kg-m^2
Iyy	0.083823364	
Izz	0.070838523	
Ixy	0.00084333816	
Ixz	0.0021969757	
Iyz	-0.00012560933	

5.2. Demonstration of Analysis Capabilities

In this part, the demonstration of analysis capabilities of the developed software has been implemented.

The optomechanical system is assumed to be mounted on the instrument panel of OH-6A helicopter as shown in Figure 5.3. Using the military standard, MIL-STD-810 [32], it is possible to obtain the information on exposed random and harmonic vibration levels of the corresponding mounting platform as given in Figure 5.4 and

Table 5.2. According to the standard, both random and harmonic vibrations exist in three orthogonal axes simultaneously.

The mechanical structure is assumed to be fixed by using four elastomeric isolators with identical properties. Here the stiffness of the isolators is defined in three orthogonal axes. The value of the stiffness in each direction is set to 10 kN/m and the loss factor is 0.2. Additionally, the location information of the isolators with respect to the global reference frame on mass center is given in Table 5.3 and shown in Figure 5.21.

As mentioned before, the points of interest are the mass center and the point where the optical lens is located. The position information of these points can also be obtained from Figure 5.2 or Table 5.4.

Figure 5.3 OH-6A Helicopter [40]

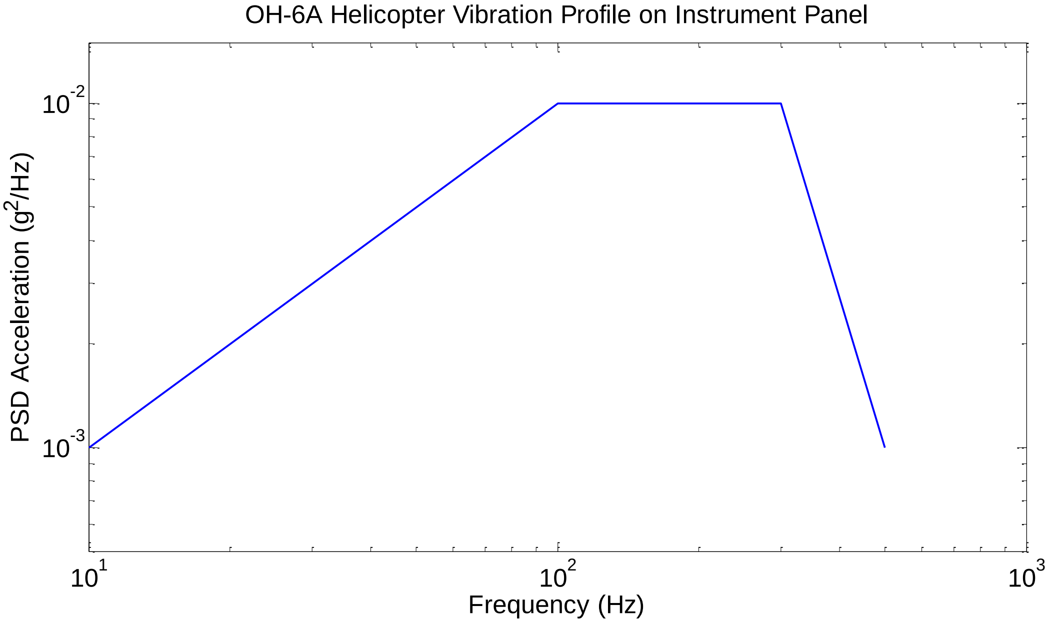

Figure 5.4 Random Vibration Profile of OH-6A Helicopter Instrument Panel

Table 5.2 Amplitudes of Harmonic Vibration of OH-6A Helicopter **[32]**

Frequency (Hz)	**Rotor Source**	**Amplitude Acceleration (g)**	**Amplitude Displacement (mm)**
8.1	Main	0.27	1.0236
32.4	Main	1.75	0.4147
51.8	Tail	1.05	0.0973
64.8	Main	1.05	0.0622
97.2	Main	1.05	0.0276
103.6	Tail	1.05	0.0243
207.2	Tail	1.05	0.0061
310.8	Tail	1.05	0.0027

Table 5.3 Isolator Location Information

Isolator	**Location w.r.t Mass Center (mm)**			**Stiffness In Each Axis (kN/m)**	**Loss Factor**
	X	Y	Z		
1	-78	0	121.5	10	0.2
2	120	0	121.5	10	0.2
3	120	0	-128.5	10	0.2
4	-78	0	-128.5	10	0.2

Table 5.4 Location Information of the Points of Interest

Point of Interest	**Location w.r.t Global Reference Frame (mm)**		
	X	Y	Z
Mass Center	0	0	0
Optical Lens	-78.4	-54.4	-53.5

5.2.1. Numerical Results

In this section, the numerical results that can be obtained using the developed software are shared. In Table 5.5, the natural frequencies are listed by implementing modal analysis. The static deflection analysis, on the other hand, gives information on the deflection of isolators due static loading in each direction as presented in Table 5.6. If the results in the table are investigated, it can be easily observed that the deflections in each isolator occur in Y direction only. In Table 5.7, acceleration and displacement response RMS values of the points of interest for random vibration are listed in each direction. If the results are investigated, it is seen that the response RMS acceleration for both points is one fifth of the input RMS acceleration value at worst. On the contrary, the response RMS displacement value for that point is three times of the amplitude value for input vibration. In Table 5.8 and Table 5.9, harmonic acceleration and displacement amplitude values for the points of interest in X, Y and Z directions are given. If the results are studied, the amplitude values are seen to decrease gradually as the frequency increases. From the results found in those tables, it can be easily concluded that vibration isolation occurs after the first frequency of harmonic excitation.

Table 5.5 Natural Frequencies

Mode Number	**Natural Frequency (Hz)**
1	11.0
2	12.4
3	12.6
4	13.6
5	17.8
6	22.2

Table 5.6 Static Deflection of Isolators due Standard Gravitational Acceleration

Isolator Number	**Deflection (mm)**		
	X	Y	Z
1	≈ 0	1.947	≈ 0
2	≈ 0	1.281	≈ 0
3	≈ 0	1.193	≈ 0
4	≈ 0	1.859	≈ 0

Table 5.7 Response to Random Vibration Input

Point of Interest	**Response Rms Acceleration (g-rms)**			**Response Rms Displacement (mm-rms)**		
	X	Y	Z	X	Y	Z
Mass Center	0.329	0.273	0.315	0.503	0.400	0.492
Optical Lens	0.342	0.242	0.349	0.521	0.422	0.545
	Input: 1.791 g-rms			Input: 0.175 mm-rms		

Table 5.8 Response to Harmonic Vibration Input- Acceleration

Frequency (Hz)	**Input Acceleration Amplitude (g)**	**Harmonic Acceleration Amplitude (g)**					
		Mass Center			Optical Lens		
		X	Y	Z	X	Y	Z
8.1	0.27	0.446	0.467	0.452	0.398	0.519	0.471
32.4	1.75	0.317	0.320	0.320	0.401	0.288	0.230
51.8	1.05	0.067	0.067	0.067	0.082	0.060	0.053
64.8	1.05	0.042	0.042	0.042	0.051	0.037	0.033
97.2	1.05	0.018	0.018	0.018	0.022	0.016	0.015
103.6	1.05	0.016	0.016	0.016	0.019	0.014	0.013
207.2	1.05	0.004	0.004	0.004	0.005	0.004	0.003
310.8	1.05	0.002	0.002	0.002	0.002	0.002	0.001

Table 5.9 Response to Harmonic Vibration Input- Displacement

Frequency (Hz)	Input Displacement Amplitude (g)	Harmonic Displacement Amplitude (mm)					
		Mass Center			Optical Lens		
		X	Y	Z	X	Y	Z
8.1	1.0236	1.690	1.770	1.712	1.509	1.965	1.785
32.4	0.4147	0.075	0.076	0.076	0.095	0.068	0.054
51.8	0.0973	0.006	0.006	0.006	0.008	0.006	0.005
64.8	0.0622	0.002	0.002	0.002	0.003	0.002	0.002
97.2	0.0276	≈ 0	≈ 0	≈ 0	0.001	≈ 0	≈ 0
103.6	0.0243	≈ 0	≈ 0	≈ 0	≈ 0	≈ 0	≈ 0
207.2	0.0061	≈ 0	≈ 0	≈ 0	≈ 0	≈ 0	≈ 0
310.8	0.0027	≈ 0	≈ 0	≈ 0	≈ 0	≈ 0	≈ 0

5.2.2. Figures

In this section, the possible curves that can be plotted using the developed software are given. The curves for transmissibility functions for the points at mass center and the optical lens are given from Figure 5.5 to Figure 5.10. Here, those transmissibility curves are obtained for the listed directions of input and response.

- Input in Y Direction – Responses in X, Y and Z Directions,
- Input in X Direction – Responses in X, Y and Z Directions,
- Input in Z Direction – Responses in X, Y and Z Directions.

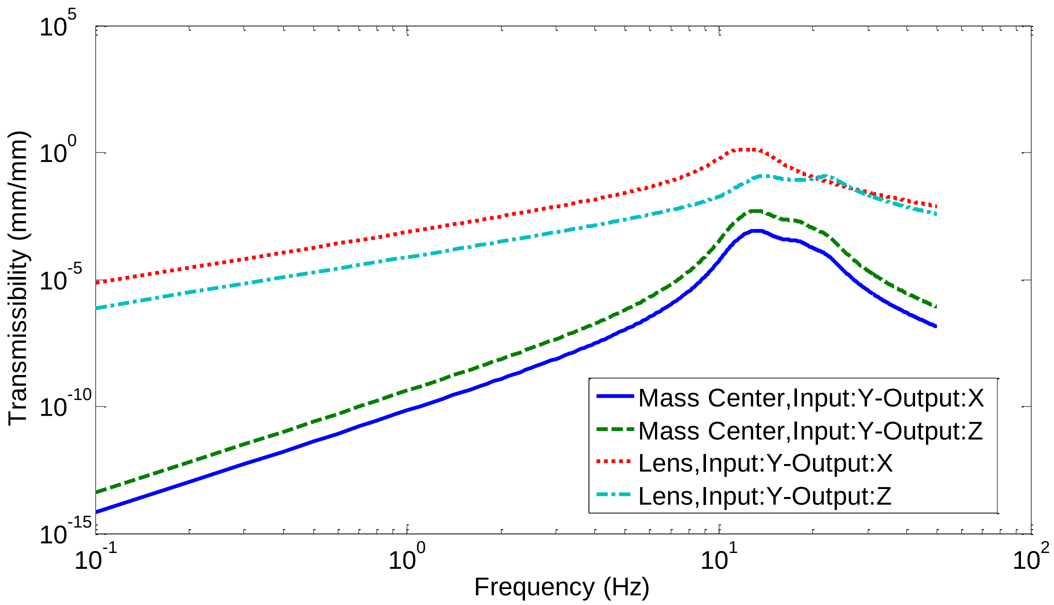

Figure 5.5 Transmissibility Curves for Points of Interest – Input:Y, Output:X/Z

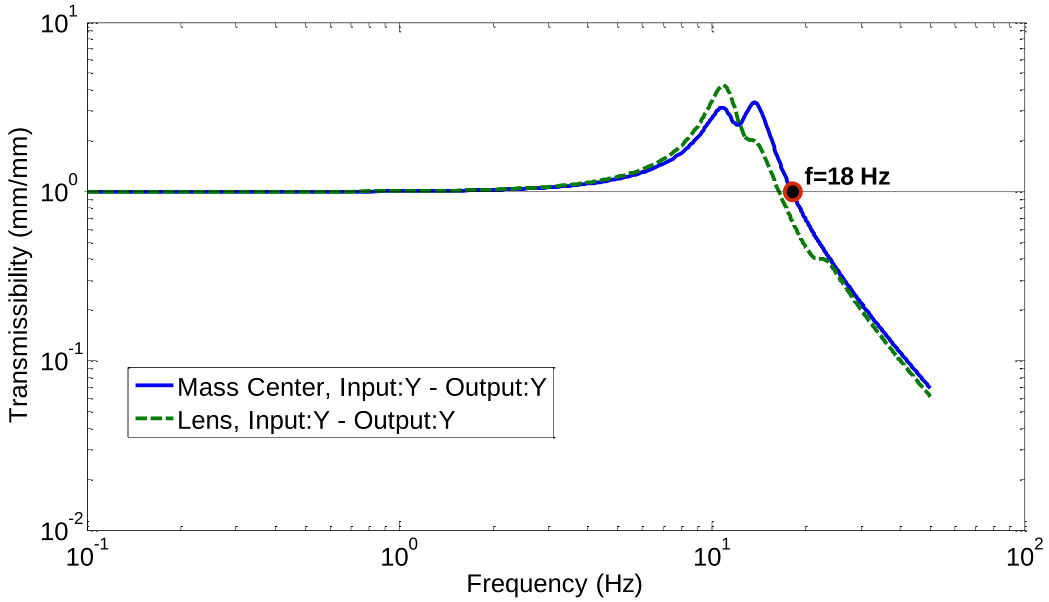

Figure 5.6 Transmissibility Curves for Points of Interest – Input:Y, Output:Y

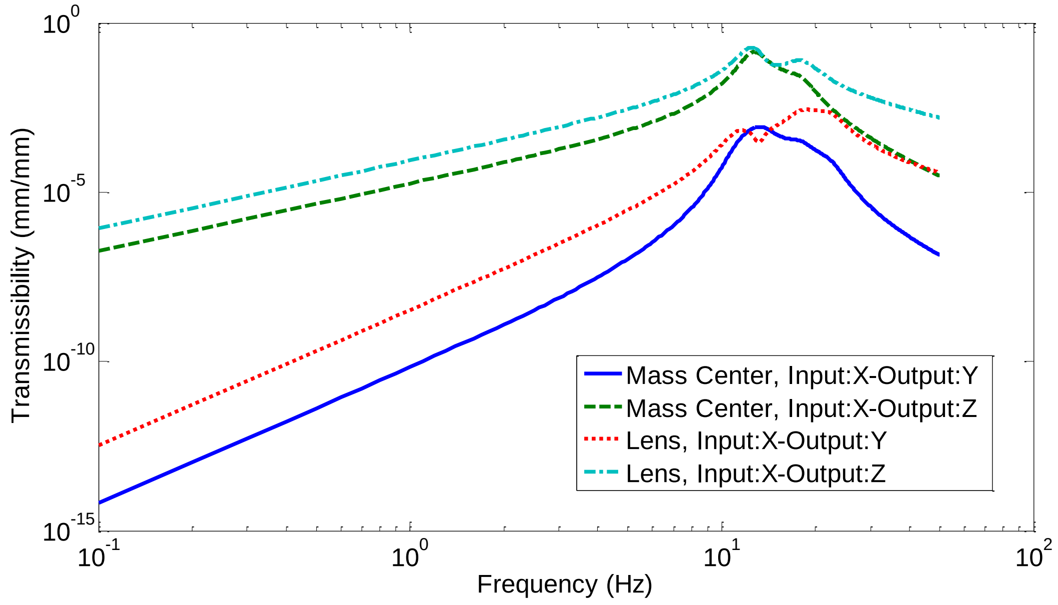

Figure 5.7 Transmissibility Curves for Points of Interest – Input:X, Output:Y/Z

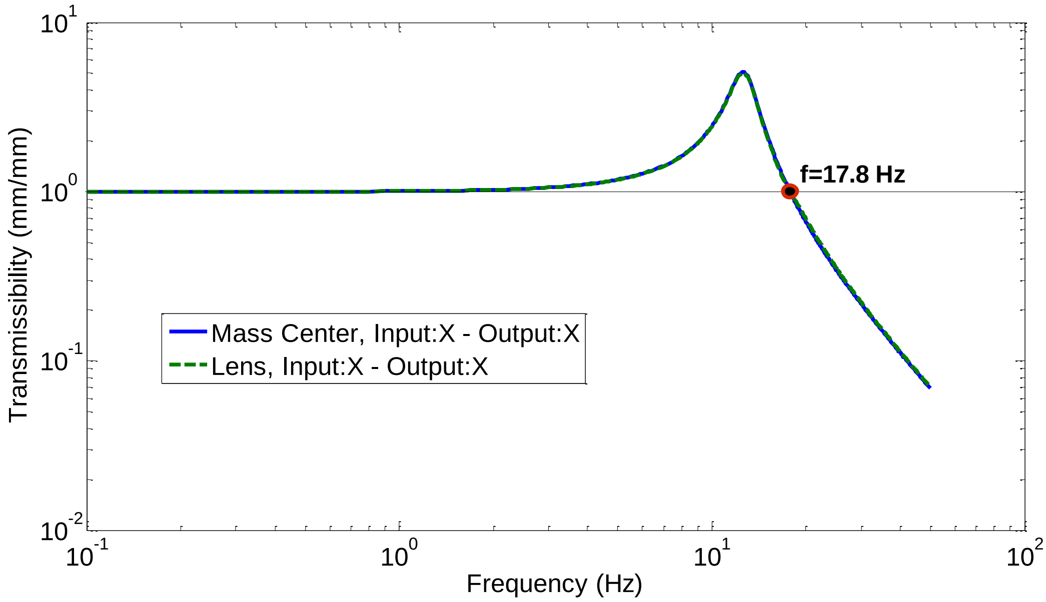

Figure 5.8 Transmissibility Curves for Points of Interest – Input:X, Output:X

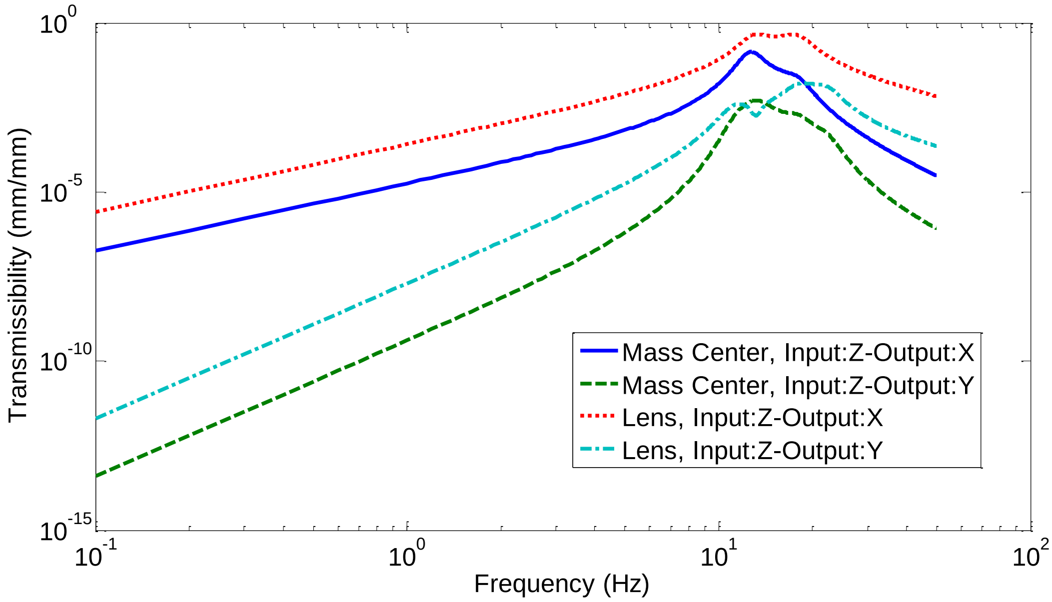

Figure 5.9 Transmissibility Curves for Points of Interest – Input:Z, Output:X/Y

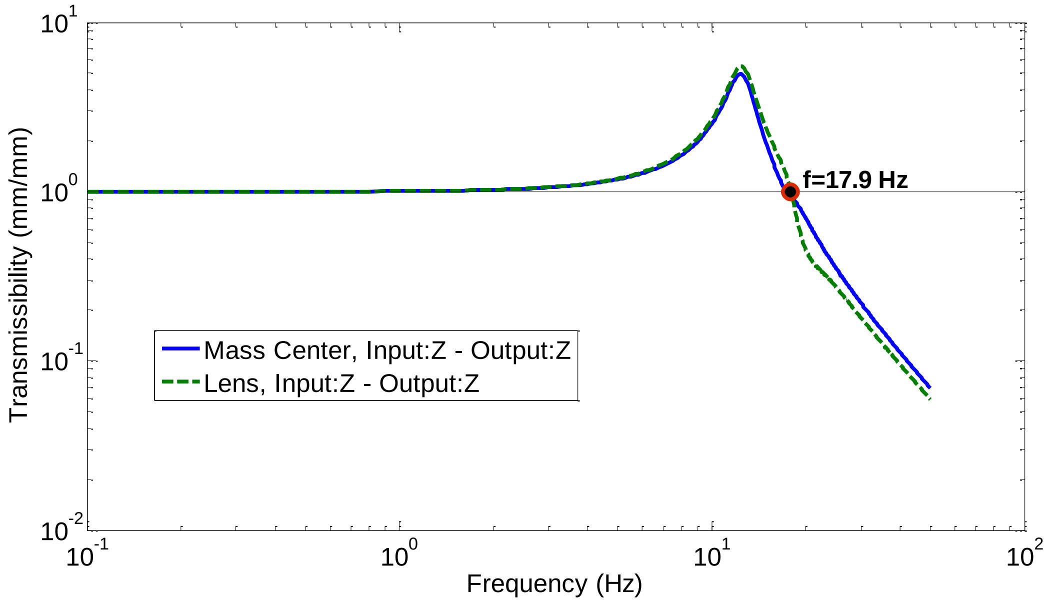

Figure 5.10 Transmissibility Curves for Points of Interest – Input:Z, Output:Z

The response PSD acceleration and displacement curves for the points of interest in each orthogonal axis are given in Figure 5.11 and Figure 5.12, respectively.

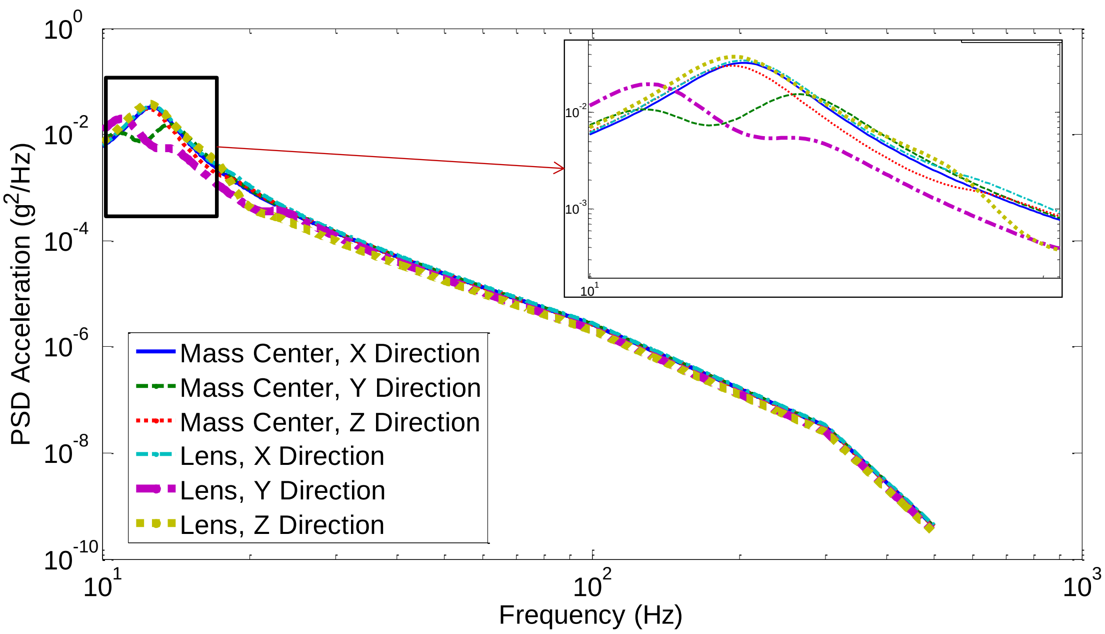

Figure 5.11 Response PSD Acceleration

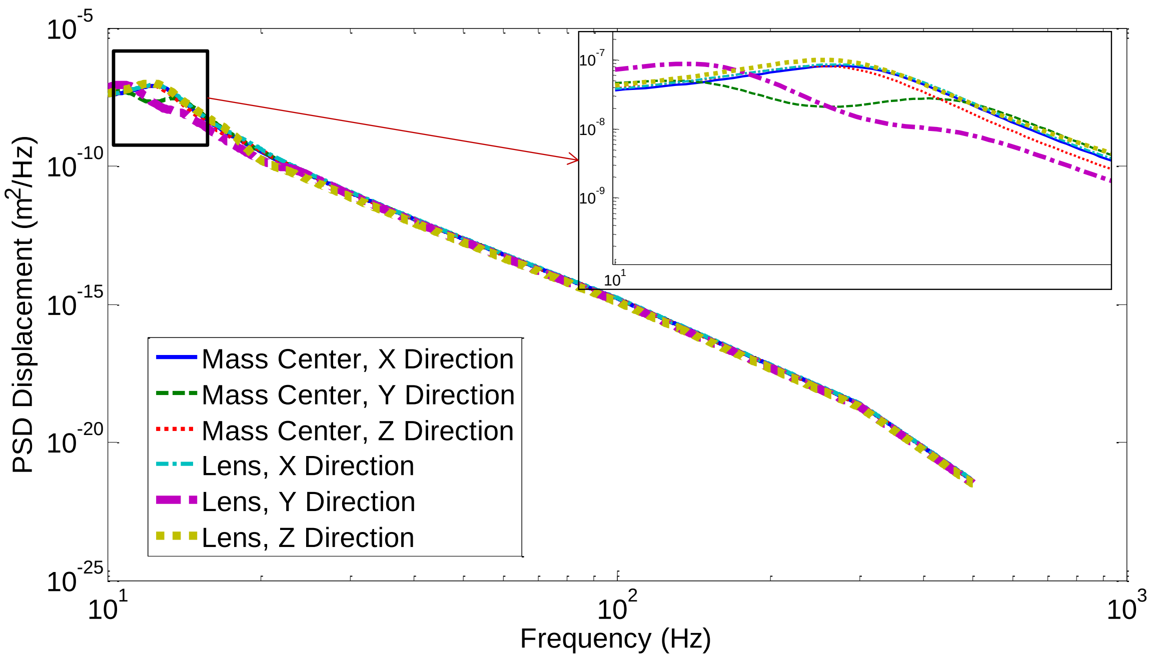

Figure 5.12 Response PSD Displacement

5.2.3. Monte Carlo Simulations

In this section, the results obtained by implementing Monte Carlo simulation found in the vibration isolation analysis software are given.

Here, the number of simulation is set to 100. In all the cases, the maximum allowable deviation in stiffness values of isolators in each direction and the loss factor is fixed and set to 10% of the assigned values. The maximum deviation in the position of each isolator for each axis due to static loading is set to 2.0 mm. Additionally, the maximum value of the orientation angle of the isolators is set to 2 degrees about each orthogonal axis.

Monte Carlo simulation is run in accordance with the above points and the results are presented in the following figures. Below, the deviation in the values of the first 6 natural frequencies is given in Figure 5.13; the deviation of static deflection of each isolator in each axis is given in Figure 5.14; the deviations in the response PSD acceleration and displacement curves and the corresponding rms acceleration and displacement amplitudes for the point at mass center in each axis are given in Figure 5.15 and Figure 5.16. Finally, the deviations in the harmonic acceleration and displacement amplitudes of the point at mass center for the corresponding excitation frequencies in each axis is given in Figure 5.17. Additionally, in order to investigate the corresponding deviations more clear, the normalized acceleration values with respect to natural frequencies are figured out in Appendix-B.

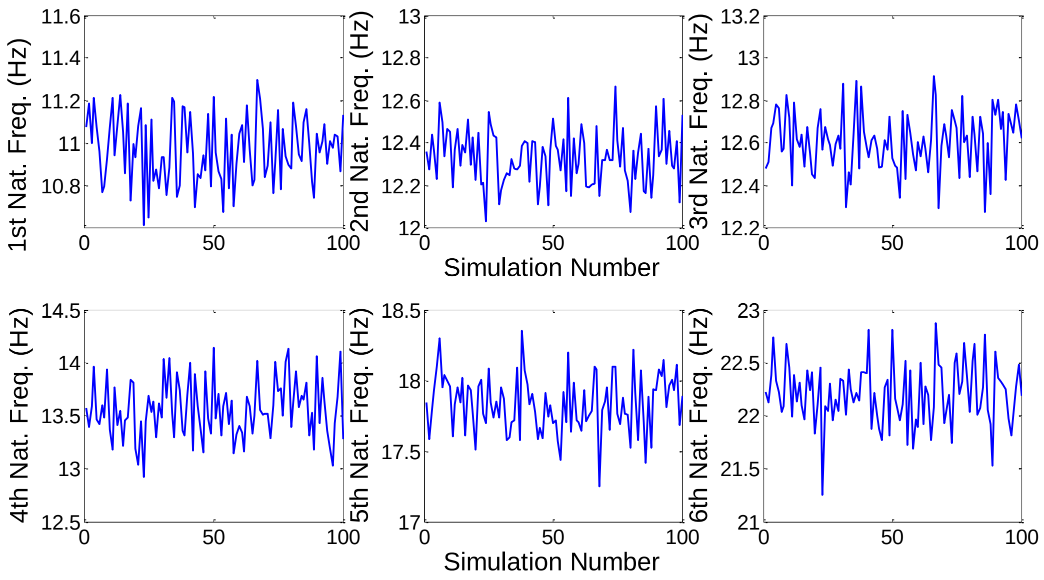

Figure 5.13 Deviation in Natural Frequencies

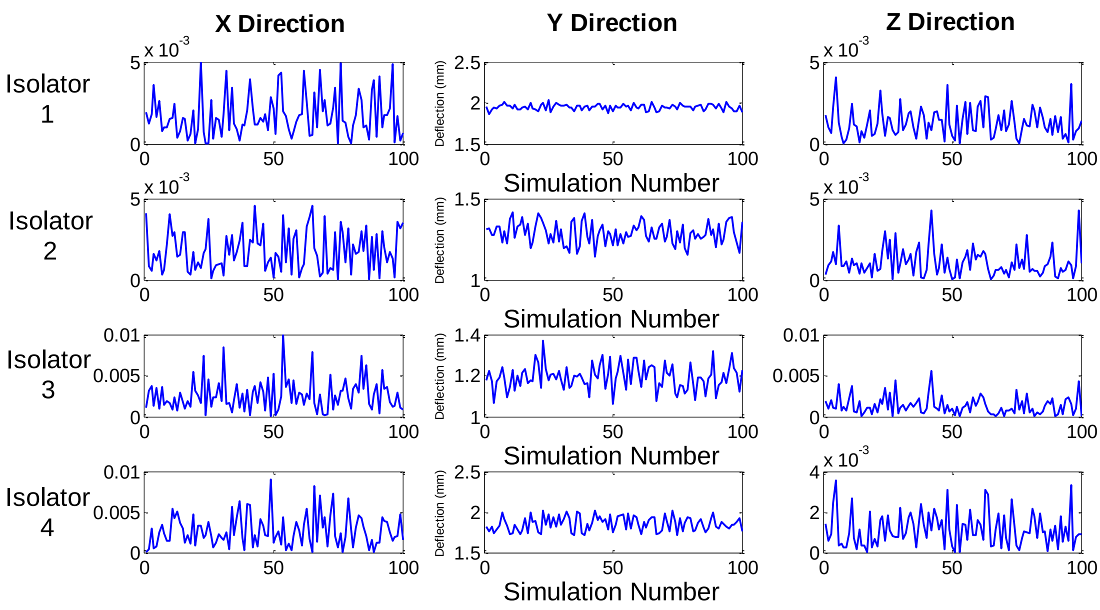

Figure 5.14 Deviation in Static Deflection of Isolators in Each Axis

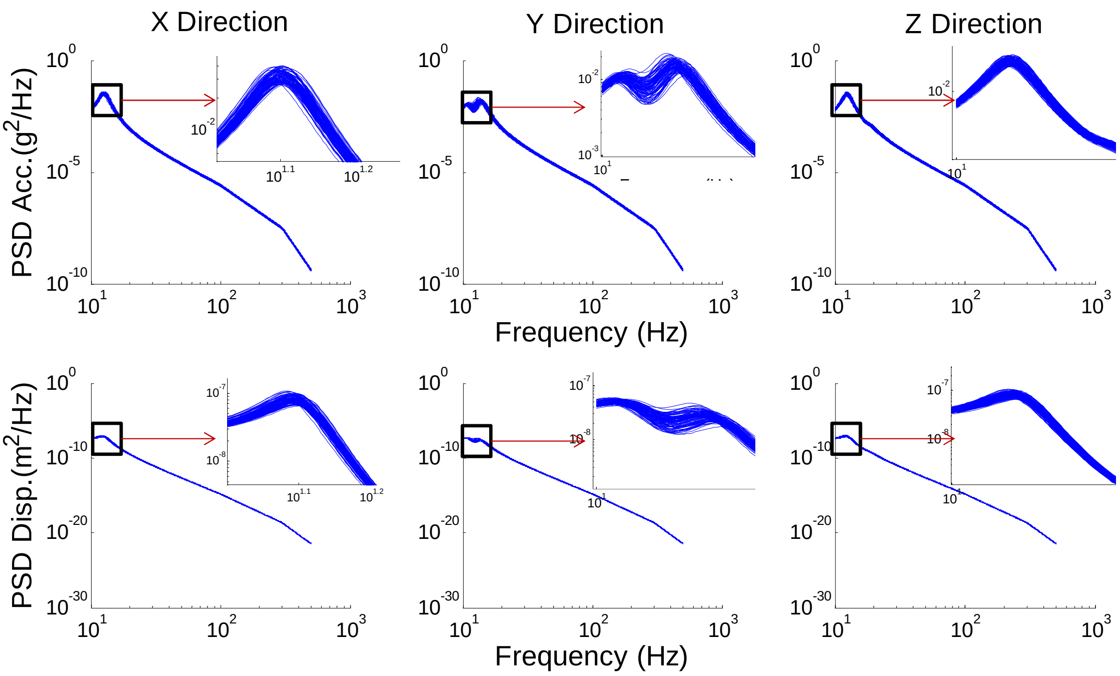

Figure 5.15 Deviation in Response PSD Acceleration and Displacement of Mass Center

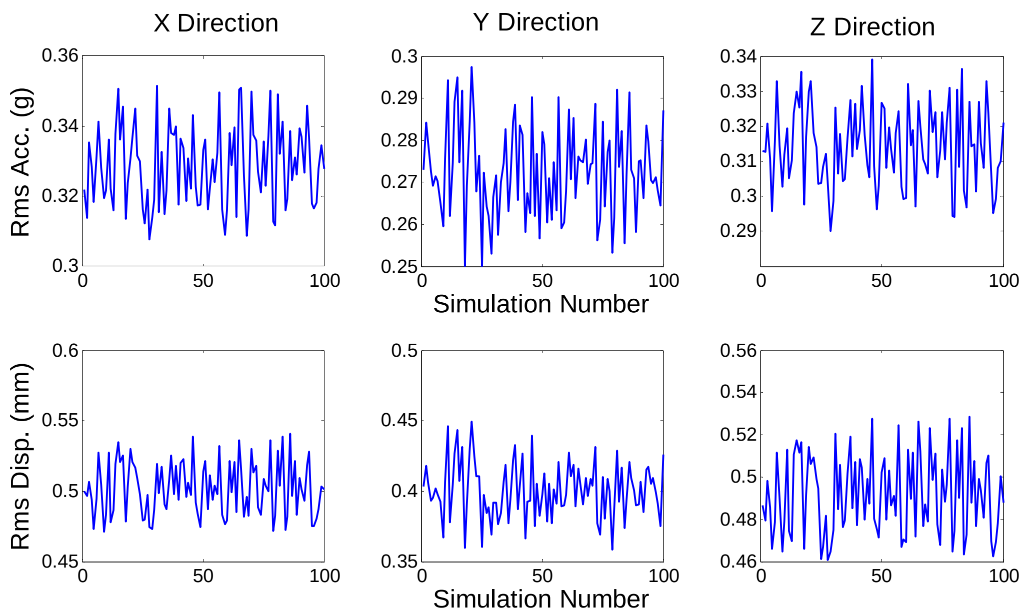

Figure 5.16 Deviation in rms Acceleration and Displacement of Mass Center

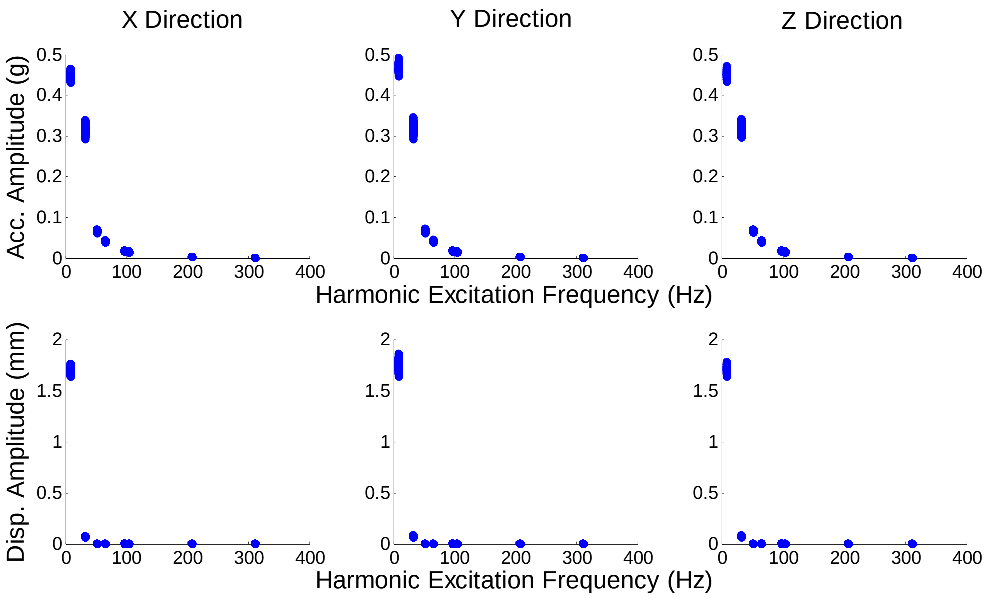

Figure 5.17 Deviation in Harmonic Acceleration and Displacement Amplitudes of Mass Center

5.3. Demonstration of Optimization Capabilities

This section aims to demonstrate the optimization capabilities of the developed software. Here, two types of optimization studies are investigated. One is the parameter optimization and the other is location optimization. The mechanical structure that is taken into consideration is the same as mentioned in the previous case study. However, in this section, the mechanical system is assumed to be mounted on a military aircraft, C130-B as seen in Figure 5.18.

Figure 5.18 C-130B Aircraft [41]

The aircraft has a random type of vibration excitation in three orthogonal axes. The harmonic vibration due to the propellers of the aircraft causes narrowband peaks on the profile. Using the military standard [32], it is possible to obtain the overall vibration profile as in Figure 5.19.

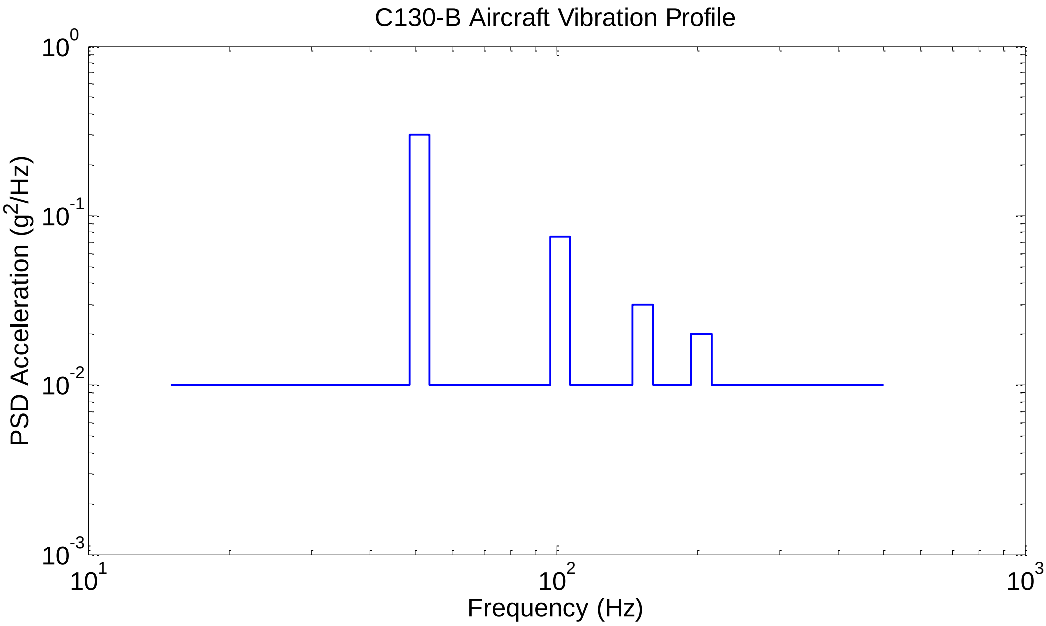

Figure 5.19 Random Vibration Profile of C130-B Aircraft

For both parameter and location optimization studies, the aim is to minimize the total acceleration encountered on the points of interest, the point at mass center and the point where the optical lens is located. In other words, the optimization algorithm is run in order to minimize the value obtained in Eq. (70). Here, the weight factor, K is the same for each point and it is set to 1, assuming both points are equally important.

The maximum deflection limit of the isolators in each direction due to static loading is set to 1.5 mm. For each case, the maximum rotation of the rigid body is limited to 2 degrees about each axis. The alignment and stability constraints are also set to the same values for each case. Those are 0.1 Hz and 10 Hz respectively. For the given vibrating platform, the maximum response RMS acceleration limit in each direction is set to 0.8 g-rms; in addition, the maximum response RMS displacement limit in each direction is set to 1 mm-rms for the points of interest.

Below, in Figure 5.20, both parameter and location optimization studies are divided into 4 sub-cases. Here, Case-1 and Case-2 are for single type of isolator with fixed and unfixed mounting; Case-3 and Case-4 are for different type of isolator with fixed and unfixed mounting, respectively. Additionally, Case-5 and Case-6 investigate discrete location optimization with fixed and unfixed parameters; on the other hand, Case-7 and Case-8 investigate continuous location optimization with fixed and unfixed parameters, respectively.

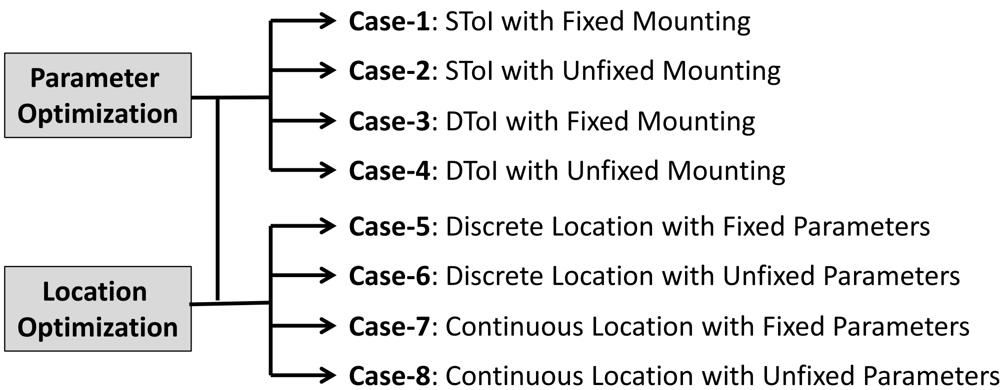

Figure 5.20 Types of Optimization and Case Studies Investigated

5.3.1. Parameter Optimization

For this type of optimization study, the position of the isolators is fixed as in Figure 5.21, from which it can be seen that the number of isolators used to support the mechanical structure is 4. Here, the optimization algorithm is run in order to find the optimum values for the stiffness and inclination angle of the isolators. The loss factor is set to 0.2 for each case.

For this type of optimization study, four different cases are investigated as seen in Figure 5.20.

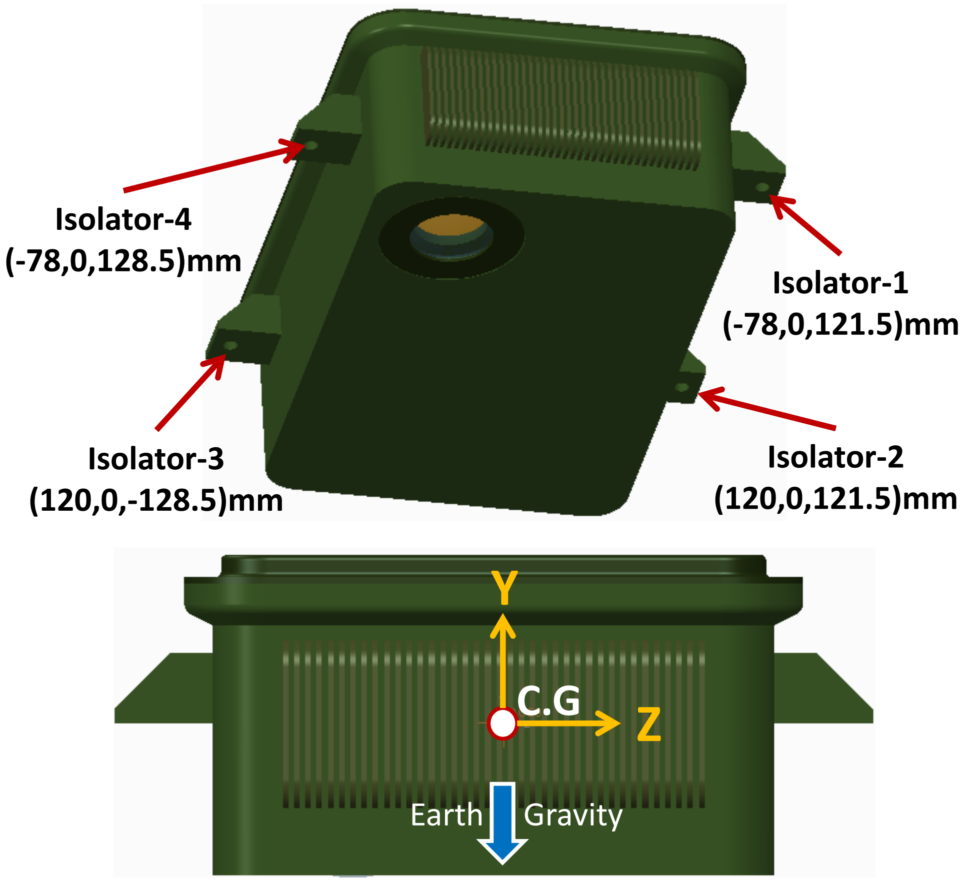

Figure 5.21 Isolator Location Information Used In Location Optimization

5.3.1.1. Case-1 and Case-2: Single Type of Isolators with Fixed and Unfixed Mounting

In this section, a single type of isolator is assumed to be used in vibration isolation design. The optimization software is run for a few times and the best three results are listed as in Table 5.10 and Table 5.11. In those tables, the optimum values are found for both fixed and unfixed types of isolators as described in Table 2.1. In other words, for the former case, the optimization design parameters are defined as the stiffness coefficients only; on the other hand, for the latter case, the optimization design parameters are the stiffness and the inclination angle. Here, for both Case-1 and Case-2, the axial to radial stiffness ratio is fixed. This ratio is set to 1.0 for the isolators mounted in orthogonal direction. However, to be reasonable, the ratio should be different than 1.0 for the inclined isolators. For Case-2, it is assumed to be 1.2. Additionally, the stiffness coefficient for the isolator is limited from 10 kN/m to 20 kN/m. Finally, for the case of inclined isolators, the rotational angle about each axis is limited from -45° to $+45^{\circ}$.

The objective function values for each attempt are given in Table 5.10 and Table 5.11. Additionally, from Table 5.12 to Table 5.16, the corresponding acceleration and displacement response RMS values, natural frequencies for all modes, static deflection of each isolator in each axis in addition to the values of the rotation of the rigid body due to static loading can be obtained for each attempt respectively. Here, it should also be remarked that the initial design of the engineer for the acceleration minimization is shown as in the zeroth attempt. For this trial, in order to implement minimization for acceleration, the stiffness value for the isolators is manually selected as the minimum of the given range which is 10 kN/m. For this assumption, the maximum static deflection limit is exceeded and penalty function is added to the overall objective function, since it is an undesired condition.

Assuming the stiffness values are the optimum values found from the optimization study, the results for the objective function of single type isolators are listed in Table 5.10 for Case-1. Additionally, considering the inclined isolator case (Case-2), the results for objective functions can be compared in Table 5.11. If those tables are investigated, it is easily observed that the predefined design constraints are not exceeded for each attempt of optimization study for single type of isolators for fixed and unfixed type of mounting conditions.

Table 5.10 Optimum Design Parameters, Objective Function and Penalty Function for SToI with Fixed Mounting

Case-1: Single Type of Isolators with Fixed Mounting				
Attempt	**Optimization Parameter**	**Axial to Radial Stiff. Ratio**	**Objective Function (g-rms)**	**Penalty Function**
	Stiffness (N/m)			
0	10000	1.0	0.94	Static Deflection
1	13542	1.0	1.81	None
2	13323	1.0	1.75	None
3	13366	1.0	1.76	None

Table 5.11 Optimum Design Parameters, Objective Function and Penalty Function for SToI with Unfixed Mounting

Case-2: Single Type of Isolators with Unfixed Mounting								
Attempt	**Optimization Parameter**					**Axial To Radial Stiff. Ratio**	**Objective Function (g-rms)**	**Penalty Function**
	Axial Stiffness (N/m)	**Inclination Angle (degree)**						
		Isolator Number	**Around**					
			X	**Y**	**Z**			
1	14637	1	-7.9	-0.3	5.4	1.2	1.56	None
		2	-7.5	40.1	-10.0			
		3	-0.2	1.9	-0.7			
		4	6.5	2.5	5.8			
2	14998	1	-15.9	2.9	-17.0	1.2	1.64	None
		2	-2.8	5.3	-15.0			
		3	1.2	-1.6	-1.7			
		4	4.5	44.3	24.9			
3	14625	1	-0.9	-1.4	-0.1	1.2	1.56	None
		2	-0.4	1.1	-2.2			
		3	2.4	-37.9	-2.3			
		4	3.9	0.1	7.3			

Table 5.12 Acceleration and Displacement Response rms Values for SToI with Fixed and Unfixed Mounting

Condition	Attempt Number	Axis	Acceleration (g-rms)		Displacement (mm-rms)	
			C.G.	Lens	C.G.	Lens
Case-1 Fixed Mounting	0	X	0.32229	0.34138	0.26673	0.28095
		Y	0.34454	0.2429	0.29087	0.19039
		Z	0.30107	0.32493	0.23932	0.28525
	1	X	0.65909	0.68716	0.58975	0.61208
		Y	0.61273	0.40016	0.51711	0.32289
		Z	0.59151	0.66938	0.52187	0.60531
	2	X	0.63363	0.66132	0.5661	0.5882
		Y	0.60119	0.3916	0.51079	0.31687
		Z	0.56787	0.64295	0.49912	0.58082
	3	X	0.63864	0.66641	0.57078	0.59293
		Y	0.60352	0.39329	0.51212	0.31806
		Z	0.57248	0.64812	0.50358	0.58562
Case-2 Unfixed Mounting	1	X	0.51268	0.54308	0.45061	0.47556
		Y	0.65729	0.44133	0.53633	0.3532
		Z	0.45868	0.5148	0.39269	0.45982
	2	X	0.56055	0.58936	0.49654	0.51914
		Y	0.65157	0.43031	0.52255	0.33944
		Z	0.48944	0.55056	0.42308	0.49234
	3	X	0.5073	0.54957	0.44552	0.4809
		Y	0.65913	0.44249	0.53587	0.35366
		Z	0.45583	0.51294	0.38979	0.45889

Table 5.13 Natural Frequencies for SToI with Fixed and Unfixed Mounting

Mode Number	Natural Frequency (Hz)						
	Case-1 Fixed Mounting				Case-2 Unfixed Mounting		
	Attempt Number				Attempt Number		
	0	1	2	3	1	2	3
1	11.0	12.8	12.7	12.7	13.2	13.2	13.2
2	12.4	14.4	14.3	14.3	13.7	13.8	13.7
3	12.6	14.6	14.5	14.5	13.9	14.2	13.9
4	13.6	15.8	15.7	15.7	16.4	16.6	16.4
5	17.8	20.8	20.6	20.6	19.8	20.1	19.7
6	22.2	25.8	25.6	25.6	26.8	26.9	26.8

Table 5.14 Static Deflection Values for the Isolators for SToI with Fixed Mounting

Isolator Number	Case-1 Static Deflection (mm)											
	Attempt 0			Attempt 1			Attempt 2			Attempt 3		
	X	Y	Z	X	Y	Z	X	Y	Z	X	Y	Z
1	0	1.94	0	0	1.44	0	0	1.46	0	0	1.46	0
2	0	1.28	0	0	0.94	0	0	0.96	0	0	0.96	0
3	0	1.19	0	0	0.89	0	0	0.89	0	0	0.89	0
4	0	1.86	0	0	1.34	0	0	1.39	0	0	1.39	0

Table 5.15 Static Deflection Values for the Isolators for SToI with Unfixed Mounting

Isolator Number	Case-2 Static Deflection (mm)								
	Attempt 1			Attempt 2			Attempt 3		
	X	Y	Z	X	Y	Z	X	Y	Z
1	0.01	1.34	0	0.03	1.34	0.01	0	1.33	0.01
2	0.01	0.88	0.01	0.03	0.86	0.04	0	0.87	0
3	0.01	0.82	0.01	0.02	0.80	0.04	0.01	0.82	0
4	0.01	1.27	0	0.02	1.28	0.01	0.01	1.27	0.01

Table 5.16 Rotation of the Rigid Body Due to Static Loading for SToI with Fixed and Unfixed Mounting

Condition	Attempt Number	Rotation Due to Static Loading (^{0})		
		About X Axis	About Y Axis	About Z Axis
Case-1 Fixed Mounting	**0**	0.0201	0	0.1925
	1	0.0149	0	0.1421
	2	0.0151	0	0.1445
	3	0.0151	0	0.144
Case-2 Unfixed Mounting	**1**	0.0152	-0.0036	0.1316
	2	0.0134	-0.0124	0.1393
	3	0.0132	-0.0025	0.1323

5.3.1.2. Case-3 and Case-4: Different Types of Isolators with Fixed and Unfixed Mounting

Different from the previous case, the isolators supporting the optomechanical structure is not a single type. In this section, the isolators are made available to have different stiffness values. In other words, rather than using a one type of isolator on the predefined locations, the designer is free to use isolators with different stiffness values. Here, by doing so that it is aimed to decrease the value of the objective function more to some extent.

The best three results obtained from the software are listed in Table 5.17 and Table 5.18 for Case-3 and Case-4, respectively.. In these tables, the optimum values are found for both fixed and unfixed types of isolators as mentioned in the previous section. However, for this case, the axial to radial stiffness ratio is assumed to be another optimization design parameter. The limit for the ratio is defined between 1.0 to 1.2. Additionally, the stiffness coefficient for the isolator is also limited from 10 kN/m to 20 kN/m. Finally, for the inclined isolators case, the rotational angle about each axis is limited from -45° to $+45^{\circ}$ as in the previous case study.

Below, from Table 5.17 and Table 5.18, the optimum values of the stiffness for each isolator, the axial to radial stiffness ratio and the inclination angles of each isolator are obtained. The objective values can also be compared using those corresponding tables. Additionally, from Table 5.19 to Table 5.23, the corresponding acceleration and displacement response RMS values, natural frequencies for all modes, static deflection of each isolator in each axis, in addition to the values of the rotation of the rigid body due to static loading, are obtained for each attempt, respectively. If the tables below are investigated, it is easily observed that the predefined design constraints are not exceeded for each attempt.

Comparing the best values obtained for the objective functions of SToI cases (Cases 1 and 2) from the previous section and the cases investigated here, it can be concluded that the objective value decreases by 9.6%.

Table 5.17 Optimum Design Parameters, Objective Function and Penalty Function for DToI with Fixed Mounting

Case-3: Different Type of Isolators with Fixed Mounting					
Attempt Number	Isolator Number	Optimization Parameter	Axial To Radial Stiffness Ratio	Objective Function (g-rms)	Penalty Function
		Stiffness (N/m)			
1	1	19539	1.0	1.60	None
	2	10000			
	3	10000			
	4	10830			
2	1	11643	1.0	1.58	None
	2	10588			
	3	10002			
	4	18907			
3	1	11506	1.0	1.61	None
	2	10675			
	3	10000			
	4	19489			

Table 5.18 Optimum Design Parameters, Objective Function and Penalty Function for DToI with Unfixed Mounting

Case-4: Different Type of Isolators with Unfixed Mounting								
Attempt	Isolator Number	Optimization Parameter					Objective Function (g-rms)	Penalty Function
		Axial Stiffness (N/m)	Inclination Angle (degree)			Axial To Radial Stiff. Ratio		
			Around					
			X	Y	Z			
1	1	14999	-1.3	45.0	-1.3	1.2	1.41	None
	2	11001	1.6	-1.0	0.7	1.0		
	3	15000	3.5	-0.6	-0.1	1.2		
	4	11002	2.6	3.6	0.6	1.0		
2	1	14998	45	4.4	4.2	1.2	1.57	None
	2	11002	2.3	5.3	1.8	1.0		
	3	11002	0.6	0.8	3.7	1.0		
	4	14998	0.2	-43.8	43.7	1.04		
3	1	14998	-2.0	0.3	1.2	1.2	1.45	None
	2	14998	0.3	-1.3	-0.7	1.2		
	3	14000	0.1	5.4	2.6	1.2		
	4	14000	6.3	2.5	1.0	1.2		

Table 5.19 Acceleration and Displacement Response rms Values for DToI with Fixed and Unfixed Mounting

Condition	Attempt Number	Axis	Acceleration (g-rms)		Displacement (mm-rms)	
			C.G.	Lens	C.G.	Lens
Case-3 Fixed Mounting	1	X	0.50308	0.53957	0.43627	0.48255
		Y	0.50389	0.52319	0.44101	0.4585
		Z	0.55127	0.58575	0.48781	0.50727
	2	X	0.51497	0.49497	0.44739	0.40769
		Y	0.51346	0.44812	0.45003	0.35896
		Z	0.57266	0.61433	0.50836	0.53301
	3	X	0.52082	0.49998	0.4524	0.41004
		Y	0.519	0.45353	0.45523	0.36016
		Z	0.58805	0.63281	0.5231	0.54815
Case-4 Unfixed Mounting	1	X	0.46216	0.4928	0.4016	0.42741
		Y	0.5918	0.37514	0.51336	0.30617
		Z	0.41782	0.47165	0.3522	0.41994
	2	X	0.50889	0.49991	0.44611	0.4294
		Y	0.55367	0.46493	0.48956	0.40003
		Z	0.53455	0.57609	0.47096	0.51607
	3	X	0.49658	0.54997	0.43525	0.48368
		Y	0.45152	0.45152	0.53511	0.36329
		Z	0.44645	0.50021	0.38044	0.44791

Table 5.20 Natural Frequencies for DToI with Fixed and Unfixed Mounting

Mode Number	Natural Frequency (Hz)					
	Case-3 Fixed Mounting			Case-4 Unfixed Mounting		
	Attempt Number			Attempt Number		
	1	2	3	1	2	3
1	12.7	13	13	12.4	12.9	13.2
2	13.9	14	14	13.4	13.9	13.6
3	14	14	14.1	13.6	14.1	13.8
4	14.1	14.2	14.3	15.3	14.4	16.4
5	19.6	19.9	20	19.3	19.6	19.6
6	25.1	25.3	25.4	25.5	24.9	26.6

Table 5.21 Static Deflection Values of the Isolators for DToI with Fixed Mounting

Isolator Number	Case-3 Static Deflection (mm)								
	Attempt 1			Attempt 2			Attempt 3		
	X	Y	Z	X	Y	Z	X	Y	Z
1	0	1.12	0	0	1.5	0	0	1.5	0
2	0	1.04	0	0	1.4	0	0	1.4	0
3	0	1.43	0	0	1	0	0	1	0
4	0	1.5	0	0	1.1	0	0	1.1	0

Table 5.22 Static Deflection Values of the Isolators for DToI with Unfixed Mounting

Isolator Number	Case-4 Static Deflection (mm)								
	Attempt 1			Attempt 2			Attempt 3		
	X	Y	Z	X	Y	Z	X	Y	Z
1	0	1.46	0	0	1.40	0.05	0	1.31	0.01
2	0	0.95	0	0	1.19	0.02	0	0.85	0
3	0	0.96	0	0.03	1.06	0.02	0.01	0.86	0
4	0	1.47	0	0.03	1.28	0.06	0.01	1.32	0.01

Table 5.23 Rotation of the Rigid Body Due to Static Loading for DToI with Fixed and Unfixed Mounting

Condition	Attempt Number	Rotation Due Static Loading (^{0})		
		About X Axis	About Y Axis	About Z Axis
Case-3 Fixed Mounting	1	-0.0876	0	0.0206
	2	0.0936	0	0.0285
	3	0.0993	0	0.0273
Case-4 Unfixed Mounting	1	-0.0026	0	0.1487
	2	0.0286	-0.0074	0.0630
	3	-0.0035	-0.0017	0.1333

5.3.2. Location Optimization

Different from the study of parameter optimization, the optimization parameters are selected for not only the isolator parameters but also for the location of the isolators in this section. In this type of optimization study, the possible locations of the isolator mounts involve discrete or continuous points as shown in Figure 5.22 and Figure 5.23. In Figure 5.22, the boundary of the region where the discretized points can be located is shown. Here, the distance between each discretized point is exactly 10 millimeters. Considering the dimension of the possible region which is 80x230 mm; the number of possible points on one surface is 216. Since there is one another surface on the other side, the total number of points where the isolators can be located is 432. On the other hand, in Figure 5.23, the possible region of continuous points where the isolator mounts can be located is shown in yellow color. The dimension of the region is the same with the case of discrete points.

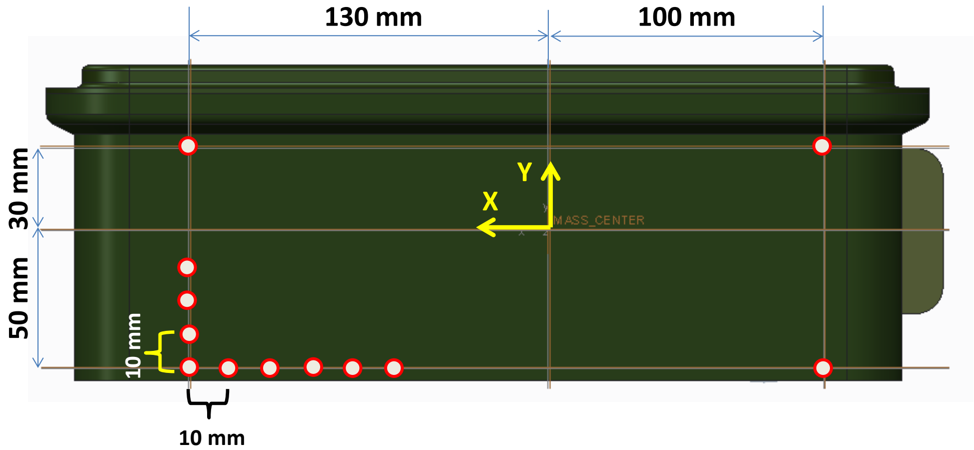

Figure 5.22 Discretized Points on the Optomechanical Structure

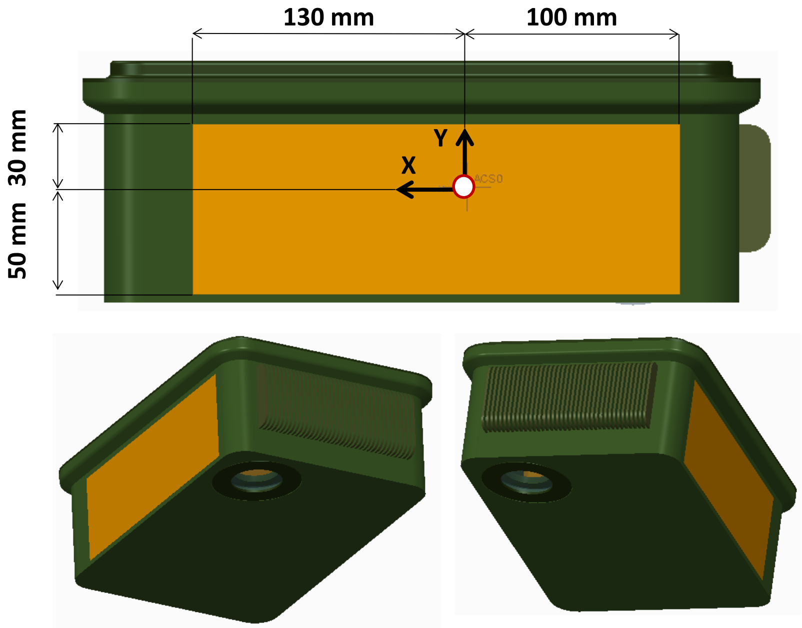

Figure 5.23 Continuous Points on the Optomechanical Structure

5.3.2.1. Case-5 and Case-6: Discrete Location Optimization with Fixed and Unfixed Parameters

In this type of optimization study, it is desired to demonstrate the capabilities of discrete location optimization with fixed and unfixed parameters using the developed software. For fixed parameters case, Case-5, the software determined the optimum location of each isolator with defined stiffness values for both axial and radial stiffnesses. On the other hand, for unfixed parameters case, Case-6, the optimum location of the isolators, axial stiffness values with the ratios of axial stiffness to radial stiffness are obtained within predefined constraints. Here, same as before, the stiffness of the isolators is limited between 10 kN/m and 20 kN/m. Additionally, the axial to radial stiffness ratio is assumed to be between 1.0 and 1.2.

The optimization software is run and the best three results are listed in Table 5.24 and Table 5.25 for Case-5 and Case-6, respectively. In Case-5, the stiffness values for the isolators are selected as the minimum of the given range for stiffness which is 10 kN/m. In this section, for the minimum value of the stiffness, the study of location optimization is implemented. However, for each trial, static deflection limit is exceeded. Considering this fact, the location optimization is conducted for different stiffness values such as 11000 N/m and 12000 N/m. Comparing the best value obtained for the objective function of Case-3, which is DToI case for fixed type of mounting, and Case-5 for fixed parameters of 11000 N/m and 12000 N/m stiffness values, the objective functions get better by 26% and 11.4%, respectively. On the other hand, if the results of Case-4, which is DToI case for unfixed type of mounting and Case-6 for unfixed parameters are compared, it is observed that the objective function is improved 18.4%.

From Table 5.24 and Table 5.25, it should also be noticed that the objective function is obtained as 0.90 g-rms, which is the lowest value considering all cases. However, for both Case-5 and Case-6, static deflection constraint is exceeded as shown in Table 5.28 and Table 5.29. For those cases, the static deflections of the isolators in Y direction are found as 2.92 mm and 2.91 mm, respectively. These are about 1.9 times of the maximum deflection limit due to static loading. As a result of these excessive static deflection values, the proposed optimum values are eliminated directly.

For other design constraints such as acceleration and displacement response rms values of the points of interest for both Case-5 and Case-6, Table 5.26 can be referred. On the other hand, in order to compare the natural frequencies, static deflection of each isolator in each axis, in addition to the values of the rotation of the rigid body due to static loading for each attempt, the tables from Table 5.27 to Table 5.30 can be used.

Table 5.24 Optimum Design Parameters, Objective Function and Penalty Function for Discrete Location Optimization with Fixed Parameters

Case-5: Discrete Location Optimization							
Attempt Number	**Isolator Number**	**Input Parameter Stiffness in All Axis (N/m)**	**Optimization Parameter**			**Objective Function (g-rms)**	**Penalty Function**
			X Axis (mm)	**Y Axis (mm)**	**Z Axis (mm)**		
1	**1**	12000	120	0	-128.5	1.40	None
	2		-100	20	-128.5		
	3		130	30	121.5		
	4		-100	0	121.5		
2	**1**	11000	130	30	-128.5	1.17	None
	2		-50	30	121.5		
	3		-100	-50	-128.5		
	4		40	-20	121.5		
3	**1**	10000	-10	20	-128.5	0.90	Static Deflection
	2		20	-50	121.5		
	3		130	30	121.5		
	4		-100	30	121.5		

Table 5.25 Optimum Design Parameters, Objective Function and Penalty Function for Discrete Location Optimization with Unfixed Parameters

Case-6: Parameter and Discrete Location Optimization								
Attempt Number	**Isolator Number**	**Optimization Parameter**					**Objective Function (g-rms)**	**Penalty Function**
		Axial Stiffness (N/m)	**X Axis (mm)**	**Y Axis (mm)**	**Z Axis (mm)**	**Axial to Radial Stiff. Ratio**		
1	**1**	10001	-100	30	121.5	1.0	1.27	None
	2	13883	40	-50	-128.5	1.1		
	3	13869	130	30	121.5	1.2		
	4	10761	-100	-50	-128.5	1.05		
2	**1**	10162	-100	-30	121.5	1.01	0.90	Static Deflection
	2	10012	-90	30	121.5	1.0		
	3	10586	130	30	121.5	1.0		
	4	10085	40	-30	-128.5	1.0		
3	**1**	10924	-100	-40	121.5	1.0	1.15	None
	2	10750	-60	30	-128.5	1.01		
	3	10920	130	30	121.5	1.0		
	4	10924	30	30	-128.5	1.0		

Table 5.26 Acceleration and Displacement Response rms Values for Discrete Location Optimization with Fixed and Unfixed Mounting for Fixed and Unfixed Parameters

Condition	Attempt Number	Direction	Acceleration (g-rms)		Displacement (mm-rms)	
			C.G.	Lens	C.G.	Lens
Case-5 Fixed Parameters	1	X	0.47364	0.4323	0.4051	0.37241
		Y	0.47298	0.42992	0.40467	0.37294
		Z	0.45336	0.52868	0.3915	0.46736
	2	X	0.39525	0.40253	0.33649	0.33915
		Y	0.39636	0.36484	0.33796	0.30602
		Z	0.39275	0.39466	0.3336	0.34058
	3	X	0.304	0.1802	0.20647	0.13206
		Y	0.20805	0.28272	0.11621	0.21258
		Z	0.32095	0.50436	0.26426	0.37877
Case-6 Unfixed Parameters	1	X	0.39584	0.40366	0.33641	0.33123
		Y	0.50149	0.46243	0.44003	0.39751
		Z	0.39159	0.38085	0.33303	0.3116
	2	X	0.27618	0.23225	0.17305	0.18699
		Y	0.21282	0.21068	0.12255	0.16279
		Z	0.33684	0.53583	0.28032	0.38191
	3	X	0.39376	0.34674	0.33574	0.28716
		Y	0.38567	0.39073	0.32749	0.32572
		Z	0.37247	0.40844	0.31407	0.34643

Table 5.27 Natural Frequencies for Fixed and Unfixed Parameters

Mode Number	Natural Frequency (Hz)					
	Case-5 Fixed Parameters			Case-6 Unfixed Parameters		
	Attempt Number			Attempt Number		
	1	2	3	1	2	3
1	13.1	11.6	10.0	11.8	10.3	11.1
2	13.6	13.2	10.7	13.2	10.9	13.0
3	13.8	13.2	11.2	13.4	12.2	13.1
4	15.6	13.3	12.6	14.0	12.7	13.4
5	20.4	17.6	17.6	19.2	18.5	17.6
6	24.6	24.3	23.6	25.7	24	24.0

Table 5.28 Static Deflection Values of the Isolators for Fixed Parameters

Isolator Number	Case 5 Static Deflection (mm)								
	Attempt 1			Attempt 2			Attempt 3		
	X	Y	Z	X	Y	Z	X	Y	Z
1	0.01	1.13	0.01	0.03	1.3	0	0.01	2.92	0.09
2	0.01	1.41	0	0.02	1.5	0.01	0.05	1.11	0.41
3	0.02	1.20	0	0.03	1.48	0.01	0.02	1.02	0.17
4	0.02	1.49	0	0.04	1.43	0.01	0.02	1.22	0.16

Table 5.29 Static Deflection Values of the Isolators for Unfixed Parameters

Isolator Number	Case-6 Static Deflection (mm)								
	Attempt 1			Attempt 2			Attempt 3		
	X	Y	Z	X	Y	Z	X	Y	Z
1	0.01	1.48	0.05	0.04	1.2	0.21	0.01	1.49	0.01
2	0.01	1.18	0.03	0.05	1.2	0.24	0	1.41	0.01
3	0.01	1.25	0	0.05	0.87	0.21	0	1.46	0
4	0.01	1.32	0	0.08	2.91	0.24	0	1.41	0

Table 5.30 Rotation of the Rigid Body Due to Static Loading

Condition	Attempt Number	Rotation Due Static Loading (^{0})		
		About X Axis	About Y Axis	About Z Axis
Case-5 Fixed Mounting	1	0.0181	0.0010	0.0734
	2	0.0140	0.0028	0.0443
	3	-0.4085	0.0012	0.0493
Case-6 Unfixed Mounting	1	0.0356	0.0124	0.0554
	2	-0.4387	-0.0092	0.0849
	3	0.0157	0	0.0053

5.3.2.2. Case-7 and Case-8: Continuous Location Optimization with Fixed and Unfixed Parameters

In this type of optimization study, it is desired to demonstrate the capabilities of continuous location optimization with fixed and unfixed parameters using the developed software. Rather than having discrete positions for the possible isolator locations, in this section, the possible region for the isolator locations is continuous.

Same as before, for Case-7 which is the case of fixed parameters, the software obtained the optimum location of each isolator with predefined stiffness value. On the other hand, for Case-8 which is the case of unfixed parameters, the optimum location information for the isolators and the axial stiffness of the isolators with the ratio of axial stiffness to radial stiffness are obtained within the predefined constraints. Here, similar to the previous case studies, the stiffness of the isolators is limited between 10 kN/m and 20 kN/m. Additionally, the ratio of the axial stiffness to radial stiffness is assumed to be between 1.0 and 1.2.

The optimization software is run and the best three results for Case-7 and Case-8 are listed in Table 5.31 and Table 5.32, respectively. The stiffness value is selected as 11 kN/m for Case-7. If Table 5.24 is investigated, it is observed that the minimum value for the objective function without exceeding the design constraints has been obtained for 11 kN/m. In Case-7, it is expected to obtain a better value of the objective function for continuous location optimization. However, if the results for the objective function given in Table 5.24 and Table 5.31 are compared, the best value for each case remains constant. This shows that for a specific stiffness (which is 11 kN/m) defined in all axis has similar response amplitudes for different positions of orthogonal isolators found using the optimization software.

On the other hand, the study of continuous location optimization of unfixed parameters results in better objective functions. Here in Case-8, as mentioned before, optimum location of the isolators in addition to axial stiffness and the ratio of the axial stiffness to radial stiffness are given in Table 5.32. If the values of the objective function are compared with the values obtained from Case-6, the objective function decreases by 5.2%.

If noticed from Table 5.31 and Table 5.32, there is no violation of the design constraints for Case-7 and Case-8. Therefore, no penalty function exists for the proposed design variables. However, it would also be beneficial to share acceleration and displacement response rms values of the points of interest for both cases; the natural frequencies of each attempt, static deflections of the isolators and the rotation of the rigid body due to static loading are given in tables from Table 5.33 to Table 5.37.

Table 5.31 Optimum Design Parameters, Objective Function and Penalty Function for Continuous Location Optimization with Fixed Parameters

Case-7: Continuous Location Optimization							
Attempt Number	Isolator Number	Input Parameter Stiffness in All Axis (N/m)	Optimization Parameter			Objective Function (g-rms)	Penalty Function
			X Axis (mm)	Y Axis (mm)	Z Axis (mm)		
1	1	11000	-32	14	121.5	1.17	None
	2		-98	14	-128.5		
	3		128	-2	-128.5		
	4		22	-6	121.5		
2	1	11000	-100	-50	-128.5	1.17	None
	2		130	10	-128.5		
	3		-62	8	121.5		
	4		48	18	121.5		
3	1	11000	-100	-50	-128.5	1.18	None
	2		130	30	121.5		
	3		-94	12	121.5		
	4		70	-6	-128.5		

Table 5.32 Optimum Design Parameters, Objective Function and Penalty Function for Continuous Location Optimization with Unfixed Parameters

Case-8: Parameter and Continuous Location Optimization								
Attempt Number	Isolator Number	Optimization Parameter					Objective Function (g-rms)	Penalty Function
		Axial Stiffness (N/m)	X Axis (mm)	Y Axis (mm)	Z Axis (mm)	Axial to Radial Stiff. Ratio		
1	1	10290	130	30	121.5	1.03	1.28	None
	2	12897	-92	30	121.5	1.11		
	3	12648	102	-50	-128.5	1.04		
	4	12999	-74	-46	-128.5	1.19		
2	1	10838	-98	24	121.5	1.07	1.09	None
	2	12824	-48	-48	-128.5	1.2		
	3	11125	130	30	121.5	1.08		
	4	10040	26	8	-128.5	1.0		
3	1	10089	66	-44	-128.5	1.0	1.11	None
	2	11026	-86	18	121.5	1.0		
	3	10520	130	30	121.5	1.0		
	4	11195	-98	-50	-128.5	1.0		

Table 5.33 Acceleration and Displacement Response rms Values for Continuous Location Optimization with Fixed and Unfixed Mounting for Fixed and Unfixed Parameters

Condition	Attempt Number	Direction	Acceleration (g-rms)		Displacement (mm-rms)	
			C.G.	Lens	C.G.	Lens
Case-7 Fixed Parameters	1	X	0.39658	0.38245	0.3379	0.32102
		Y	0.39605	0.36908	0.33763	0.30963
		Z	0.39077	0.41062	0.33149	0.36017
	2	X	0.3953	0.40243	0.33654	0.33846
		Y	0.39573	0.37099	0.33729	0.31159
		Z	0.39303	0.39207	0.33408	0.33611
	3	X	0.39508	0.39795	0.33638	0.33447
		Y	0.39542	0.37905	0.33693	0.31861
		Z	0.39485	0.39037	0.3363	0.33127
Case-8 Unfixed Parameters	1	X	0.4049	0.42335	0.34503	0.3486
		Y	0.49986	0.4316	0.43783	0.36431
		Z	0.38951	0.40183	0.32915	0.34051
	2	X	0.34232	0.33494	0.28576	0.27457
		Y	0.41011	0.39129	0.35106	0.32879
		Z	0.34151	0.35166	0.28504	0.29716
	3	X	0.37621	0.39168	0.31819	0.32496
		Y	0.37241	0.37688	0.3144	0.31229
		Z	0.36259	0.34704	0.30455	0.27749

Table 5.34 Natural Frequencies for Fixed and Unfixed Parameters

Mode Number	Natural Frequency (Hz)					
	Case-7 Fixed Parameters			Case-8 Unfixed Parameters		
	Attempt Number			Attempt Number		
	1	2	3	1	2	3
1	10.3	11.5	12.5	12.4	10.8	11.5
2	13.2	13.2	13.2	13.1	12.8	12.9
3	13.2	13.2	13.2	13.5	12.8	13
4	13.3	13.2	13.3	14.2	13.3	13.3
5	17.3	17.8	18.8	19.6	17.2	18.7
6	23.5	24.0	24.0	25.8	24.1	24

Table 5.35 Static Deflection Values of the Isolators for Fixed Parameters

Isolator Number	Case-7 Static Deflection (mm)								
	Attempt 1			Attempt 2			Attempt 3		
	X	Y	Z	X	Y	Z	X	Y	Z
1	0.01	1.49	0	0.02	1.46	0	0.01	1.41	0.01
2	0.01	1.50	0	0.02	1.32	0.01	0	1.43	0
3	0.01	1.28	0	0	1.50	0.01	0	1.50	0.01
4	0.01	1.44	0	0	1.43	0	0.01	1.37	0

Table 5.36 Static Deflection Values of the Isolators for Unfixed Parameters

Isolator Number	Case-8 Static Deflection (mm)								
	Attempt 1			Attempt 2			Attempt 3		
	X	Y	Z	X	Y	Z	X	Y	Z
1	0.02	1.2	0	0	1.50	0.02	0	1.43	0.01
2	0.02	1.50	0.05	0.01	1.35	0.02	0	1.5	0.01
3	0.02	1.09	0.05	0	1.44	0.01	0	1.49	0.01
4	0.02	1.30	0.01	0.01	1.33	0	0	1.44	0.01

Table 5.37 Rotation of the Rigid Body Due to Static Loading

Condition	Attempt Number	Rotation Due Static Loading (^{0})		
		About X Axis	About Y Axis	About Z Axis
Case-7 Fixed Parameters	1	0.0137	0	0.0565
	2	0.0150	0.0041	0.0351
	3	0.0197	0.0033	0.0157
Case-8 Unfixed Parameters	1	0.0408	0.0126	0.0678
	2	0.0313	0.0034	0.0155
	3	0.0138	0.0009	0.0014

5.3.3. Comparison of Optimization Types

This section is prepared in order to list the objective functions used in each optimization study and compute the corresponding isolation performance values. Below, in Table 5.38, the values for the objective functions are listed for each case. If the table is investigated, considering the best values for each case, the objective values are reduced from 1.75 g-rms to 1.09 g-rms. In other words, the optimum value obtained in Case 1 is decreased approximately 38% in Case 8.

The proposed optimum values for the design constraints have been selected as the best three suggestions among 5 or 6 trials for each case. Being aware of the fact that the quality of the optimization design variables are dependent on the proposed initial population for genetic algorithm, the values of the objective functions may be reduced by increasing the number of trials and check for the proposed optimum values. However, in the thesis study, the number of trials for each optimization problem is considered to be sufficient.

If noticed, except from the 3rd and 2nd attempts for Case-5 and Case-6, respectively, there is no violation of the design constraints. On the other hand, for those proposed optimum values, the static deflection limit for the isolators are exceed. Therefore, although the values of the objective function for those cases are the smallest, due to the violation of design constraints, the proposed optimum values are directly eliminated.

Table 5.38 Overall Objective Functions for Each Case

Case No	**Objective Function (g-rms)**			**% Reduction**
	Attempt-1	**Attempt-2**	**Attempt-3**	
1	1.81	**1.75**	1.76	------
2	**1.56**	1.64	**1.56**	**10.9%**
3	1.60	**1.58**	1.61	9.7%
4	**1.41**	1.57	1.45	19.4%
5	1.40	**1.17**	0.90 (P)	33.1%
6	1.27	0.90 (P)	**1.15**	**34.3%**
7	**1.17**	**1.17**	1.18	33.1%
8	1.28	1.09	1.11	37.7%

Considering the best attempts for each case, the isolation performance values at mass center and the point at lens location are computed and compared with each other. The computation for isolation performance at any point is implemented as in Eq. (74). Here, the isolation performance is computed considering the acceleration response rms values encountered in all three orthogonal axes and the input acceleration rms value which is equally the same in each axes.

$$Performance = \frac{a_{in}\sqrt{3} - \sqrt{a_{out,x}{}^2 + a_{out,y}{}^2 + a_{out,z}{}^2}}{a_{in}\sqrt{3}} * 100 \qquad (74)$$

where a_{in} is the input rms acceleration value; $a_{out,x}$, $a_{out,y}$ and $a_{out,z}$ are the acceleration response rms values at the point of interest in X, Y and Z axes, respectively.

In Table 5.39, the isolation performance values for the points of interest are listed. Depending on the response values computed for X, Y and Z axes, the isolation performance increases from Case-1 to Case-8 in general. As seen from the table, the average isolation performance increases by approximately 10.6%.

Table 5.39 Isolation Performances of the Best Attempts of Each Case

Case No	Description	Axis	Input (g-rms)	Response (g-rms)		Isolation Performance (%)		
				Mass Center	Lens	Mass Center	Lens	Average
1	STOI Fixed Mounting Attempt-2	X	2.7443	0.63363	0.66132	78.1	78.9	78.5
		Y		0.60119	0.3916			
		Z		0.56787	0.64295			
2	STOI Unfixed Mounting Attempt-1	X	2.7443	0.51268	0.54308	80.0	81.7	80.9
		Y		0.65729	0.44133			
		Z		0.45868	0.5148			
3	DTOI Fixed Mounting Attempt-2	X	2.7443	0.51497	0.49497	80.5	80.9	80.7
		Y		0.51346	0.44812			
		Z		0.57266	0.61433			
4	DTOI Unfixed Mounting Attempt-1	X	2.7443	0.46216	0.4928	81.9	83.6	82.8
		Y		0.5918	0.37514			
		Z		0.41782	0.47165			
5	DiscreteLocation Attempt-2	X	2.7443	0.39525	0.40253	85.6	85.9	85.7
		Y		0.39636	0.36484			
		Z		0.39275	0.39466			
6	Parameter & Discrete Loc. Attempt-3	X	2.7443	0.39376	0.34674	86.0	86.0	86.0
		Y		0.38567	0.39073			
		Z		0.37247	0.40844			
7	ContinuousLocation Attempt-1	X	2.7443	0.39658	0.38245	85.6	85.9	85.7
		Y		0.39605	0.36908			
		Z		0.39077	0.41062			
8	Parameter & Cont. Loc. Attempt-2	X	2.7443	0.34232	0.33494	86.7	86.9	86.8
		Y		0.41011	0.39129			
		Z		0.34151	0.35166			

Using the computed optimum values for corresponding design variables, it is possible to plot the response PSD acceleration functions for each case. Below, the response PSD acceleration functions for the point at mass center in X, Y and Z axes are given in Figure 5.24, Figure 5.25 and Figure 5.26, respectively. Similarly, the same results for the point where the lens is located are given from Figure 5.27 to Figure 5.29 for each axis.

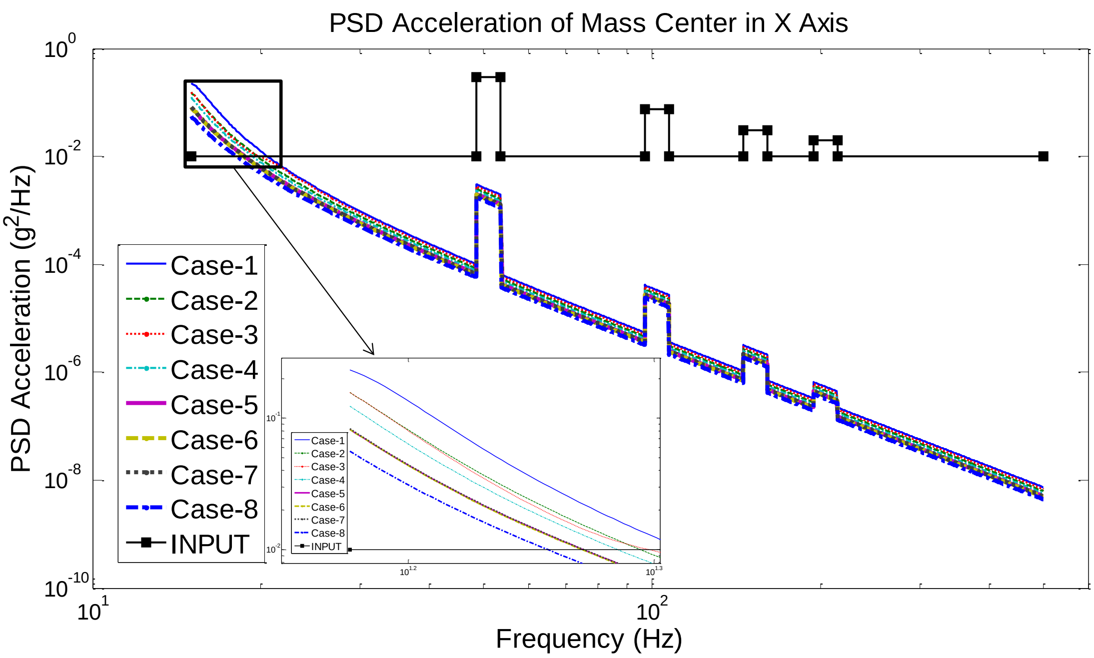

Figure 5.24 PSD Acceleration of Mass Center in X Axis

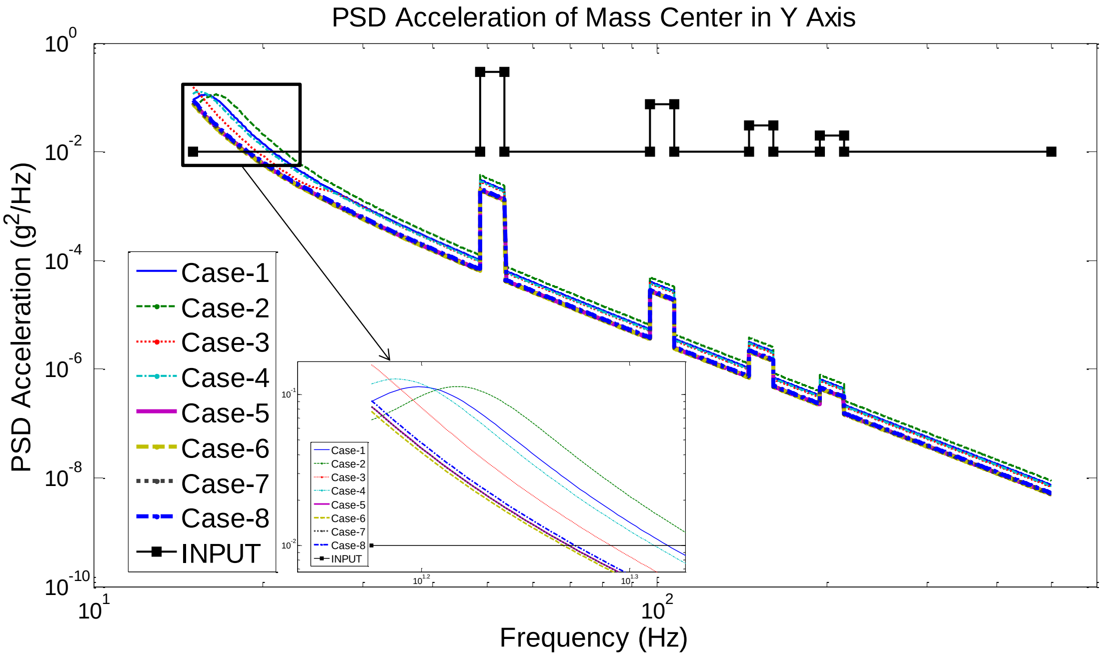

Figure 5.25 PSD Acceleration of Mass Center in Y Axis

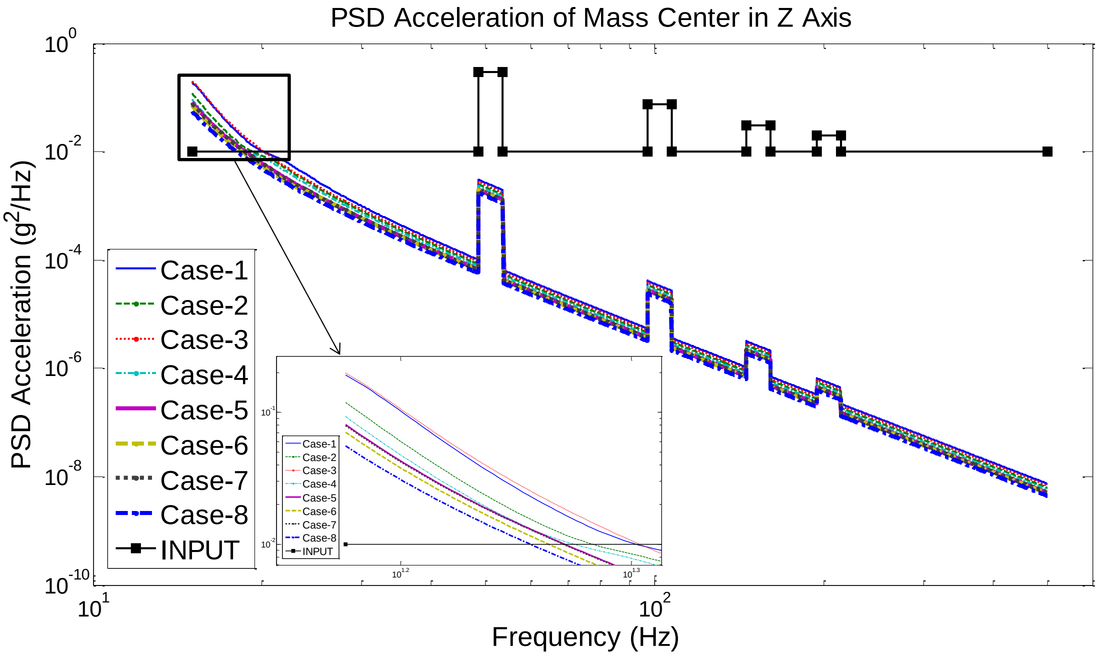

Figure 5.26 PSD Acceleration of Mass Center in Z Axis

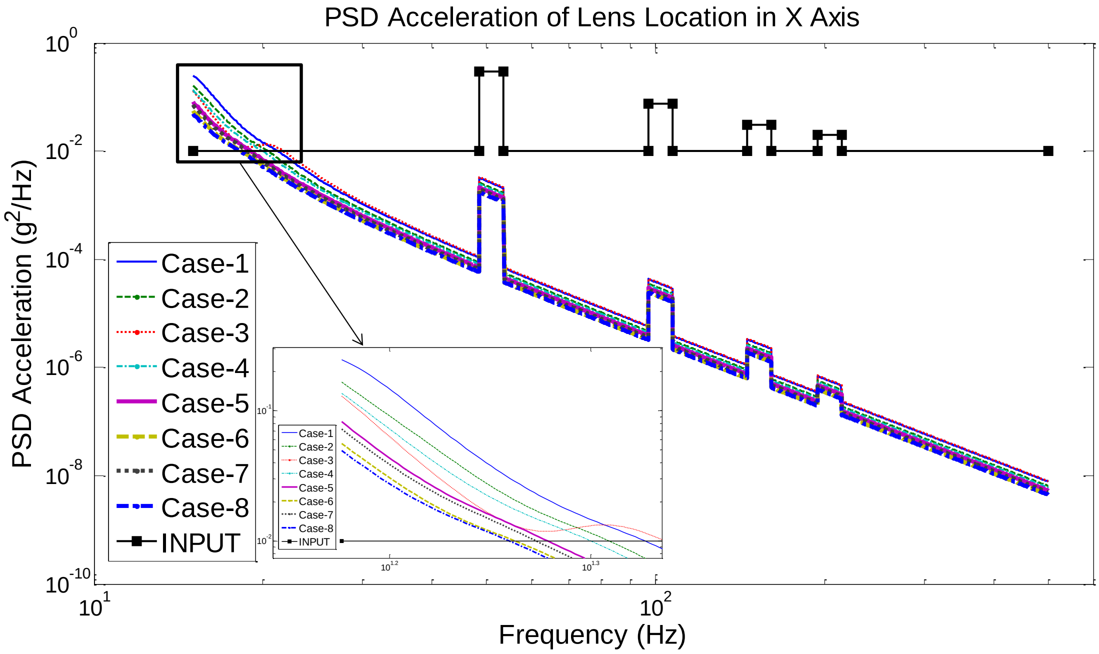

Figure 5.27 PSD Acceleration of Lens Location in X Axis

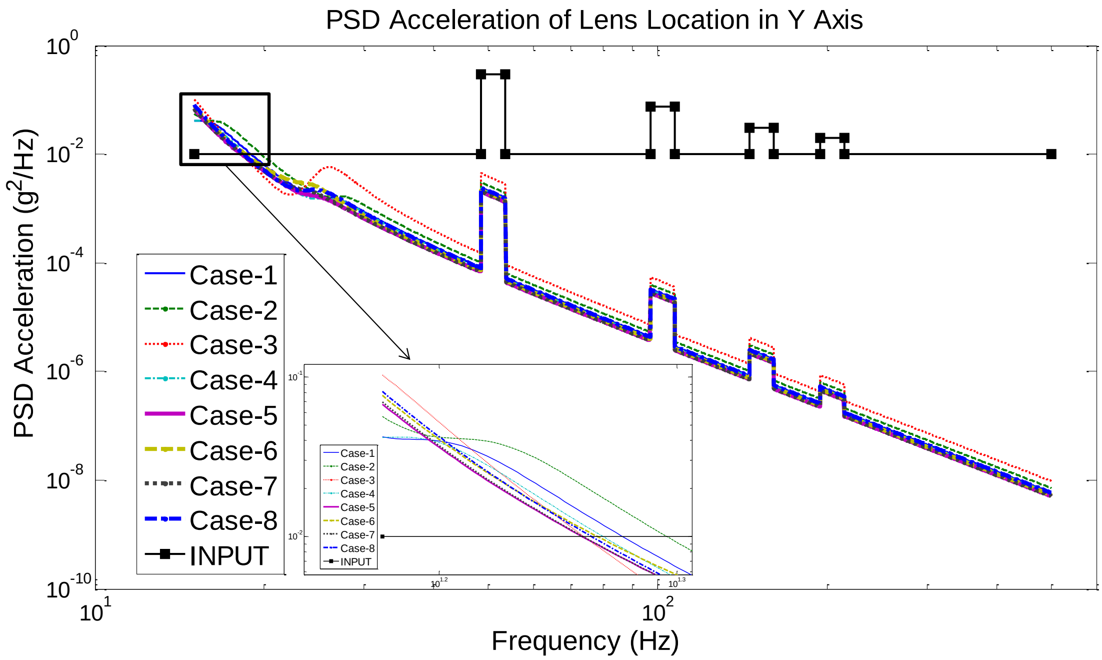

Figure 5.28 PSD Acceleration of Lens Location in Y Axis

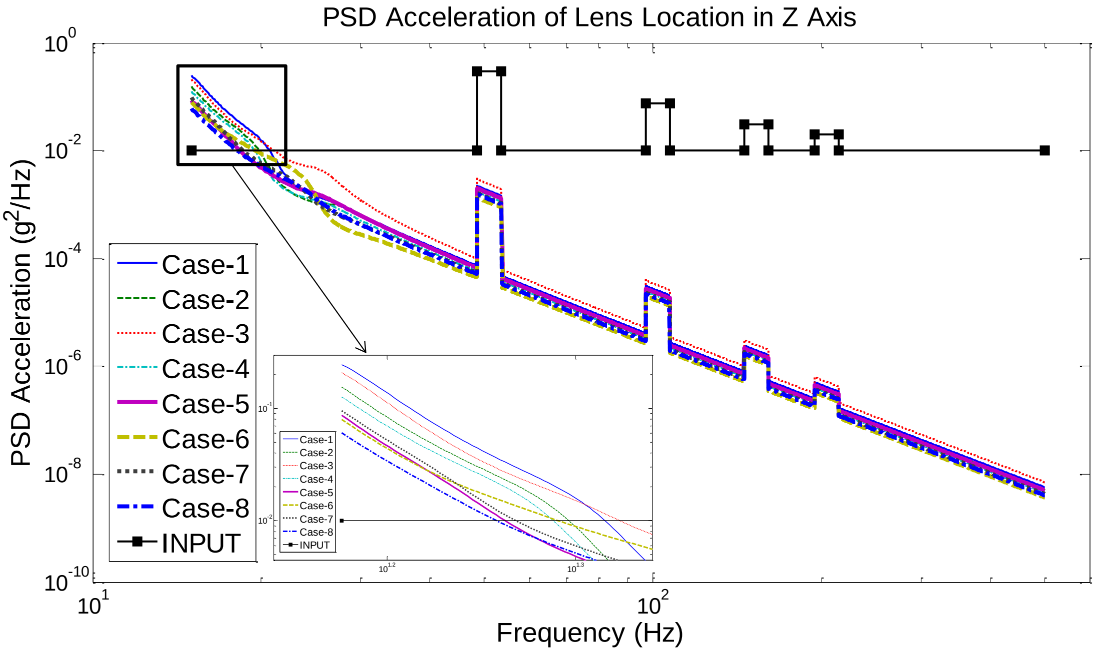

Figure 5.29 PSD Acceleration of Lens Location in Z Axis

5.4. Optimization Application on a Helicopter Platform

In this case study, the optomechanical system of which the physical properties are described in Figure 5.2 and Table 5.1 is assumed to be mounted on the instrument panel of OH-6A helicopter. The excitation of the mounted platform is harmonic vibration, which is in three orthogonal axes. The vibration level can be obtained by using the military standard, MIL-STD-810 [32].

According to the standard, the vibration source is due to both the main and tail rotors. The amplitudes of harmonic acceleration and displacement at the corresponding frequencies can be listed as in Table 5.2.

In this part of study, the objective is to find the optimized values for the defined parameters such as stiffness and location of the resilient members in order to minimize the total acceleration level of point at mass center and the point where the lens is located.

As mentioned in the previous study, there are various types of optimization methods that can be used to find the optimum values for the design parameters in order to minimize the objective function. The results of those methods are also compared with each other in those sections. However, rather than investigating and comparing different types of optimization methods, this study will cover the results of one type optimization method which is both parameter and discrete location optimization.

In this study, like mentioned in Section 5.3.2.1, the possible locations where the isolators can be mounted are discretized. The discretized surfaces are located 128.5 mm and 121.5 mm away from mass center in negative and positive Z direction, respectively. As shown in Figure 5.30, the dimension of the possible region is 80x230 mm. Different from Section 5.3.2.1, the distance between each point is set to 2.0 mm. That makes the number of possible points on one plane as 4756. Since there are two planes located on negative and positive Z direction, the total number of points where the isolators can be mounted is 9512.

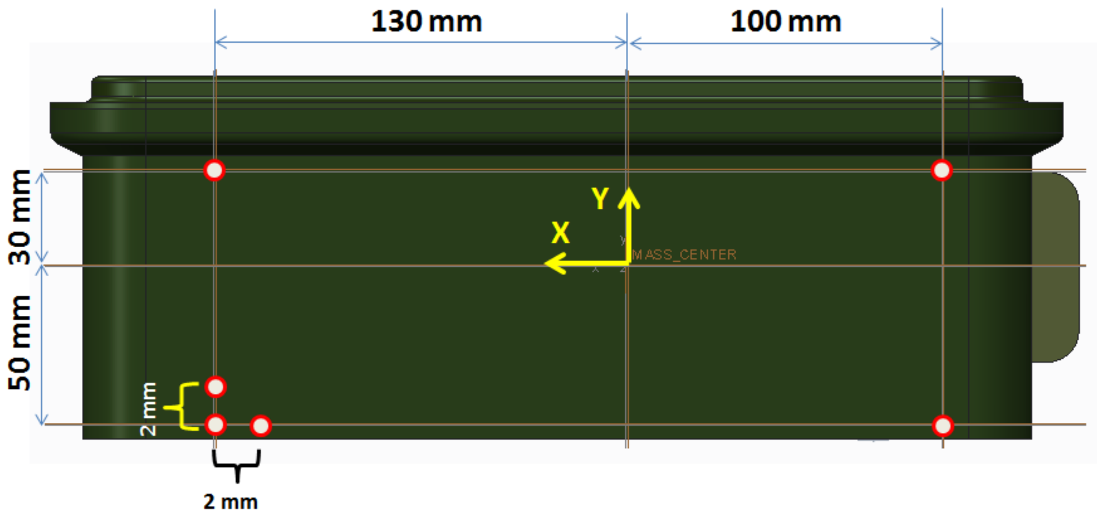

Figure 5.30 Discretized Points on X-Y Plane

In order to constitute an optimization problem, the boundary conditions, constraints and the fixed parameters should also be well defined. These are listed as follows:

- The number of isolators used is defined as 4.
- Stiffness values in each direction should be selected between 10000 N/m and 20000 N/m.
- The axial to radial stiffness ratio is selected as 1.
- The value for loss factor is 0.2.

- Maximum harmonic acceleration amplitude limit for the points of interest is 0.8 g in each direction.
- Maximum harmonic displacement amplitude limit for the points of interest is 2.0 mm in each direction.
- Maximum available deflection of each isolator due to static loading is 1.5 mm in each direction.
- Maximum available rotation of the rigid body due to static loading is 2 degrees about each axis.
- Alignment constraint is defined as 0.1 Hz.
- Stability constraint is defined as 10 Hz.

5.4.1. Parameter and Discrete Location Optimization

An engineer, at first glance, will select the minimum value for the isolator stiffness in each direction for the minimization of the total acceleration amplitude of the points of interest. In other words, considering the range set for the isolator stiffness values, the stiffness coefficients in each direction are assumed to be 10000 N/m. Additionally, the location of the isolators is selected as the same as in Section 5.3.1.

For this type of isolation system configuration, the static deflection of isolators 1 and 4 in Y direction exceed the limit set for the static deflection constraint as shown in Table 5.42. Therefore, rather than using the predefined stiffness coefficients for the isolators mounted on the predefined location, the selected optimization algorithm should be run and the optimum values for the stiffness of the isolators and their location on the predefined planes should be computed.

For parameter optimization with discrete location optimization, the algorithm is run for three times and the results for the objective function are for each trial are given in Table 5.40.

Table 5.40 Optimization Results

Parameter and Discrete Location Optimization							
Attempt Number	Isolator Number	Stiffness (N/m)	X Axis (mm)	Y Axis (mm)	Z Axis (mm)	Objective Function (g)	Penalty Function
0	1	10000	-78	0	121.5	2.76	Static Deflection (Table 5.42)
	2	10000	120	0	121.5		
	3	10000	120	0	-128.5		
	4	10000	-78	0	-128.5		
1	1	10000	86	-46	-128.5	2.78	None
	2	11262	-100	14	121.5		
	3	10330	130	30	121.5		
	4	10589	-100	-44	-128.5		
2	1	10259	-100	-30	-128.5	2.79	None
	2	10778	-94	18	121.5		
	3	10391	114	-32	-128.5		
	4	11317	80	28	121.5		
3	1	10401	68	-30	-128.5	2.99	None
	2	18869	-96	24	121.5		
	3	10000	130	30	121.5		
	4	10002	62	-12	-128.5		

For each attempt, the natural frequencies, static deflection of each isolator and rotation of the rigid body due static loading are also computed and listed in tables below from Table 5.41 to Table 5.43.

Table 5.41 Comparison of Natural Frequencies

Mode Number	**Natural Frequency (Hz)**			
	Attempt Number			
	0	**1**	**2**	**3**
1	11.0	12.2	11.9	10.0
2	12.4	12.9	13.0	13.6
3	12.6	12.9	13.0	14.0
4	13.6	13.5	13.0	14.5
5	17.8	19.0	18.4	19.5
6	22.2	23.6	23.5	25.9

Table 5.42 Comparison of Static Deflection of Isolators

Isolator Number	**Static Deflection (mm)**											
	Attempt 0			**Attempt 1**			**Attempt 2**			**Attempt 3**		
	X	Y	Z	X	Y	Z	X	Y	Z	X	Y	Z
1	0	**1.94**	0	0	1.48	0	0	1.50	0	0.06	1.47	0.07
2	0	1.28	0	0	1.50	0	0	1.48	0	0.01	1.44	0.02
3	0	1.19	0	0	1.49	0	0	1.46	0	0.04	0.52	0.13
4	0	**1.86**	0	0	1.49	0	0	1.45	0	0.01	1.50	0.02

Table 5.43 Comparison of Rotation of the Rigid Body Due to Static Loading

Attempt Number	**Rotation Due to Static Loading (^{0})**		
	About X Axis	**About Y Axis**	**About Z Axis**
0	0.0201	0	0.1925
1	0.0030	6.2281e-4	0.0035
2	-0.0042	0.0014	0.0106
3	-0.1595	0.0336	0.2335

Comparing the values for the objective function given in Table 5.40 and investigating whether the values of the first natural frequency, static deflection of isolators in each axes and the amount of rigid body rotation due to static loading are within the defined constraint limits or not, it is reasonable to use the optimized parameters obtained in the first attempt.

In Table 5.44, the amplitude values of the harmonic acceleration and displacement encountered on the mass center and at the location where the lens is mounted are listed. If the values for the corresponding input frequencies are investigated, it is easily observed that the values computed for acceleration and displacement amplitudes do not exceed the maximum acceleration and displacement amplitudes of 0.8g and of 2.0 mm, respectively.

Table 5.44 Harmonic Acceleration and Displacement Amplitude of Attempt-1

Frequency (Hz)	Axes	Mass Center		Lens Location	
		Acc. (g)	Disp. (mm)	Acc. (g)	Disp. (mm)
8.1	X	0.43455	1.6458	0.42399	1.6058
	Y	0.4309	1.632	0.45379	1.7187
	Z	0.43241	1.6377	0.42471	1.6085
32.4	X	0.33806	0.080022	0.3634	0.086021
	Y	0.33715	0.079808	0.23309	0.055175
	Z	0.3399	0.080459	0.4096	0.096957
51.8	X	0.07109	0.0065835	0.075565	0.0069979
	Y	0.071033	0.0065782	0.055749	0.0051628
	Z	0.071164	0.0065903	0.08014	0.0074216
64.8	X	0.044354	0.0026248	0.047047	0.0027841
	Y	0.044333	0.0026235	0.035407	0.0020953
	Z	0.044379	0.0026263	0.049503	0.0029295
97.2	X	0.019265	0.0005067	0.020396	0.00053643
	Y	0.019261	0.0005066	0.01561	0.00041057
	Z	0.019269	0.00050681	0.021323	0.00056081
103.6	X	0.016922	0.00039177	0.017911	0.00041468
	Y	0.016919	0.0003917	0.013729	0.00031787
	Z	0.016925	0.00039185	0.018715	0.00043329
207.2	X	0.00418	2.4196e-5	0.0044206	2.5586e-5
	Y	0.0041802	2.4195e-5	0.0034154	1.9768e-5
	Z	0.0041805	2.4197e-5	0.0046055	2.6657e-5
310.8	X	0.001854	4.769e-6	0.0019601	5.0422e-6
	Y	0.0018538	4.7689e-6	0.0015165	3.9011e-6
	Z	0.0018539	4.7691e-6	0.002041	5.2505e-6

5.4.2. Monte Carlo Simulation

In this part of the case study, Monte Carlo simulation is implemented for the optimized system obtained in Attempt-1.

The number of simulation is set to 250. In all these cases, the maximum allowable deviation in stiffness of the isolators in each direction and the loss factor is set to 10%. The maximum deviation in the position of each isolator is set to 2.0 mm. Additionally, the maximum value of the mounting orientation angle of the isolators is set to 2 degrees about each axis.

In Table 5.45, the minimum and maximum deviations in the first 6 natural frequencies are shown, where the most critical one is the first natural frequency. As mentioned before, in all optimization methods, the stability constraint is defined such that the first natural frequency is larger than 10 Hz. Here, the minimum frequency value for the first mode is 11.9 Hz. Additionally, if the results for other modes are investigated, it is seen that the maximum deviation is 4.7% or the 3rd mode which seems also reasonable.

In Table 5.46 and Table 5.47, the deviations in the static deflection of each isolator along Y axis are shown. On the other hand, since the values of the static deflection for the isolators along X and Z axes are very small compared to the allowable limit which is 1.5 mm, those values along X and Z axes are not listed. If the results for the maximum deviations of static deflection of isolators in Y direction are investigated, it is seen that the allowable limit is exceed by 6.3%, 11.9%, 9.1% and 9.9% for each isolator, respectively. Knowing this fact, the designer should pay attention in mounting the isolators with the correct stiffness and in exactly predefined locations.

In Table 5.48, the deviations in acceleration and displacement response amplitudes of the points of interest in each direction are shown. If the given data is investigated, it is observed that the maximum acceleration limit, which is 0.8 g in each direction, is not exceeded. The maximum values among the Monte Carlo simulation results are 0.45 g and 0.49 g for mass center in X direction and the lens location in Z direction, respectively. In addition to the acceleration constraint, the constraint defined for the amplitude of displacement of the harmonic vibration is not exceeded. From the given list, the maximum values among the Monte Carlo simulation results are 1.73 mm and 1.83 mm for mass center along X axis and the lens location along Y axis, respectively. Considering the limit for the acceleration and displacement response constraints, the deviations encountered are feasible.

Table 5.45 Deviation in Natural Frequencies

Mode Number	**Frequency (Hz)**			**Deviation (%)**	
	Optimum Value	Monte Carlo Simulation			
		Minimum	Maximum	Minimum	Maximum
1	12.2	11.9	12.5	2.5	2.5
2	12.9	12.5	13.1	3.1	1.6
3	12.9	12.6	13.5	2.3	4.7
4	13.5	13.1	13.8	3.0	2.2
5	19.0	18.4	19.4	3.2	2.1
6	23.6	22.9	24.4	3.0	3.4

Table 5.46 Deviation in Static Deflection

Isolator	**Static Deflection (mm)**		
	Optimum Value	**Monte Carlo Simulation**	
	Y	**Y**	
		Min.	**Max.**
1	1.4751	1.375	1.594
2	1.4993	1.342	1.679
3	1.4854	1.338	1.636
4	1.4864	1.367	1.648

Table 5.47 Percentage Deviation in Static Deflection

Isolator	**Deviation (%)**	
	Y	
	Min.	Max.
1	6.8	8.1
2	10.5	12.0
3	9.9	10.1
4	8.0	10.9

Table 5.48 Maximum Deviation in the Amplitudes of Acceleration and Displacement

Location	Axis	f (Hz)	Acceleration (g)			f (Hz)	Displacement (mm)		
			M.C. Sim.	Optimum Value	Dev. (%)		M.C. Sim.	Optimum Value	Dev. (%)
Mass Center	X	8.1	0.455	0.435	4.4	8.1	1.7268	1.646	4.7
	Y	8.1	0.450	0.431	4.2	8.1	1.7034	1.632	4.2
	Z	8.1	0.453	0.432	4.6	8.1	1.7167	1.638	4.6
Lens Location	X	8.1	0.438	0.424	3.3	8.1	1.66	1.606	3.3
	Y	8.1	0.483	0.454	6.1	8.1	1.8299	1.7197	6.1
	Z	32.4	0.493	0.410	16.9	8.1	1.6999	1.609	5.4

CHAPTER 6

CONCLUSION AND FUTURE STUDIES

Considering the 21st century engineering problems worldwide, it is easily observed that the designers are forced to tackle with difficult cases including more sensitive electronic and optical devices operating in more severe environmental conditions. In order to sustain the endurance and operational performance of such mechanical systems, the study for vibration isolation system design involving the parameter and location optimization processes are considered as a critical stage in all design phases.

In this thesis report, similar studies in literature investigating the passive vibration isolation system design in order to minimize the destructive effects of vibration for various types of applications are reviewed. The studies are tabulated in detail and compared with each other considering their capabilities on vibration isolation system analysis and optimization. Examining the softwares used on these studies, it is realized that there is no reference developing a software-based tool that is capable of implementing all modal analysis, static deflection analysis and response analysis in addition to simulations and optimization studies in one platform, simultaneously.

Being aware of this necessity, within the scope of the present thesis, a MATLAB based graphical user interface has been developed for analysis, simulation and optimization processes for a general vibration isolation system design problem. Here, the isolated system is assumed to be mounted on elastomeric isolators. Those elastomeric isolators are defined by 3 mutually orthogonal springs with axial and radial stiffness coefficients and constant loss factor. The mechanical system is assumed to be a rigid body with 6 degrees of freedom. The equations representing the whole motion of the isolation system is obtained from literature, which are converted into matrix form. Having obtained the information for the input vibration profile together with the system matrices, the software is capable of implementing dynamic response analysis. Not only the modal analysis for the isolation system, but also response analysis at any point on the rigid body can be conducted easily. Additionally, setting the amplitude and direction of the gravitational acceleration, the static deflection of each isolator in each orthogonal axis can be computed separately.

Realizing the deviations in the characteristics of the resilient members in addition to the possibility of the offsets in the position and orientation of those isolators in real life, Monte Carlo simulations are also made available in the developed software. By setting the maximum deviation quantities for the predefined design parameters, it is also possible to observe the deviations in a number of results such as natural frequencies, static deflections and response functions.

In this thesis study, a set of optimization problem scenarios is generated and studied by utilizing the developed software. Here, the user is allowed to select the proper optimization scenario considering the structure of the vibration isolation problem. Parameter optimization of single and different types of isolators; in addition to location optimization for discrete and continuous set of points are the major types in optimization alternatives. According to the type of the optimization study, the design variables are the stiffnesses, locations or the orientation angles of the isolators. For each type, a hybrid method involving both global search and gradient based methods is used in order to minimize the selected objective function. In this study, the objective function is the minimization of acceleration or displacement of the points of interest. Additionally, in order not to exceed the predefined design constraints, constant and gradual types of penalty functions have been defined.

The verification of the theoretical model used in the developed software is performed by using a commercial finite element analysis program, ANSYS Workbench 14.0. In this thesis, the verification is applied for a simple rigid body mounted on springs with different stiffness coefficients. Here, the isolators are assumed to be mounted in orthogonal and inclined directions with respect to the global reference frame. For both case, the results obtained from modal analysis, static deflection analysis, response analysis for random and harmonic types of input excitation in addition to transmissibility functions are compared.

Finally, a set of case studies are investigated in order to demonstrate the capabilities of the developed software for vibration isolation analysis and optimization. In all cases, the isolated system is selected as an optomechanical system, which is used to determine the altitude of any air-platform. In the first case study, the mechanical system is assumed to be mounted on a helicopter platform. Considering the harmonic and random type of input vibration and the gravitational acceleration, dynamic and static responses are analyzed. Additionally, Monte Carlo simulations are performed and the deviations in a number of results have been studied. In the second case study, the optimization capabilities of the software are demonstrated. Here, several types of optimization scenarios are considered for the same mechanical system mounted on an aircraft. For each optimization scenarios, the optimum values for predefined design parameters are computed and the objective functions, in addition to the isolation performances, are compared. Considering the computational time required and the results obtained for the selected objective function, it can be concluded that the discrete location optimization with unfixed parameters is the most preferred one among other optimization alternatives. In the final case study, the same mechanical system is assumed to be exposed to harmonic vibration only. For this type of problem, location optimization for discrete set of points with unfixed parameters is considered and Monte Carlo simulations are performed for the best attempt.

In order to improve the present study, the assumptions made in isolator and isolation system modeling should be restored. In this study, the isolators are modeled as 3 mutually orthogonal springs with linear and constant stiffness, and constant structural damping characteristics. For this type of modeling, the isolator properties are independent from the excitation frequency, temperature and the load on the isolator. However, in real life, due to the viscoelastic properties of the elastomeric isolators, the isolator characteristics are directly dependent on those factors. Therefore, the reliable characterization of the isolators should be done by implementing various types of experiments and the results should be reflected in isolator modeling. In addition to this, the isolators are assumed to be massless. Therefore, in isolation system modeling, the system mass matrix does not involve any information on the mass values of the isolators. In order to observe the effects of the mass of the isolators, the isolation system modeling should be revised.

It is also important to investigate the effects of platform acceleration on the resilient members. Although it is not included in the present thesis, redefining the forcing vector, it is possible to compute the amplitude values of deflection and force on each isolator. By computing those values, it would be possible to check whether the dynamic limits of the isolators are exceeded or not when the mechanical structure is exposed to steady acceleration.

Finally, in order to obtain better isolation performance values, the number of options that can be managed for the optimization algorithm should be increased. In this study, only the population size, stall generation limit in addition to time limit are changeable. In order to improve the quality of the optimum design variables, according to the optimization problem, the options such as population, reproduction, mutation, crossover and migration should be added in the developed software.

REFERENCES

[1] A. M. Veprik, "Vibration Protection of Critical Components of Electronic Equipment in Harsh Environmental Conditions," Journal of Sound and Vibration, 2003.

[2] D. Kamesh, R. Pandiyan and A. Ghosal, "Modeling, Design and Analysis of Low Frequency Platform for Attenuating Micro-Vibration in Spacecraft," Journal of Sound and Vibration, 2010.

[3] S. W. Yoon, Vibration Isolation and Shock Protection for MEMS, Electrical Engineering, The University of Michigan, 2009.

[4] A. Hati, C. W. Nelson, D. A. Howe, N. Ashby, J. Taylor, K. M. Hudek, C. Hay, D. Seidel and D. Eliyahu, "Vibration Sensitivity of Microwave Components," IEEE, 2007.

[5] D. C. Griffith, "Phase Error Compensation Technique for Improved Synthetic Aperture Radar Performance," JOHNS HOPKINS APL TECHNICAL DIGEST, 1997.

[6] P. Knott, «Deformation and Vibration of Conformal Antenna Arrays and Compensation Techniques,» Research Institute for High Frequency Physics, Germany, 2006.

[7] C. Y. Song, "Design Optimization and Development of Vibration Analysis Program for Engine Mount System," Technical Division, AhTTi Co., Korea.

[8] E. R. Ponslet and M. S. Eldred, "Discrete Optimization of Isolator Locations for Vibration Isolation Systems: an Analytical and Experimental Investigation," Structural Dynamics Department Sandia National Laboratories, New Mexico, May 17, 2006.

[9] I. I. Esat and H. Bahai, "Vibratory System Synthesis For Multi-Body Systems Based On Genetic Algorithm," Journal of Sound and Vibration, 2000.

[10] D. A. Swanson and H. T. Wut, Optimization of Aircraft Engine Suspension Systems, Journal of Aircraft, 1992.

[11] Vibrant Technology Inc., «Mathematics of a Mass-Spring-Damper System,» 2005. [Accessed 11 August 2013].

[12] Federal Institute for Occupational Safety and Health, "http://www.baua.de/en/Practical-experience/Practical-

solutions/ISOMAG/ISOMAG.html," BAuA, June 2007. [Accessed August 2013].

[13] Mechartes Simulation Experts, "http://www.mechartes.com/casestudy/mechartes_case_studies_VISP.html," Mechartes Simulation Experts. [Accessed 11 August 2013].

[14] T. H. Vejsz, Vibration Analysis of a Computer Hard Drive Subjected to a Random Vibration Input Using Integrated Solid Modeling and Simulation Software, Long Beach: Mechanical Engineering Department, California State University, 2002.

[15] S. Chen, Q. Wei, J. Huang, G. Yin ve Z. Li, «An Equivalent Model for Modal Analysis of Engine Mounting System,» Atlantis Press, France, 2012.

[16] M. Zehsaz, M. Sadeghi, M. Ettefagh ve F. Shams, Tractor Cabin's Passive Suspension Parameters Optimization, Iran: Journal of Terramechanics, 2011.

[17] Y. Basavaraj ve T. Manjunatha, Design Optimization of Automotive Engine Mount System, International Journal of Engineering Science Invention, 2013.

[18] S. Mallick and D. Zimmerman, "Multi-Axis Vibration Isolation of Sensitive Electronics in Police Trunks," University of Houston, Houston, 2004.

[19] R. F. Alkhatib, Modeling and Vibration Control of Turboprop Installations, Canada: Mechanical Engineering Department, University o f Waterloo, 2002.

[20] S. Kaul, Modeling Techniques for Vibration Isolation in Motorcycles, Milwaukee: University of Wisconsin, 2006.

[21] R. Wang, A Study of Vibration Isolation of Engine Mount System, Canada: Mechanical and Industrial Engineering Department, Concordia University, 2005.

[22] D. Cinarel, "Vibration Isolation of Inertial Measurement Unit," Mechanical Engineering Department, METU, Ankara, 2012.

[23] S. Kelly, Fundamentals of Mechanical Vibrations, 2nd Edition, McGraw-Hill, 2000.

[24] C. Silva, Vibration: Fundamentals and Practice, CRC Press, 2000.

[25] S. Rao, Mechanical Vibrations, 2nd Edition, Addison-Wesley Publishing, 2000.

[26] İ. Baran, «Optimization of Vibration Characteristics of a Radar Antenna Structure,» Mechanical Engineering Department, The Middle East Technical Unitversity, Ankara, 2011.

[27] Y. Yu, N. Naganathan and R. Dukkipati, "A Literature Review of Automotive Vehicle Engine Mounting Systems," Mechanism and Machine Theory, 1999.

[28] J. Zhang, "The Application of Maxwell Elements for Modeling, Identification and Analysis of Passive and Semi-Active Vibration Systems," Department of Mechanical Engineering, University of Louisville, Kentucky, 2006.

[29] J. Zhang and C. M. Richards, "Parameter identification of analytical and experimental rubberisolators represented by Maxwell models," Elsevier Ltd, 2007.

[30] H. Himelblau and S. Rubin, "Chapter 3: Vibration of a Resiliently Supported Rigid Body," in Harris' Shock and Vibration Handbook, McGraw-Hill, 2010.

[31] Barry Controls, "Barry Controls: Application Matrix," Barry Controls, [Online]. Available: www.novibration.com/applicationsmatrix/aircraft.htm. [Accessed 11 8 2013].

[32] Department of Defense, USA, "Department of Defense Test Method Standard for Environmental Engineering Considerations and Laboratory Tests," Department of Defense, USA, 2000.

[33] R. Wheeler, "Helicopter Anatomy," GNU Free Documentation License, 19 11 2006. Available: http://en.wikipedia.org/wiki/File:Helicopter_Anatomy.png. [Accessed 15 8 2013].

[34] C. F. Beards, Structural Vibration: Analysis and Damping, New York: Arnold, 1996.

[35] J. S. Tao, G. R. Liu and K. Y. Kam, "Design Optimization Of Marine Engine–Mount System," Journal of Sound and Vibration, Singapore, 2000.

[36] E. I. Rivin, Passive Vibration Isolation, ASME Press, 2003.

[37] Lord Corperation, *Vibration, Shock and Motion Control Products,* USA, 2000.

[38] Tech Products Corperation, Vibration and Shock Isolation Products, Tech Products Corperation.

[39] D. Çınarel and E. Ciğeroğlu, "Ataletsel Ölçüm Biriminin Titreşim Yalıtımı," in SAVTEK 2012, 6th Defence Technologies Congress, Ankara, 2012.

[40] S. Homewood, "flugzeuginfo.net," 11 8 2013. [Online]. Available: http://www.flugzeuginfo.net/acdata_php/acdata_oh6_en.php. [Accessed 1 9 2013].

[41] Wikipedia, «Lockheed C-130 Hercules,» 16 8 2013. Available:

http://en.wikipedia.org/wiki/Lockheed_C-130_Hercules. [Accessed: 18 8 2013].

APPENDIX A

TRANSMISSIBILTY FUNCTION DEFINED IN MODAL DOMAIN

In this section, a two degree of freedom system is considered as shown in Figure A-1.

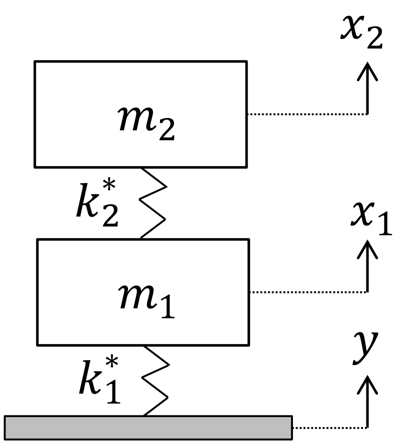

Figure A-1 Two Degree of Freedom System

Here, the body 1 of mass m_1 is connected to the moving platform and the body 2 of mass m_2. The connection is implemented by using resilient members with stiffness values k_1^* and k_2^* which are defined as follows.

$$k_1^* = k_1 + i\,\lambda\,k_1, \qquad \text{(A.1)}$$

$$k_2^* = k_2 + i\,\lambda\,k_2. \qquad \text{(A.2)}$$

The equation of motion of the system can be obtained in matrix form as follows.

$$[M]\{\ddot{q}\} + i\,\lambda[K]\{q\} + [K]\{q\} = \{F\} \qquad \text{(A.3)}$$

where,

$$[M] = \begin{bmatrix} m_1 & 0 \\ 0 & m_2 \end{bmatrix}, \tag{A.4}$$

$$[K] = \begin{bmatrix} k_1 + k_2 & -k_2 \\ -k_2 & k_2 \end{bmatrix} , \tag{A.5}$$

$$\{F\} = \{\begin{matrix} k_1\, y \\ 0 \end{matrix}\} , \tag{A.6}$$

$$\{q\} = \{\begin{matrix} x_1 \\ x_2 \end{matrix}\} . \tag{A.7}$$

The coordinate transformation can be applied as follows.

$$\{q\} = [\phi]\,\{\eta\} . \tag{A.8}$$

Using the Equation (A.8) in Equation (A.3), the following equality is obtained.

$$[M][\phi]\{\ddot{\eta}\} + i\,\lambda[K][\phi]\{\eta\} + [K][\phi]\{\eta\} = \{F\} \quad . \tag{A.9}$$

If each side of the equality in Equation (A.9) is multiplied by $[\phi]^T$, then the following equation is obtained.

$$[\phi]^T[M]\phi\{\ddot{\eta}\} + i\,\lambda[\phi]^T[K][\phi]\{\eta\} + [\phi]^T[K][\phi]\{\eta\} = [\phi]^T\{F\} . \tag{A.10}$$

If Equations (66) and (68) are used in Equation (A.10), then a simplified equation is obtained as follows.

$$\{\ddot{\eta}\} + i\,\lambda \begin{bmatrix} {\omega_1}^2 & \cdots & 0 \\ \vdots & \ddots & \vdots \\ 0 & \cdots & {\omega_n}^2 \end{bmatrix} \{\eta\} + \begin{bmatrix} {\omega_1}^2 & \cdots & 0 \\ \vdots & \ddots & \vdots \\ 0 & \cdots & {\omega_n}^2 \end{bmatrix} \{\eta\} = [\phi]^T \{F\}\,. \tag{A.11}$$

For a two degree of freedom system, mass normalized modal matrix and its transpose are defined as follows.

$$[\phi] = \begin{bmatrix} \phi_1^1 & \phi_1^2 \\ \phi_2^1 & \phi_2^2 \end{bmatrix}, \tag{A.12}$$

$$[\phi]^T = \begin{bmatrix} \phi_1^1 & \phi_2^1 \\ \phi_1^2 & \phi_2^2 \end{bmatrix}. \tag{A.13}$$

Using Equations (A.12) and (A.13) in Equation (A.11), the two independent equations are obtained as follows.

$$\ddot{\eta}_1 + {\omega_1}^2(1 + i\,\lambda)\eta_1 = \phi_1^1 k_1 y\,, \tag{A.14}$$

$$\ddot{\eta}_2 + {\omega_2}^2(1 + i\,\lambda)\eta_2 = \phi_1^2 k_1 y\,. \tag{A.15}$$

Considering the Equations (A.14) and (A.15), it is possible to obtain the following two free body diagrams satisfying both equations.

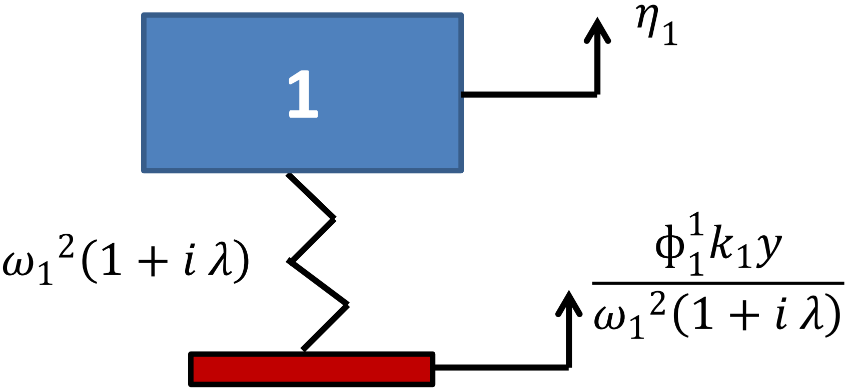

Figure A-2 Unit Mass in Modal Domain

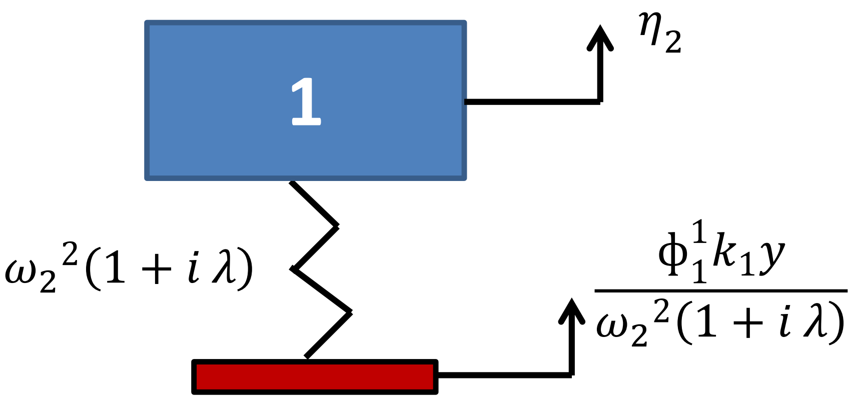

Figure A-3 Unit Mass in Modal Domain

From the figures given, it is possible to obtain transmissibility functions for each. Please note that the defined transmissibility functions are in modal domain.

$$\bar{T}_1 = \frac{\eta_1}{\dfrac{\phi_1^1 k_1 y}{{\omega_1}^2(1 + i\,\lambda)}} \tag{A.16}$$

$$\bar{T}_2 = \frac{\eta_2}{\dfrac{\phi_1^2 k_1 y}{{\omega_2}^2(1 + i\,\lambda)}} \tag{A.17}$$

Additionally, from Equations (A.14) and (A.15), it is possible to find the solution for η_1 and η_2 as follows.

$$\eta_1 = \frac{\phi_1^1 k_1 y}{{\omega_1}^2(1 + i\,\lambda) - \omega^2} \tag{A.18}$$

$$\eta_2 = \frac{\phi_1^2 k_1 y}{{\omega_2}^2(1 + i\,\lambda) - \omega^2} \tag{A.19}$$

Using Eqs. (A.18) and (A.19) in Eqs. (A.16) and (A.17), it is possible to make some simplifications and obtain the following equalities.

$$\bar{T}_1 = \frac{{\omega_1}^2(1 + i\,\lambda)}{{\omega_1}^2(1 + i\,\lambda) - \omega^2} \tag{A.20}$$

$$\bar{T}_2 = \frac{{\omega_2}^2(1 + i\,\lambda)}{{\omega_2}^2(1 + i\,\lambda) - \omega^2} \tag{A.21}$$

Considering the end results for transmissibility functions defined in modal domain, it is possible to make the generalization for this function as follows.

$$\bar{T} = [\bar{K}](1 + i\,\lambda)\,[\bar{\alpha}]\,. \tag{A.22}$$

APPENDIX B

NORMALIZED ACCELERATION VALUES

In this Appendix, the results obtained from Monte Carlo Simulations in Section 5.2.3 are used. Here the aim is to see the level of the deviations in the harmonic acceleration amplitudes of the point at mass center in each axis. Otherwise, the deviations in the results of Monte Carlo Simulations cannot be observed clearly for the frequencies of vibration input except for the first and second frequencies as seen in Figure 5.17.

Here, the normalized acceleration values are computed using the numerical results obtained for the mass center as in Table 5.8 and the results for the acceleration amplitudes obtained from the Monte Carlo Simulations as in Figure 5.17. Those results are used as in Eq. (B.1) and plotted for each natural frequency in each axis as in Figure B-1, Figure B-2 and Figure B-3.

$$a_n = \frac{a_{M.C.}}{a} \tag{B.1}$$

where a_n is the normalized acceleration value; $a_{M.C.}$ is the acceleration value found from Monte Carlo Simulations and a is the amplitude of the acceleration computed at mass center for the given direction and input vibration frequency.

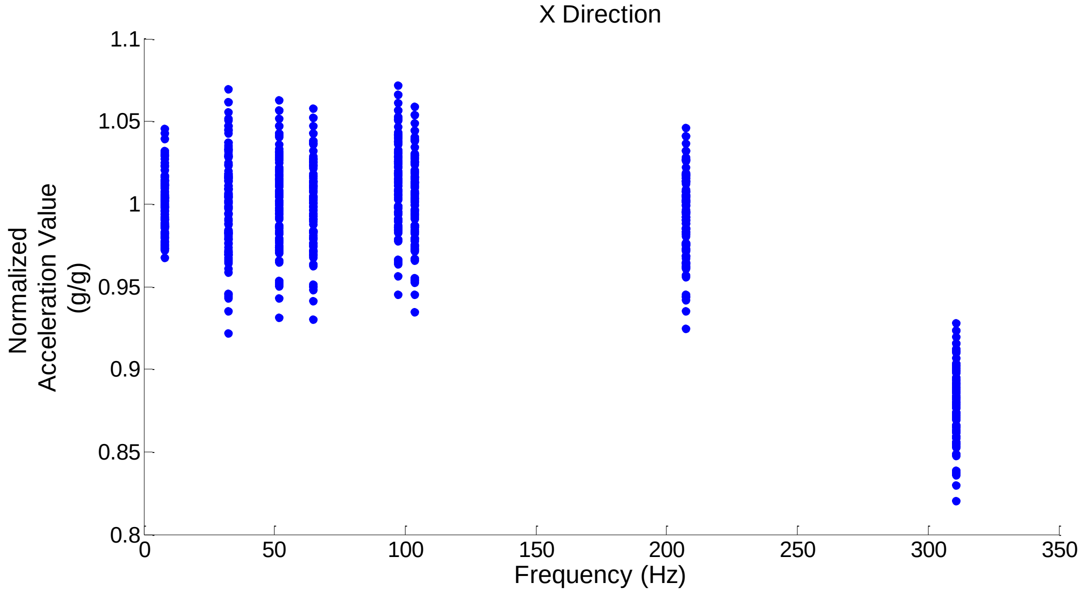

Figure B-1 Normalized Acceleration Values in X Direction

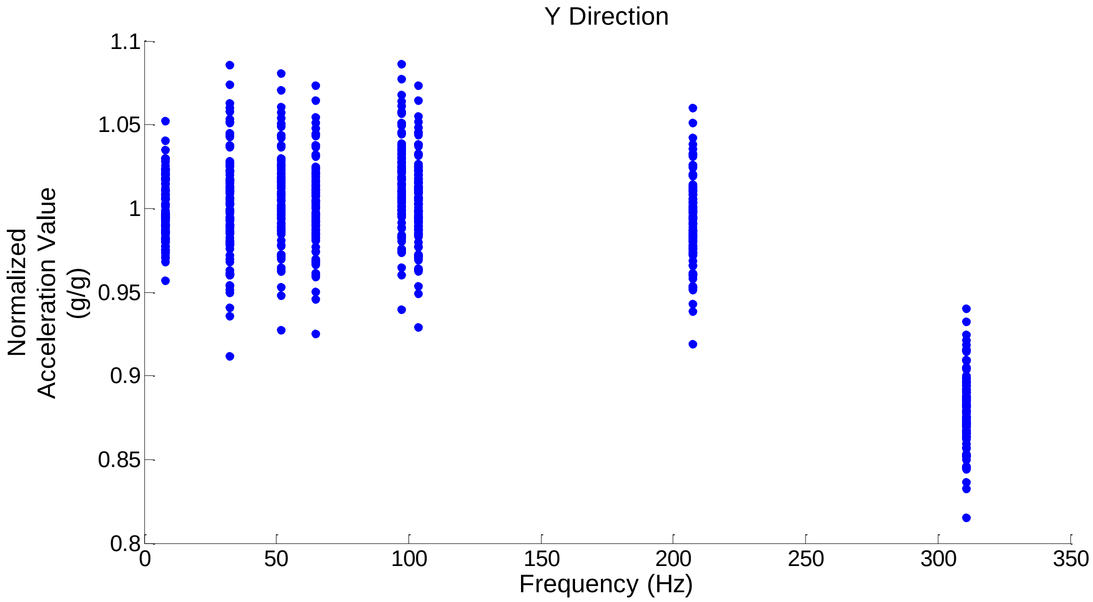

Figure B-2 Normalized Acceleration Values in Y Direction

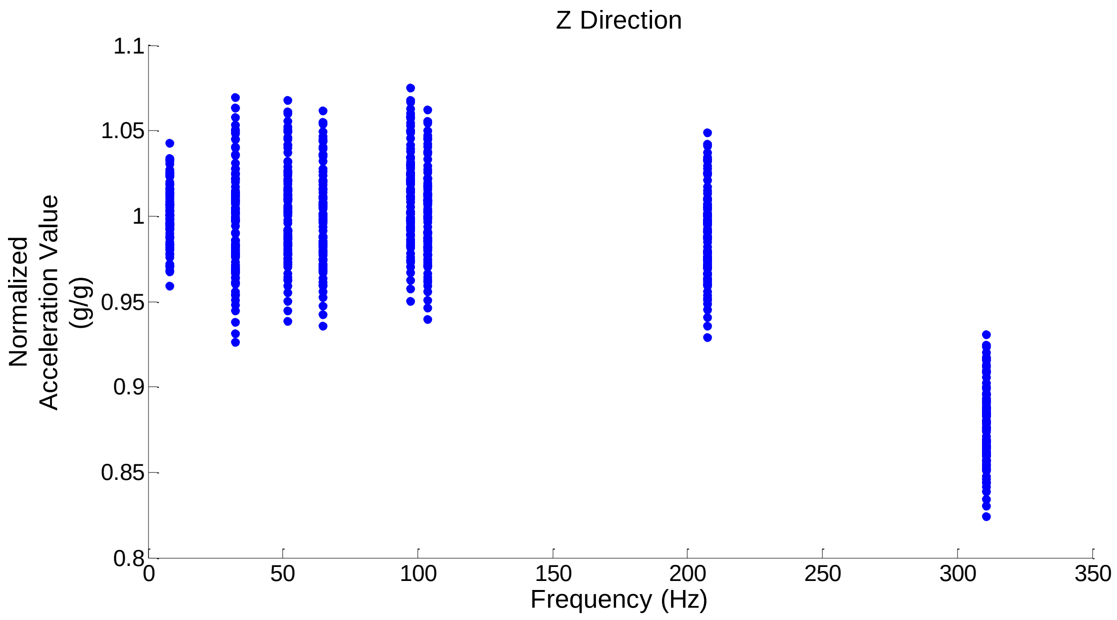

Figure B-3 Normalized Acceleration Values in Z Direction